TECHNISCHE UNIVERSITÄT MÜNCHEN

am Institut für Pflanzenernährung

High-Throughput Phenotyping the Nitrogen and Carbon Dynamics in Maize at the Reproductive Phase

Friederike Gnädinger

Vollständiger Abdruck der von der Fakultät Wissenschaftszentrum Weihenstephan für Ernährung, Landnutzung und Umwelt der Technischen Universität München zur Erlangung des akademischen Grades eines

Doktor der Naturwissenschaften (Dr.-rer. nat.)

genehmigten Dissertation.

Vorsitzender: Prof. Dr. Kay H. Schneitz

Prüfer der Dissertation:

1. Prof. Dr. Urs Schmidhalter
2. apl. Prof. Dr. Eckart Priesack

Die Dissertation wurde am 29.11.2017 bei der Technischen Universität München eingereicht und durch die Fakultät Wissenschaftszentrum Weihenstephan für Ernährung, Landnutzung und Umwelt am 06.03.2018 angenommen.

CINTEOTL - "Hombres de maíz" nennen sich die Maya.
Mais ist eine Gabe der Götter, ihm verdanken sie ihre Existenz.
(Geschichte der Maya)

Acknowledgement

With greatest respect and admiration I want to express my most sincere thanks to Prof. Dr. Urs Schmidhalter, who advised me through three years of difficulties, success and personal development. I am especially grateful for all his comments on this thesis and his support that causes one or another night shift. Thank you for giving me the opportunity to write my thesis at the chair of plant nutrition, I really appreciated that.

Apl.-Prof. Dr. Eckard Priesack and Florian Heinlein from the HelmholtzZentrum München, thank you for your time discussing opportunities in modeling maize architecture and for your help creating 3-D models of my maize cultivars. It helped me a lot to better understand breeding targets. Additionally, I want to thank Apl.-Prof. Dr. Eckard Priesack for his consent to be my second expert.

Dr. Joachim Eder from the Bayerische Landesanstalt für Landwirtschaft (LfL) who has agreed to be my mentor, thank you for great inspiring discussions and your comprehensive support during my thesis, I really appreciated that.

Dr. Sabine von Tucher, thanks for being there whenever I needed your help. Thanks for having always an open door. I really enjoyed my time sitting next to your office – you’re my role model, in terms of personality and scientific way of working.

Big thanks goes to Amanda Araujo de Franca, Sibel Yildirim and Karolin Kunz, who gave me always the feeling to be welcome and gave me the strength to endure. I really enjoyed our activities together and I hope some more will follow. Thanks Lukas Prey for all the constructive discussions we had about agriculture, harvest, and statistic problems and thanks for yours and Samuel`s Knapp help in R. Equally, I would like to thank the Dürnast Team, who enabled harvest and data collection. Special thanks to Robert Gottschalk who helped me even at the weekend and patently answered, with his many year`s experiences, every single question about crop cultivation and fertilization use.

Thanks for proof reading to Carola, Dorothee, Evi, Michi, and Lukas whom spend their private time to help me. I would like to express my deep gratitude to all of you.

Writing their master thesis with me as their supervisor, Michael, Sascha and Jan helped me a lot to prepare samples, to discuss data, and to get an overview of all my work. Thank you for that.

I would like to thank all the students Johannes, Sophia, Linh, Corinna and Bernadette without whom I would still stand in the lab grinding or extracting samples. Special thanks to Monika Heilmeier, Züleyha Öztürk, and Claudia Buchhart for analyzing and evaluating thousands of samples.

Thanks to Andrea, Marina, Johanna and Jule who accompanied me during these three years in Munich and made the weekends more colorful. Because of you I felt like home – thank you for being one of my best friends.

I am particularly grateful to Andreas who has always been on my side, solving Matlab problems in five minutes and helping me to complete my presentations even at midnight. Thank you for your encouragement to finish my thesis and for your effort to see situations sometimes from different perspectives. Thank you for being in my life.

Besonderer Dank gebührt auch meiner Familie, die in den letzten drei Jahren immer hinter mir standen und mir halfen wo es nur ging. Danke Mama und Papa für ein tolles Zuhause am Bodensee indem ich es immer geschafft habe Abstand und Ruhe zu finden. Danke auch für eure Unterstützung und euer Verständnis während meines ganzen Studiums. An meine lieben Geschwister, Dorothee und Urs, die ich so sehr bewundere und liebe. Vielen Dank an Ike für dein offenes Ohr und deine ansteckende positive Art, die mir vor allem den Anfang in München sehr erleichtert hat. Auch möchte ich mich bei Evi bedanken für konstruktive Beiträge, viele wertvolle Diskussionen über die deutsche Forschungslandschaft und über meinen beruflichen Werdegang, sowie deinen unermüdlichen Einsatz kurz vor knapp. Danke, dass ich immer auf euch zählen kann.

München, 28.09.17 Friederike Gnädinger

Table of content

List of abbreviations

abbreviation	meaning
BDW	Total above-ground biomass dry weight (kg ha^{-1})
LDW	Leaf biomass dry weight (kg ha^{-1})
SDW	Stem biomass dry weight (kg ha^{-1})
GDW	Grain biomass dry weight (kg ha^{-1})
TNU	Total above-ground nitrogen uptake (kg N ha^{-1})
LNU	Leaf nitrogen uptake (kg N ha^{-1})
SNU	Stem nitrogen uptake (kg N ha^{-1})
GNU	Grain nitrogen uptake (kg N ha^{-1})
HI	Harvest index
NHI	Nitrogen harvest index
UAV	Unmanned aerial vehicle

Formula directory

variable	unit	meaning
Nrem	kg N ha^{-1}	Remobilized nitrogen in the generative phase
Crem	t ha^{-1}	Remobilized carbon in the generative phase
NU silk	kg N ha^{-1}	Above-ground nitrogen uptake till flowering/ silk emergency
NU stover	kg N ha^{-1}	Nitrogen uptake of total above-ground biomass on grain maturity expect grain nitrogen uptake
BDW vegetative	t ha^{-1}	Above-ground biomass dry weight at flowering/silk emergency
BDW stover	t ha^{-1}	Above-ground biomass dry weight at grain maturity expect corn dry weight
Nrep	kg N ha^{-1}	Reproductive nitrogen in the generative phase
TNU grain maturity	kg N ha^{-1}	Nitrogen uptake of the total above-ground biomass at grain maturity
TNU silk emergency	kg N ha^{-1}	Nitrogen uptake of the total above-ground biomass at flowering/silk emergency
Crep	t ha^{-1}	Reproductive carbon in the generative phase
BDW grain maturity	t ha^{-1}	Total above-ground biomass dry weight at grain maturity
BDW silk emergency	t ha^{-1}	Total above-ground biomass dry weight at silk emergency
Heritability	(hÂ²)	Ratio of the genetic variability to phenotypic variability

Abstract

Increasing environmental concerns and thus more restricted official regulations for fertilizer and pesticides utilization require nitrogen efficient maize plants, as well as an optimized input of scarce resources. The aim of this work was the estimation of nitrogen and carbon allocation within different maize hybrids (*Zea mays* L.) under low (50 kg N ha^{-1}), medium (150 kg ha^{-1}) and higher fertilization levels (250 kg ha^{-1}). A better knowledge in the optimization of the nitrogen use efficiency could improve the selection for nitrogen uptake in plant breeding programs and field management decisions of farmers. For better data acquirement in regard to nitrogen and carbon uptake as well as nitrogen utilization, image processing (images made by unmanned aerial vehicles) and hyperspectral sensor techniques were established. Furthermore, precision phenotyping techniques (unmanned aerial vehicles and hyperspectral reflectance techniques) were used before the reproductive phase at plant emergence and flowering in order to detect plant density and to predict biomass production and grain yield of hybrids at grain maturity. Experimental field trials were conducted in the alpine upland close to the research station Dürnast, Freising, in Germany in the years 2014-2016. Images made by UAV were collected regularly from plant emergence till silage maturity and additionally high throughput sensor measurements were performed along with biomass sampling at flowering, silage and grain maturity. During plant emergence maize plant counting was successful through image processing and to detect the emergence quality. This observation helped to determine the final yield in regard to in situ emerged plants. Furthermore biomass detection on the basis of green pixel estimation was successfully demonstrated. During the further development of plants, sensor measurement at flowering displayed very good correlations between spectral indices and total nitrogen uptake, total above-ground biomass, leaf biomass and leaf nitrogen uptake. Moreover, cultivar differences due to the degree of maturity as well as biomass production could be distinguished through partial least square regression (PLSR). At silage maturity the quality of hyperspectral sensor measurements decreased due to beginning senescence, and grouping of cultivars with regard to above-ground biomass detection showed equally weak values. Therefore hyperspectral reflectance measurements performed better at flowering with increased correlations found for leaf biomass and nitrogen uptake. Within the nitrogen fertilization levels spectral indices showed significantly higher correlations at lower and higher fertilization levels to destructively assessed parameters based on further differentiation of cultivars regarding to the nitrogen use efficiency. For that reason the nitrogen and carbon allocation of above-ground biomass (including leaves, stem and corn) was studied more precisely to gain future knowledge regarding the nitrogen use efficiency with a focus on remobilized N and reproductive N. The sink driven remobilized N which is primarily associated with vegetative N and the reproductive N which is driven by ear demand are antagonistically related to each other. The results show that both allocation processes are primarily dependent on the stage of ripening among different hybrids and are therefore important indicators for the nitrogen use efficiency.

Our results support the integration of phenotyping techniques into breeding processes as well as daily agriculture practices to improve fertilization recommendations in a sustainable crop management.

Zusammenfassung

Zunehmendes Umweltbewusstsein und damit einhergehende behördliche Regulierungen des Dünger- und Pestizideinsatzes erfordern stickstoffeffiziente Maissorten. Ziel dieser Arbeit war es, den Stick- und Kohlenstoffhaushalt verschiedener Maissorten unter drei verschiedenen Düngerstufen – Unterversorgung (50 kg N ha^{-1}), Normalversorgung (150 kg ha^{-1}) und Überversorgung (250 kg N ha^{-1}) – zu untersuchen, um ein erweitertes Verständnis bezüglich einer effizienten Stickstoffausnutzung zu gewinnen. Dies ermöglicht eine verbesserte Auswahl von Maishybriden in Pflanzenzüchtungsprogrammen sowie Feldmanagemententscheidungen von Landwirten. Hierzu wurden hyperspektrale Sensortechniken und die Bildbearbeitung für eine erweiterte Datenerfassung der Stick- und Kohlenstoffaufnahme etabliert. Des Weiteren wurde versucht durch Nutzung von bildgebender Drohnen und Sensoren Rückschlüsse auf die Enderträge verschiedener Sorten von der Frühentwicklung bis zur Blüte zu ziehen, mit dem Zweck die Selektion in Züchtungsprogrammen zu beschleunigen. In den Jahren 2014 bis 2016 wurden Feldversuche im Voralpenland bei Dürnast, Freising, in Deutschland durchgeführt, in denen regelmäßige Drohnenbefliegungen sowie Sensormessungen mit destruktiven Probenahmen der Biomasse zur Blüte, Silo- und Körnerreife durchgeführt wurden. Die Qualität des Pflanzenaufgangs und die Anzahl der Maispflanzen konnten erfolgreich mit Drohnenbildern erfasst werden und zur genaueren Ertragsbestimmung herangezogen werden. Darüber hinaus konnte die Erkennung der Biomasse auf Basis der Grünpixelerfassung erfolgreich aufgezeigt werden. In der weiteren Entwicklung der Pflanzen zur Blüte zeigten etablierte Indizes und destruktive Pflanzenparameter, wie die gesamte oberirdische Biomasse und deren Stickstoffaufnahme sowie die Biomasse und Stickstoffaufnahme in den Blättern sehr gute Korrelationen. Zusätzlich konnten Sortenunterschiede auf Grund des Reifegrades und der Biomassenproduktion mittels PLSR unterschieden werden. Während der Siloreife wiesen schwächere Korrelationen zwischen hyperspektralen Messungen und destruktiven Parametern auf den Beginn der Abreife hin und auch die Sortengruppierung mittels PLSR war weniger präzise. Eine bessere Erfassung von Pflanzenparametern ist somit während der Blüte möglich. Innerhalb der Stickstoffstufen konnten signifikante Korrelationen und damit eine verbesserte Differenzierung von Sorten durch hyperspektrale Messungen in der niedrigsten und höchsten Düngerstufe gefunden werden, da sich in diesen Stufen eine effizientere Stickstoffnutzung sowie die Ausschöpfung der Stickstoffreserven besser erkennbar macht. Diese Erkenntnis führte zu weiteren pflanzenphysiologischen Untersuchungen, die durch ein erweitertes Verständnis der N- und C Allokation, insbesondere von remobilisiertem (Nrem) und reproduziertem

N (Nrep), Rückschlüsse auf die Stickstoffeffizienz ermöglichen sollen. Remobilisiertes und reproduktives N verhielten sich antagonistisch zueinander, während das remobilisierte N sehr stark von der N-Aufnahme in der vegetativen Phase beeinflusst wird und das reproduzierte N hingegen vom N Bedarf des Korns gesteuert wird. Die Ergebnisse zeigen, dass beide Translokationsprozesse primär von der Reifegruppe der unterschiedlichen Sorten abhängig sind und daher wichtige Indikatoren für die Bestimmung und Optimierung der Stickstoffeffizienz bilden.

Diese Arbeit zeigt die mögliche Einbindung von Phänotypisierungsmethoden in die Pflanzenzüchtung und in der Optimierung der N-Düngung auf. Dies trägt zu einer nachhaltigen und zukunftsorientierten Agrarwirtschaft bei.

1 General Introduction

The rising world population and the accompanying food demand is a big global challenge. Until 2050 it is expected that the world population will reach approximately more than nine billion people who have to be fed. Furthermore, higher living standards (especially in Asia and Latin America) demand a higher use of resources, which has put further strains on food supply and the environment. Some of these challenges include: a constantly changing environment including globally rising temperatures, soil salinity, desertification and eutrophication of lakes. Due to the socio-economic changes and the prognosis of a high agricultural yield, key goals for the crop production have been defined: economic success and a low environmental impact (Mistele, 2006).

1.1 The importance of maize worldwide and in Europe

In 2016, the world cereal production reached 2569 million tonnes and topped the previous peak of 2014 by 5.5 million tonnes. Maize yield even exceeded 800 million tonnes. The global utilization of maize increased by 1.5 percent in 2016, largely driven by industrial use and animal feeding – especially in the United States and China (FAOSTAT, 2017). Maize was grown on 148 million hectares (ha) on a global level. Together with rice and wheat, maize provides at least 30% of the food calories to more than 4.5 billion people (Shiferaw et al., 2011). After the USA, Brazil and China, the European Union (EU) is the fourth most important maize producer in the world, covering 14 million ha of fertile land (Table1).

Table 1: The global yield production (Mio t) of grain maize and corn-cob-mix in 2014 (FAOSTAT, 2017)

Country	**2014**	
	Yield (Mio t)	Area (1000 ha)
United States	**361**	**33645**
China	215	37105
Brazil	79	15432
European Union	**77**	**14800**
Mexico	23	7060

Maize is not only used for human consumption. Especially in highly developed countries maize is used multivarious as livestock feed, in industrial processes and for seed production with up to 70% (Shiferaw et al., 2011) of the whole maize production. Within the EU, the production of green maize for energy and silage production is significantly higher compared to grain maize cultivation (Tables 2 and 3). Germany is the biggest maize producer in the EU (producing 96 Mio tonnes, of which 5% is grain maize). The major interest is to ensure high biomass production for animal feeding and energy production through biogas (eurostat, 2017). The race between increasing food demand (in the future) and bio-energy production to replace fossil energy resources could become a fierce competition, mostly driven by economic interests. As maize cultivation already covers a remarkable area of fertile land, an increase in the cultivation area for increasing the future food production is not a sustainable solution due to the environmental cost in form of land degradation (Tilman et al., 2002). An enhanced utilization of nitrogen fertilization is another option to increase maize yield but limitations of a certain fertilization amount and drastic consequences for environmental ecosystems have to be taken into account.

Table 2: Yield production (1000 t) and area utilization (1000 ha) of green maize production in the EU (including 28 countries) compared to the most important maize producing European countries in 2014, 2015 and 2016 (eurostat, 2017)

Country	**2014**		**2015**		**2016**	
	yield (1000 t)	area (1000 ha)	yield (1000 t)	area (1000 ha)	yield (1000 t)	area (1000 ha)
Eurpean Union (28 countries)	**268565.2**	**6076.5**	**211872.5**	**6185.6**	**240043.5**	**6217.2**
Germany	99203.7	2092.6	87218.9	2100.4	92087.7	2137.60
Poland	25844.3	541.2	19801.8	555.2	29684.9	602.2
France	20105.6	1411.8	17259.4	1475.2	16084.0	1506.8
Netherlands	10788.0	226.0	8222.4	223.8	8271.7	202.3
UK	6847.0	171.0	7160.0	179.0	7440.0	186.0

Table 3: Yield production (1000 t) and area utilization (1000 ha) of grain maize and corn-cob-mix in the EU (including 28 countries) and of the most important maize producers of Europe in 2014, 2015 and 2016 (eurostat, 2017)

Country	**2014**		**2015**		**2016**	
	yield (1000 t)	area (1000 ha)	yield (1000 t)	area (1000 ha)	yield (1000 t)	area (1000 ha)
European Union (28 countries)	**77460.3**	**9610.2**	**58905.6**	**9255.3**	**61097.5**	**8583.5**
Germany	5142.1	481.3	3973.0	455.5	4017.8	416.3
Spain	4776.2	418.5	4564.4	398.7	3981.7	357.3
France	18541.8	1848.1	13738.2	1639.5	12191.8	1488.7
Italy	9250.1	869.9	7073.9	727.4	6839.5	660.7
Romania	11988.6	2513.6	8984.7	2607.4	8901.9	2552.4

1.2 The global meaning of nitrogen – “The challenge to produce more food and energy with less pollution”

At the beginning of the 20th century, the Haber-Bosch process - where energy is used to convert unreactive atmospheric N_2 into reactive nitrogen compounds - initiated the “green revolution” of the 20th century in agriculture (Erisman et al., 2008). The production of industrial nitrogen has steadily increased the utilization of nitrogen in agriculture (Fig 1).

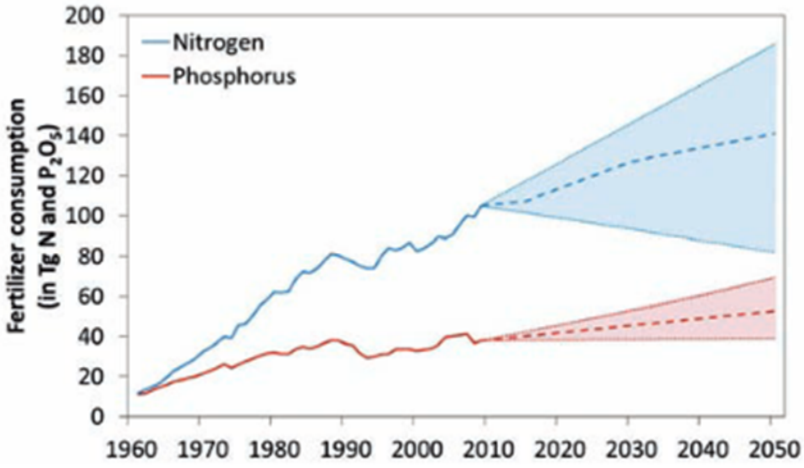

Fig. 1: Trends in global mineral fertilizer consumption for nitrogen and phosphorous and projected possible futures (Sutton et al., 2013a)

The enhanced utilization of nitrogen potentially contributes to a number of environmental concerns, for example water eutrophication and an increase in greenhouse gases - which have a significant effect on climate change, air pollution, soil degradation and biodiversity losses. The nitrogen biochemical cycle is strongly influenced by agriculture and fossil fuel energy, whereas a dominant impact of N from 15 × 10^9 kg N in 1869 to 187 × 10^9 kg N in 2005 is indebted by farming (Galloway et al., 2008). Losses in form of NH_3 emissions from agriculture and livestock reach an amount of 37 × 10^9 kg N per year (Sutton et al., 2013b) and additional leaching and denitrification from soils were calculated with amounts higher than 100 × 10^9 kg N per year (Billen et al., 2013).

A lack of sufficient nitrogen demand for fertilization has become apparent in several developing countries, which points toward a problematic shift in nitrogen fertilizer-use worldwide (Galloway et al., 2008). For some developing countries synthesized nitrogen as fertilizer has been very costly due to the lack of local resources and poor infrastructure. Many farmers have not been able to afford synthesized nitrogen as fertilizer, which has made it difficult for developing countries to keep up with the production capacity of industrial nations. A rising population has further increased the pressure (Fig. 2).

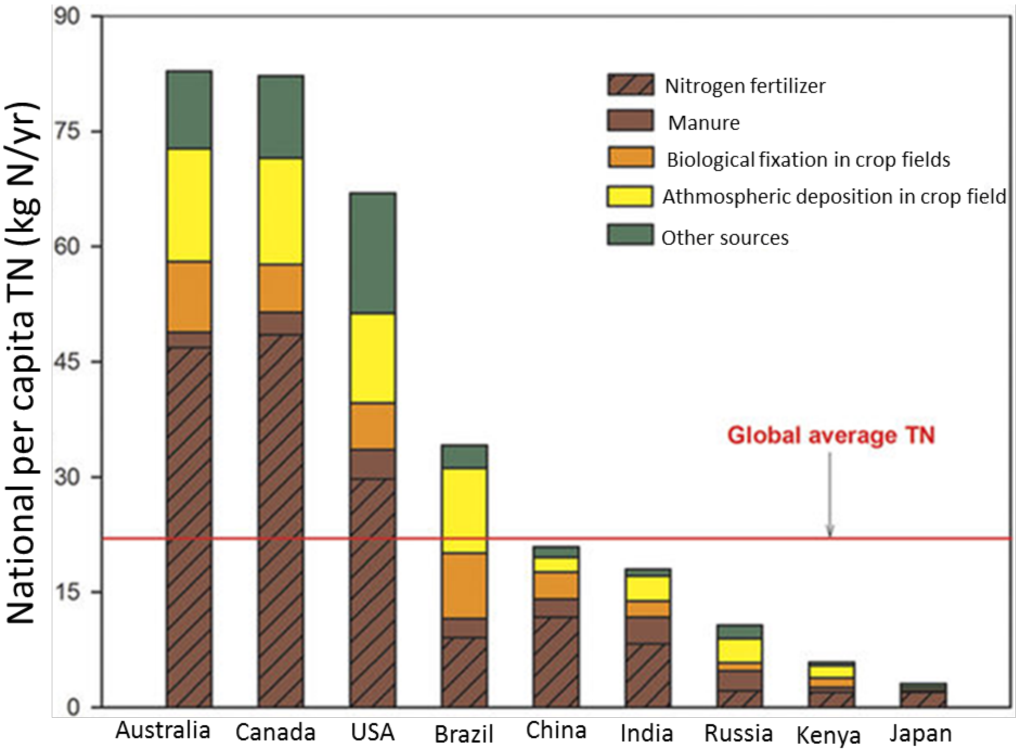

Fig. 2: The national per capita utilization of different plant available nitrogen of countries with the highest N impact (Liu et al., 2016)

The challenge in future agriculture is to secure higher food production while ensuring high quality food, by not endangering human health, preservation of the biodiversity, and sustainable agriculture (Tilman et al., 2002; Tilman et al., 2001). To be able to address these challenges, it is essential to find the right balance of nitrogen utilization, regarding the overestimation and shortage of N. Additionally, new movements in precision farming systems and innovations in breeding targets is expected to optimize nitrogen efficiency in a sustainable way.

1.3 Precision farming systems as a solution for agricultural challenges

Precision farming has a high potential in terms of re-organizing today's entire agricultural system towards a low-input, high efficiency and sustainable agriculture. Many innovations have already been presented. Yet, precision farming practices on a local level have not widely been established, as many farmers are uncertain about its applicability (Zhang et al., 2002). However, precision farming techniques benefit agriculture in at least economic and ecological/environmental matters. Innovative techniques support decisions on whether the use of costly parameters like fertilizers, pesticides and virility can be covered by an increased output in form of yield. Decision-making based on calculated economic benefits is often applied to re-organize marginal land in low income areas, which are subject to a higher biodiversity impact. With regard to new official requirements, sustainable practices in agriculture are becoming increasingly important and precision farming techniques help to fulfill these requirements. Precision farming provides the opportunity for targeted and efficient application of fertilizer, agro-chemicals and record field information on a metric scale which helps with further management practices (Stafford, 2000). Furthermore, the opportunity to combine topological data of a cropland with information collected by precision farming techniques provides the means to detect the interactions of tillage and field morphology and eventually reduce soil degradation and water contamination (Schumacher et al., 2005).

1.3.1 Unmanned aerial vehicles

One of various precision farming tools is the unmanned aerial vehicle (UAV) which has high potential in future applications in agriculture. UAV is a very promising instrument in agricultural sciences (Floreano and Wood, 2015). Flights are fairly independent of weather conditions and time. Images can be captured even on cloudy days, when image recording by satellite is not possible (Zhang and Kovacs, 2012). Hence, a higher degree of information can be obtained because the higher flexibility allows for an extended range of measurement days. Furthermore, UAVs offer time-saving and cheaper image recording, enable flexible and immediate image processing and give a survey of the health of the farm systems (Tripicchio et al., 2015). In addition UVAs enable the flexible handling options for aim-oriented use, e.g. in form of variable flight height and better image resolution (Pena et al., 2013). UAVs also represent new opportunities in agricultural sciences, especially in precision farming and precision phenotyping. Precision farming has created a critical need for spatial data on plant density, crop yield and related soil characteristics (Geesing et al., 2014). Recent technological advances in UAV technology offer new opportunities for assessing agricultural plot experiments using UAV imagery (Rasmussen et al., 2016).

Fig 3: RGB image recorded with an unmanned aerial vehicle (UAV) model MK EASY Okto V3 (HiSystems GmbH, Moormerland, Germany) at the field site Dürnast in July 2016

1.3.2 Field sensors

The above-ground biomass is a potential source to estimate plant performance and health. Canopy reflectance data has proven to be an appropriate parameter to characterize the plant physiology (Mistele, 2006) and has already been successfully tested in various experiments under controlled conditions using handheld spectrometers (Hackl et al., 2013; Kipp et al., 2014). However, to estimate plant physiological parameters with sensors, field experiments are indispensable and were conducted with various cultivars and treatments, such as N uptake (Erdle et al., 2013; Winterhalter et al., 2011), phosphorus deficiency (Osborne et al., 2002), water deficiency (Weber et al., 2012) and biomass detection (Liebler et al., 2001; Mistele and Schmidhalter, 2008). Despite the high potential of sensors in field experiments, technical limits due to environmental disturbances have to be considered. Field measurements can only be conducted during midday due to shadow effects resulting from the position of the sun. As most of the measurements run on nadir, the position shadow effect caused by a rising or fading sun negatively affect the reflected wavelength detection (Mistele and Schmidhalter, 2010). Furthermore, disturbances of soil background (Daughtry et al., 2000), temperature (Schlemmer et al., 2005) as well as annual influences (Osborne et al., 2002) are additional reasons why spectral measurements are not always exactly comparable among different field experiments and years.

The use of high-throughput phenotyping is expected to improve crop performance and hence accelerates the breeding progress (Barmeier and Schmidhalter, 2016). Field-based phenotyping is the most promising approach for delivering the required throughput in terms of numbers of plants as well as populations for a precise description of plant traits in cropping systems (Winterhalter et al., 2013).

1.4 Thesis objectives

This thesis aims to increase the knowledge about high throughput phenotyping of maize in the reproductive phase and nitrogen allocation in general within different cultivars. More precisely, this thesis studies the effects of different nitrogen levels 50, 150 and 250 kg N ha^{-1} on above ground nitrogen allocation in various maize cultivars (*Zea mays* L.), representing the dominant agricultural cultivar in the world. Special focus is set on the reproductive phase from flowering until corn maturity where translocation processes and the grain filling period start. The thesis aims to answer the following research questions:

1) In relation to claim settlement: can precision farming techniques as UAV and sensors help to asses economic related parameters like yield, post-emergency nitrogen uptake? And are they able to predict final yield increases in an early plant growth stage?

2) With regard to the environmental aspect and official requirements: do sensors and image processing detect nitrogen demand in the exact dimensions for reliable field management. And do sensors and image processing provide the means for targeted and needs-oriented fertilizer and agro-chemical application?

3) With respect to the breeding progress: is the utilization of sensors a reliable and potential tool to detect efficient traits of maize cultivars by providing accurate maize performance forecasts and does it thereby accelerate the trustworthy breeding processes? Followed by the next question: How should future breeding targets consider physiological aspects?

4) Which importance do translocation processes have - remobilized and reproductive N in future breeding targets and which loadings can be given to these two allocations? Can allocation processes be optimized, in regard to nitrogen use efficiency and predicted environmental and climate changes?

1.5 Thesis outline

This chapter has given a broad overview and a comprehensive basis for the following detailed examination of nitrogen and carbon allocation and phenotypic techniques. In the following chapters, the above-mentioned research questions are addressed using phenotyping approaches.

In **Chapter 2**, a methodical approach to count young maize plants in a field is presented. RGB images recorded with a 10 Mega pixel compact camera mounted on an unmanned aerial vehicle (UAV) were analysed with the aim to detect the amount of plants in a plot by clustering pixels. With the help of a decorrstrech filter, which enhances the contrast of each pixel, the segmentation of a particular plant part was made possible. Additionally, a loop to analyse images in a batch and detect biomass by counting green pixels was coded.

Chapter 3 focuses on the physiological processes in the generative phase of different maize cultivars. The above-ground carbon and nitrogen allocation were determined by calculating the differences among dry weight biomass plant compartments in different growth stages. The main objective of this work was to distinguish differences in the nitrogen uptake capacity, remobilization strength and nitrogen tolerance of different maturing maize cultivars to optimize breeding targets with regard to enhanced nitrogen use efficiency.

Chapter 4 addresses the methodological aspect of measuring the biomass and nitrogen uptake of maize plants in situ with active and passive sensors. The quality and capacity of three active sensors and of a bidirectional passive sensor were estimated and best performing indices were calculated. Furthermore, cultivar-specific differences by sensor detection could be successfully implemented.

1.6 References

Barmeier, G., and Schmidhalter, U. (2016). High-Throughput Phenotyping of Wheat and Barley Plants Grown in Single or Few Rows in Small Plots Using Active and Passive Spectral Proximal Sensing. Sensors 16, 1860.

Billen, G., Garnier, J., and Lassaletta, L. (2013). The nitrogen cascade from agricultural soils to the sea: modelling nitrogen transfers at regional watershed and global scales. Phil. Trans. R. Soc. B 368, 20130123.

Daughtry, C., Walthall, C., Kim, M., De Colstoun, E. B., and McMurtrey, J. (2000). Estimating corn leaf chlorophyll concentration from leaf and canopy reflectance. Remote sensing of Environment 74, 229-239.

Erdle, K., Mistele, B., and Schmidhalter, U. (2013). Spectral assessments of phenotypic differences in spike development during grain filling affected by varying N supply in wheat. Journal of Plant Nutrition and Soil Science 176, 952-963.

Erisman, J. W., Sutton, M. A., Galloway, J., Klimont, Z., and Winiwarter, W. (2008). How a century of ammonia synthesis changed the world. Nature Geoscience 1, 636.

eurostat (2017).In "eurostat Ihr Schlüssel zur europäischen Statistik", Vol. 2017, pp. eurostat meta data European Commission, Retrieved from http://ec.europa.eu/eurostat/cache/metadata/de/apro_acs_esms.htm.

FAOSTAT (2017). Food and Agriculture Organization of the United Nations (FAO), Vol. 2017. Retrieved from http://www.fao.org/faostat/en/#data.

Floreano, D., and Wood, R. J. (2015). Science, technology and the future of small autonomous drones. Nature 521, 460-466.

Galloway, J. N., Townsend, A. R., Erisman, J. W., Bekunda, M., Cai, Z., Freney, J. R., Martinelli, L. A., Seitzinger, S. P., and Sutton, M. A. (2008). Transformation of the Nitrogen Cycle: Recent Trends, Questions, and Potential Solutions. Science 320, 889-892.

Geesing, D., Diacono, M., and Schmidhalter, U. (2014). Site-specific effects of variable water supply and nitrogen fertilisation on winter wheat. Journal of Plant Nutrition and Soil Science 177, 509-523.

Hackl, H., Mistele, B., Hu, Y. C., and Schmidhalter, U. (2013). Spectral assessments of wheat plants grown in pots and containers under saline conditions. Functional Plant Biology 40, 409-424.

Kipp, S., Mistele, B., and Schmidhalter, U. (2014). The performance of active spectral reflectance sensors as influenced by measuring distance, device temperature and light intensity. Computers and Electronics in Agriculture 100, 24-33.

Liebler, J., Sticksel, E., and Maidl, F. (2001). Field spectroscopic measurements to characterise nitrogen status and dry matter production of winter wheat. In "Proceedings of the third European conference on precision agriculture, Montpellier", pp. 18-20.

Liu, J., Ma, K., Ciais, P., and Polasky, S. (2016). Reducing human nitrogen use for food production. Scientific reports 6, 30104.

Mistele, B. (2006). Tractor based spectral reflectance measurements using an oligo view optic to detect biomass, nitrogen content and nitrogen uptake of wheat and maize and the nitrogen nutrition index of wheat (Doctoral dissertation).

Mistele, B., and Schmidhalter, U. (2008). Spectral measurements of the total aerial N and biomass dry weight in maize using a quadrilateral-view optic. Field Crops Research 106, 94-103.

Mistele, B., & Schmidhalter, U. (2010). Tractor-based quadrilateral spectral reflectance measurements to detect biomass and total aerial nitrogen in winter wheat. Agronomy Journal, 102(2), 499-506.

Osborne, S. L., Schepers, J. S., Francis, D. D., and Schlemmer, M. R. (2002). Detection of phosphorus and nitrogen deficiencies in corn using spectral radiance measurements. Agronomy Journal 94, 1215-1221.

Pena, J. M., Torres-Sanchez, J., de Castro, A. I., Kelly, M., and Lopez-Granados, F. (2013). Weed Mapping in Early-Season Maize Fields Using Object-Based Analysis of Unmanned Aerial Vehicle (UAV) Images. PloS one 8(10),e7715.

Rasmussen, J., Ntakos, G., Nielsen, J., Svensgaard, J., Poulsen, R. N., and Christensen, S. (2016). Are vegetation indices derived from consumer-grade cameras mounted on UAVs sufficiently reliable for assessing experimental plots? European Journal of Agronomy 74, 75-92.

Schlemmer, M. R., Francis, D. D., Shanahan, J. F., & Schepers, J. S. (2005). Remotely measuring chlorophyll content in corn leaves with differing nitrogen levels and relative water content. Agronomy journal, 97(1), 106-112.

Schumacher, J., Kaspar, T., Ritchie, J., Schumacher, T., Karlen, D., Venteris, E., McCarty, G., Colvin, T., Jaynes, D., and Lindstrom, M. (2005). Identifying spatial patterns of erosion for use in precision conservation. Journal of soil and water conservation 60, 355-362.

Shiferaw, B., Prasanna, B. M., Hellin, J., and Bänziger, M. (2011). Crops that feed the world 6. Past successes and future challenges to the role played by maize in global food security. Food Security 3, 307.

Stafford, J. V. (2000). Implementing precision agriculture in the 21st century. Journal of Agricultural Engineering Research 76, 267-275.

Sutton, M. A., Bleeker, A., Howard, C., Bekunda, M., Grizzetti, B., De Vries, W., Van Grinsven, H., Abrol, Y., Adhya, T., and Billen, G. (2013a). "Our Nutrient World: The challenge to produce more food and energy with less pollution," NERC/Centre for Ecology & Hydrology.

Sutton, M. A., Reis, S., Riddick, S. N., Dragosits, U., Nemitz, E., Theobald, M. R., Tang, Y. S., Braban, C. F., Vieno, M., and Dore, A. J. (2013b). Towards a climate-dependent paradigm of ammonia emission and deposition. Philosophical Transactions of the Royal Society of London B: Biological Sciences 368, 20130166.

Tilman, D., Cassman, K. G., Matson, P. A., Naylor, R., and Polasky, S. (2002). Agricultural sustainability and intensive production practices. Nature 418, 671.

Tilman, D., Fargione, J., Wolff, B., D'Antonio, C., Dobson, A., Howarth, R., Schindler, D., Schlesinger, W. H., Simberloff, D., and Swackhamer, D. (2001). Forecasting agriculturally driven global environmental change. Science 292, 281-284.

Tripicchio, P., Satler, M., Dabisias, G., Ruffaldi, E., and Avizzano, C. A. (2015). Towards Smart Farming and Sustainable Agriculture with Drones. 2015 International Conference on Intelligent Environments Ie 2015, 140-143.

Weber, V. S., Araus, J. L., Cairns, J. E., Sanchez, C., Melchinger, A. E., and Orsini, E. (2012). Prediction of grain yield using reflectance spectra of canopy and leaves in maize plants grown under different water regimes. Field Crops Research 128, 82-90.

Winterhalter, L., Mistele, B., Jampatong, S., & Schmidhalter, U. (2011). High-throughput sensing of aerial biomass and above-ground nitrogen uptake in the vegetative stage of well-watered and drought stressed tropical maize hybrids. Crop Science, 51(2), 479-489.

Winterhalter, L., Mistele, B., and Schmidhalter, U. (2013). Evaluation of active and passive sensor systems in the field to phenotype maize hybrids with high-throughput. Field Crops Research 154, 236-245.

Zhang, C., and Kovacs, J. M. (2012). The application of small unmanned aerial systems for precision agriculture: a review. Precision Agriculture 13, 693-712.

Zhang, N., Wang, M., and Wang, N. (2002). Precision agriculture—a worldwide overview. Computers and electronics in agriculture 36, 113-132.

2 Digital Counts of Maize Plants by Unmanned Aerial Vehicles (UAVs)

Precision phenotyping, especially the use of image analysis, allows researchers to gain information on plant properties and plant health. Aerial image detection with unmanned aerial vehicles (UAVs) provides new opportunities in precision farming and precision phenotyping. Precision farming has created a critical need for spatial data on plant density. The plant number reflects not only the final field emergence but also allows a more precise assessment of the final yield parameters. The aim of this work is to advance UAV use and image analysis as a possible high-throughput phenotyping technique. In this study, four different maize cultivars were planted in plots with different seeding systems (in rows and equidistantly spaced) and different nitrogen fertilization levels (applied at 50, 150 and 250 kg N ha^{-1}). The experimental field, encompassing 96 plots, was overflown at a 50m height with an octocopter equipped with a 10-megapixel camera taking a picture every 5s. Images were recorded between BBCH 13–15 (it is a scale to identify the phenological development stage of a plant which is here the 3- to 5-leaves development stage) when the color of young leaves differs from older leaves. Close correlations up to $R^2 = 0.89$ were found between in situ and image-based counted plants adapting a decorrelation stretch contrast enhancement procedure, which enhanced color differences in the images. On average, the error between visually and digitally counted plants was ≤5%. Ground cover, as determined by analyzing green pixels, ranged between 76% and 83% at these stages. However, the correlation between ground cover and digitally counted plants was very low. The presence of weeds and blurry effects on the images represent possible errors in counting plants. In conclusion, the final field emergence of maize can rapidly be assessed and allows more precise assessment of the final yield parameters. The use of UAVs and image processing has the potential to optimize farm management and to support field experimentation for agronomic and breeding purposes.

2.1 Introduction

Unmanned aerial vehicles (UAVs) are very promising instruments in agricultural sciences (Floreano and Wood, 2015; Sankaran et al. 2015).Flights are fairly independent of weather conditions and time. Images can be captured on cloudy days, whereas image recording in similar conditions by satellite is not possible (Zhang and Kovacs, 2012). Hence, a higher degree of information can be obtained because the higher flexibility allows for an extended range of measurement days. Furthermore, UAVs offer time-saving and cheaper image recording, enable flexible and immediate image processing and give a survey of the health of farm systems (Tripicchio et al., 2015). In addition to the time-saving and cheaper image processing, the flexible handling options for aim-oriented use, e.g., variable flight height and better image resolution (Pena et al., 2013; Pérez-Ortiz et al., 2016), UAVs represent new opportunities in the agricultural sciences, especially in precision farming and precision phenotyping. Precision farming has created a critical need for spatial data on plant density, crop yield and related soil characteristics (Geesing et al., 2014). Recent technological advances in UAV technology offer new opportunities for assessing agricultural plot experiments using UAV imagery (Rasmussen et al., 2016). The use of high-throughput phenotyping is expected to improve crop performance and hence accelerate the breeding progress (Barmeier and Schmidhalter, 2016). Field-based phenotyping is the most promising approach for delivering the required throughput in terms of numbers of plants as well as populations for a precise description of plant traits in cropping systems (Winterhalter et al., 2013).

The human eye is a sensitive system, which recognizes contrast better than absolute luminance as well as the structural properties of an object. However, image analysis could provide a wealth of metric information about positions, size and interrelationships between objects (Dharani et al., 2016) The human eye is always combined with subjective perception, and therefore the degree of ground cover in a cropping system can be only relatively assessed compared with imaging (Kipp et al., 2014), scaling-up is difficult and a comparison of ground cover and the number of plants is not feasible. Weeds between and within crop rows were successfully recorded using the k-means clustering method (Pérez-Ortiz et al., 2016) and crop row detection was accomplished by mounting a camera on a tractor. Rows were counted by evaluating pixel values, and their positioning was demonstrated (Romeo et al., 2012). Burgos-Artizzu, et al. (2011) and Berge et al. (2008) successfully detected weeds with RGB images (with three channels: red, green and blue to define color space) using a camera mounted on a tractor. Additionally, nitrogen level and the LAI can be detected with aerial visible and near-band images by calculating the Normalized Difference Vegetation Index (NDVI) and Grassland drought index (GDI) (Gautam and Panigrahi, 2007; Lelong et al., 2008). Even object detection is possible through image processing using the mathematical Bernoulli distribution (Martin et al., 2012). Whereas detection of weeds, biomass and ground cover with aerial RGB and remote imaging has already been successfully shown in previous works (Kipp et al., 2014; Pena et al., 2013; Pérez-Ortiz et al., 2016); the counting and segmentation of individual plants has not yet been demonstrated and represents the goal of this work.

The aim of this work is to advance UAV use and image analysis as a possible high-throughput phenotyping technique. Therefore, image analysis applied to two different sowing systems, conventional row and equidistant planting, was performed. In theory, plants growing in triangular planting systems should have better light and water availability and therefore competition between plants is reduced (Maddonni et al., 2001a; Maddonni et al., 2001b; Weiner et al., 2010). Additionally, soil erosion due to heavy rainfall, which can exert a strong influence on plant cultivation, particularly maize, could also be diminished or even prevented. Moreover, with faster row cover development in triangular plantings, competition with weeds may be suppressed (Abdin et al., 2000), growth potential may be enhanced and the intensive application of pesticides and soil tillage could be reduced (Goetz, 2010).

Determination of the plant number per hectare represents an important index to assess plant density as well as field emergence. Ultimately, the final yield can be best determined by including the exact plant number. Identifying optimal plant density and row spacing is a critical management decision for maize production to investigate grain yield response to plant density and to explore genotype x environment interactions (Assefa et al., 2016; Testa et al., 2016). The goal of this work is to use aerial images to detect ground cover and to determine the plant number of different maize cultivars grown in different row spacings.

2.2 Materials and Methods

The field experiment was conducted in 2016 in Dürnast (48°24′10.3″, 11°41′37.5″), close to Freising in southern Bavaria, at the experimental station of the Chair of Plant Nutrition belonging to the Technical University of Munich. The silty cambisol is characterized by a homogeneous soil texture across the whole experimental site, which is exposed from north to south. The average annual temperature was 8.1 °C and the average precipitation reached 791 mm. The phenological plant growth proceeded regularly during the season. Optimal climate conditions with sunny days and enough rain led to above average yield. The fully randomized block design consisted of 96 plots with four cultivars, three nitrogen levels (50, 150 and 250 kg N ha^{-1}), four replicates and two planting systems—row planting (RP) and triangular planting (TP). Cultivars were from different maturity groups representing different agronomic purposes (Table 1). Conventional farming was applied using the herbicides Roundup PowerFlex (20 April 2016) and Gardo Gold + Callisto (10 June 2016). Different fertilization levels were applied on 1 June 2016.

Table 1. Intended use, maturity class and number of the different maize cultivars.

Cultivar	**Usage**	**Maturity Group**	**FAO Number**
Cannavaro	biogas	very late	S 310
Lapriora	corn	early	K 190
Saludo	silage, corn	early	S10, K210
Vitallo	silage	late	S270

Aerial images were taken on 16 June 2016, when plants reached the BBCH stage 13–15 (it is a scale to identify the phenological development stage of a plant which is here the 3- to 5-leaves development stage). The flying height was 50 m above the field, covering an area of 9000 m^2, to obtain a seamless orthophoto mosaic photo and to cover all plots.

The flight direction of the UAV called MKSET_BASIS_OKTO2 (KS Model Company Ltd., Hong Kong, China) was perpendicular to the plots. One image was captured on average per three plots as illustrated in Figure 1. The recorded images overlapped on average by one third. After the flyover of one plot row, the UAV was navigated back to the first plot of the second row to maintain a perpendicular and centered flight direction (over the next row).

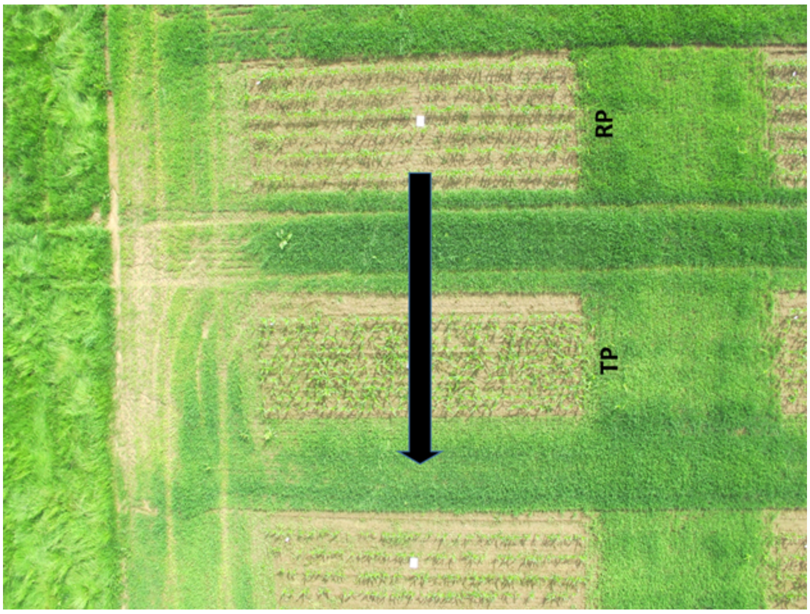

Figure 1. Part of the trial design, where black arrow indicate the flight direction of the unmanned aerial vehicles (UAVs) and illustrate the field section that was captured in the image (in general three plots). The abbreviations RP and TP indicate row planting and triangular (equidistant) planting.

DINA4 posters (210x297 millimeter) labeled with the plot number were placed on each plot. Images were taken with a Canon G12 digital camera (Canon, Tokyo, Japan) with 1/1.7 inch CDD sensor, 10 megapixels, 28-mm focal length, an image quality of 180 pixels/inch, triggering time of 281 milliseconds, f-stop of 2.97 and disk size of 4.91 MB mounted on the octocopter. Images were captured in auto mode due to changing light conditions and to avoid wrong ISO (light sensitivity of the camera sensor) the f-stop and shutter speed settings. Despite the stable mounting of the camera on the UAV, the camera with an outstanding position was partly affected by the wind and vibrations of the UAV comparatively to integrated cameras fixed within the UAV. Additionally, the focus of the camera could not be used properly due to limited remote tripping contrasting to integrated cameras where the focus is fixed at infinity. Therefore, occasionally blurry images resulted, however, not affecting the subsequent image analysis. The position of the octocopter could be detected by GNSS (Differential Global Positioning System) and a magnetic compass to maintain flight direction. The height could be detected by measuring barometric air pressure; air pressure was calibrated as zero at the beginning of the flight campaign. The UAV used is a vertical take-off and landing aircraft with eight brushless external rotor motors. The UAV is air-remotely controlled with a bidirectional transmission frequency of 2.4 GHz that receives data of the battery voltage, temperature of the motor controller, Global Positioning System (GPS) reception and the height differences from the starting point. The angle of the camera can be changed remotely. With a lithium polymer battery, the octocopter has a flight time of 16 min when carrying the camera.

2.2.1 Description of the Image Analysis Process

To detect the number of plants and their spatial distribution in the field, weed-free conditions on the field are required. All images of the plots were cut into correct form using the program Adobe Photoshop CC (Adobe Systems Software Ireland Limited, Dublin, Ireland). Segmentation of the green pixels and detection of the plant numbers were completed using MATLAB (Mathworks, Natick, MA, USA).

2.2.2 Creation of the Color Histograms and Employment of the Contrast Enhancement Procedure

Color histograms help to judge, correct and optimize the brightness and contrast of images. For RGB images, four histograms are created per image: the red channel histogram, the green channel histogram, the blue channel histogram, and the gray histogram, which explain the luminance of the image. A histogram has values ranging from 0 to 255, where zero is black and 255 is white. Between these border values are gray values. The height of the bars (deducted from the histogram) demonstrates the frequency of the appearing color value in the image represented by pixels. The color histogram is created to evaluate the quality of the image and to collect more information for further processing (MathWorks, 2016). The decorrstretch contrast enhancement procedure, which is suitable for visual interpretation, was adapted to enhance and stretch the color difference in the original picture (used in images with significant band–band correlations) and produces an image with high correlation among its bands (Sankaran et al,.2015). Every pixel of the three channels of the original RGB image was transformed into the color eigenspace, where a new, wider and stretched range of color values was created (Figure 2) and transformed back to the original band (Figure 2). During the process all three bands were stretched through decorrelation into a new 3 × 3-bands correlation matrix and equalized to maintain the band variances. Additionally, a linear contrast stretch is applied to further expand the color range in all three bands equally and to find limits to contrast the stretch in an image because pixel values must be located in the range [0, 255] (MathWorks, 2016).

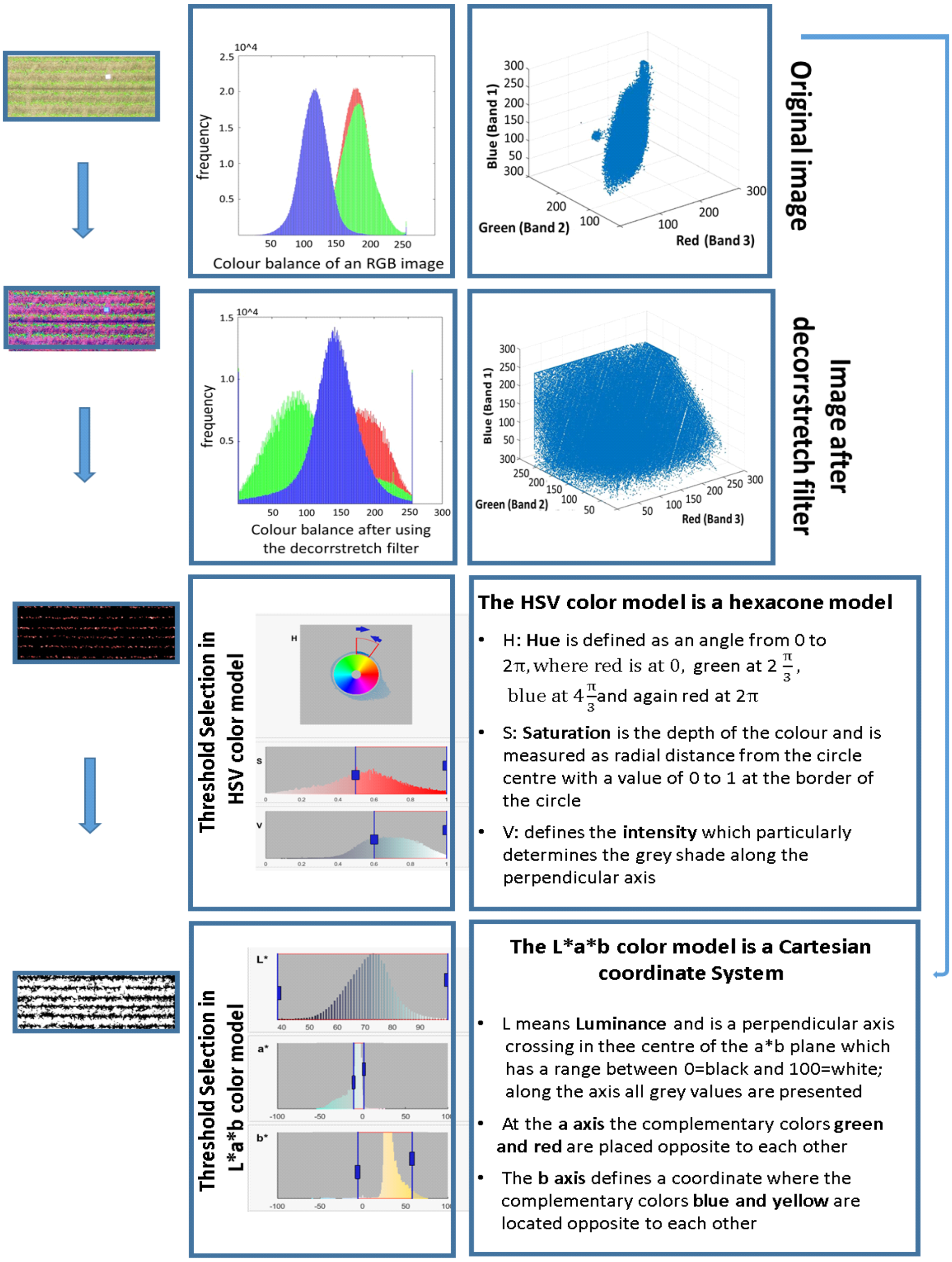

The HSV color model is a hexacone model

- H: **Hue** is defined as an angle from 0 to 2π, where red is at 0, green at $2\frac{\pi}{3}$, blue at $4\frac{\pi}{3}$ and again red at 2π
- S: **Saturation** is the depth of the colour and is measured as radial distance from the circle centre with a value of 0 to 1 at the border of the circle
- V: defines the **intensity** which particularly determines the grey shade along the perpendicular axis

The L*a*b color model is a Cartesian coordinate System

- L means **Luminance** and is a perpendicular axis crossing in thee centre of the a*b plane which has a range between 0=black and 100=white; along the axis all grey values are presented
- At the **a axis** the complementary colors **green and red** are placed opposite to each other
- The **b axis** defines a coordinate where the complementary colors **blue and yellow** are located opposite to each other

Figure 2. Flowchart of the theoretical image processing steps in MATLAB, where the color scatter plot of the original RGB image is first transformed in a new, wider scatter plot with the decorrstrech contrast enhancement procedure and a pixel segmentation of the light green pixel with a threshold selection in the HSV color model (with the three channels: hue, saturation and value) followed by count the plants at the end. Additionally the L*a*b* color model (where L stays for luminosity, and a and b are vectors to create a color space) was used to select green pixels from the original image to detect ground cover.

2.2.3 Creation of the Threshold Value

The HSV color model is a nonlinear transformation of the RGB mode since it separates out the luminance from the color information. There are three channels which describe the HSV color model: the hue (channel 1), the saturation (channel 2) and the intensity values of an image pixel (channel 3) (Sural et al., 2002). The HSV color model is described as a hexacone where the color values are split up in a circle with red at angle 0, green at $2\pi/3$, blue at $4\pi/3$ and red again at 2π. The saturation channel defines the depth or purity of the color and passes from the center of the circle where S = 0% (white) to the edge of the circle where S = 100% (complete saturation). Along the perpendicular axis the hue channel can be measured, between H = 100% and H = 0%. Along the vector S-H the grey scale between black and white is defined. It should be considered that the HSV color model is referenced to the RGB color space and lightness and hue could be confounded—for example two saturated colors could designated as the same lightness but have wide differences in perceived lightness. To express brightness, saturation and hue numerically could show some problems. The HSV color model of the already processed (decorrstrechted) image was used to select the threshold. To define the threshold, the “Color Thresholder App of MATLAB” was used once and channel limits were implemented in the attached script. The thresholds were defined for the three HSV channels and set as follows:

channel 1: channel1Min = 0.115; channel1Max = 0.436;

channel 2: channel2Min = 0.526; channel2Max = 1.000;

channel 3: channel3Min = 0.627; channel3Max = 1.000;

Selected pixels were set at zero after thresholding, and thereafter the objects could be counted.

2.2.4 Creation of the “Open Area”

With the command bwareaopen (BW, p), combined clusters/objects under the defined pixel value p were removed from the binary image and were not counted (MathWorks, 2016).

2.2.5 Creation of the Threshold Value to Complete Total Green Pixel Segmentation/Classification

The L*a*b* model is similar to the HSV model and is defined as a rectangular coordinate system with the two vectors color value and saturation. The L*a*b* color model was used to select green pixels because the distribution of the color area was only in this model sufficient. Euclidean distance of two complementary colors in the L*a*b* model space is directly proportional to the visual similarity of the colors. This can provide simple metrics for a clustering. The clustering can be performed only in the “a”, ”b” space, which represents the color value component. The “L” component in the CIE-Lab space represents the luminosity (Recky and Leberl, 2010). The command used was “I2 = im2double(I)”, which increases the intensity of the original image twofold, rescaling the data if necessary. The second image appears like the original. The command “im2double” converts the images to double precision. Green pixels were set to zero and pixels could then be counted to capture the degree of coverage. Additionally, the percentage of green pixels was calculated (MathWorks, 2016).

2.2.6 Creation of a Table

At the end of the loop, all information collected from each image was saved in a table, including the number of plants, the amount of green pixels and the percentage of green pixels.

2.3 Results and Discussion

Most of the images were sharp, but in some images slight blurriness resulted from the motion of the platform created by wind; however, all images were still useable and did not require different processing for image analysis, and a batch-mode was feasible. Figure 3 indicates the original image, illustrates the segmentation of the green pixels and the ground cover of the plot.

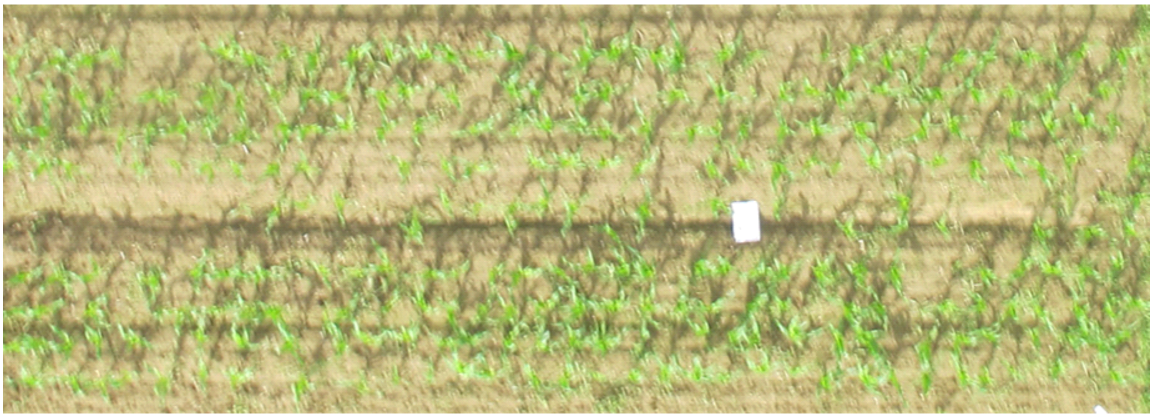

Figure 3. Nadir view of an RGB image acquired with a drone from an equidistantly planted plot.

The correlation of the green pixel percentage and the plants recorded visually in the plots indicated little relationship (R^2 = 0.023), which suggests that no relationship between ground cover and plant number existed. Digital detection of plants was thus not possible. Ground cover obtained from the segmentation of the green pixels could be detected quite well (Figure 4) and indicates the health of the crop. At the BBCH stages 13–15, the ground cover ranged between 76 and 83% green pixels for all cultivars (Figure 5).

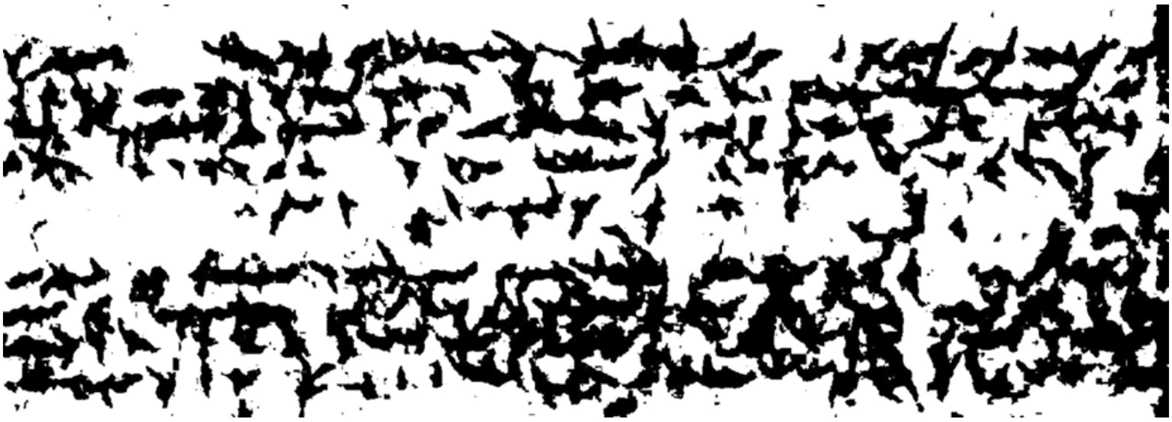

Figure 4. Example of ground cover segmentation of the green area. The black-filled area represents the amount of green pixels in the same plot as shown in Figure 2.

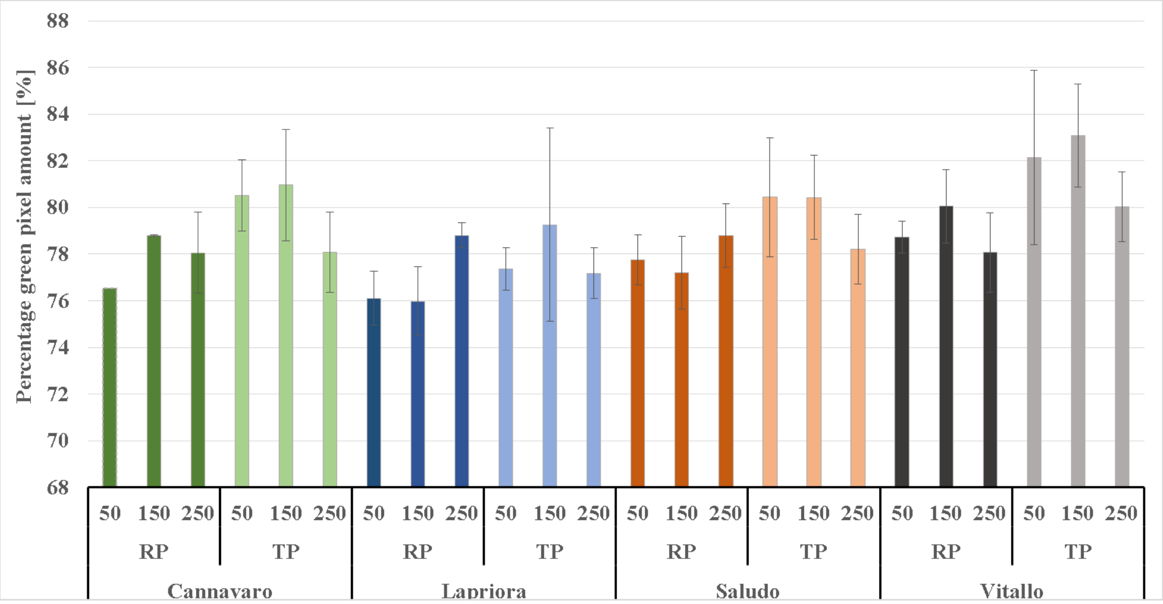

Figure 5. Ground cover of four different cultivars at the BBCH 13–15 development stages. Segmentation of the percentage of green pixel amounts (%) for different nitrogen application levels (50, 150 and 250 kg N ha−1) and different planting systems, row planting.

The equidistantly cropped plots tended to exhibit a higher amount of green pixels, indicating enhanced growth and biomass production. Goetz (2010) and Bullock et al. (1988) also detected a higher ground cover two months after sowing in equidistant plantings compared with row plantings, and a slightly higher grain yield as observed by Hoff and Mederski (1960), in equidistant plantings compared with row plantings. Detection of green pixels to assess ground cover and biomass production is considered an adequate and reliable digital technique to replace destructive methods in line with observations by Kipp et al. (2014). However, ground cover did not reflect the plant number in the plots, as shown by low correlation coefficients. An increased number of plants does not automatically result in increased biomass as shown in Figure 6. This was also shown by Turgut et al. (2005) who reported no significant increase in dry weight at more than 85,000 plants/ha. To record the digital number of plants in each image, the original image was processed with the decorrstretch contrast enhancement procedure in Figure 7.

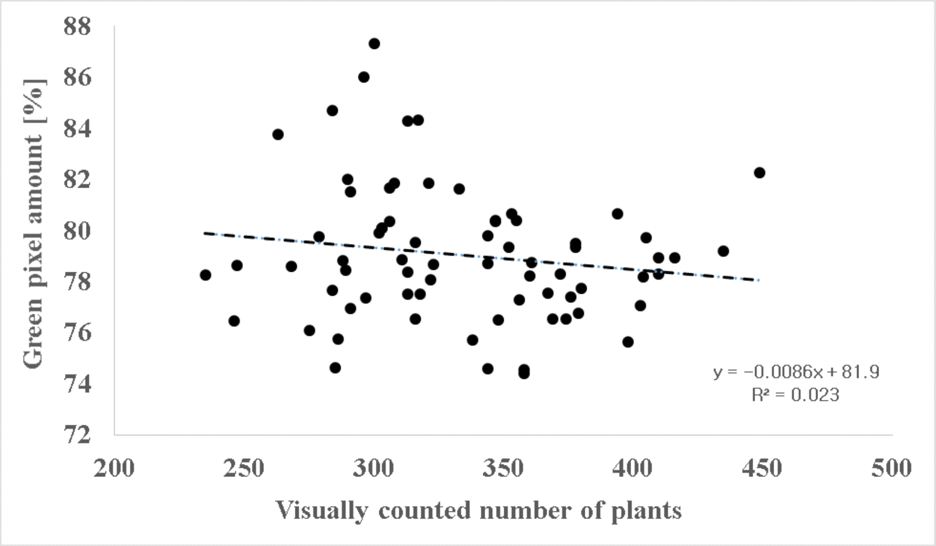

Figure 6. Correlation of the percentage of green pixel amounts (%) indicating the ground cover and the number of plants as counted in the experimental plots.

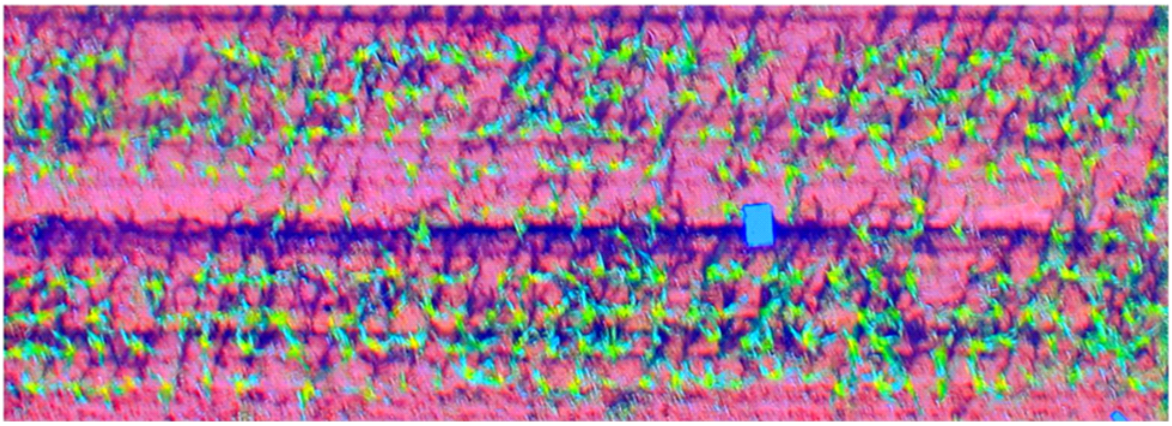

Figure 7. Image after adapting the contrast with a decorrelation of MATLAB. The function highlights elements by enhancing the color differences indicated for plot number 12. Moreover, MATLAB offers various parameters to be set for the decorrelation stretch. We used the following command: P_Contrast = decorrstretch(P, 'Tol', 0.01); where "P" is the image, "Tol" is the linear contrast stretch, which further expands the color range and additionally finds limits to contrast the stretch because pixel values must be located in the range [0, 255] and "0.01" (which defines the level of the contrast stretch).

Using the decorrstretch contrast enhancement procedure command and producing higher color contrasts in the images (Figure 7) enabled the counting of plants digitally with a close correlation. This offers reliable information about plant emergence, which also serves as basis to correctly determine the aerial yield per plant (Figure 8). A threshold that selects only the yellow and light green pixels in the range from 0.115 to 0.436 (V = channel one, HSV model) from the young leaves, which are located in the center of the plants, was used. It is defined with the HSV channels as indicated in the M & M section. Only the light green and yellow pixels were selected to ensure that overlapping plants were not counted as one single plant (Figure 9).

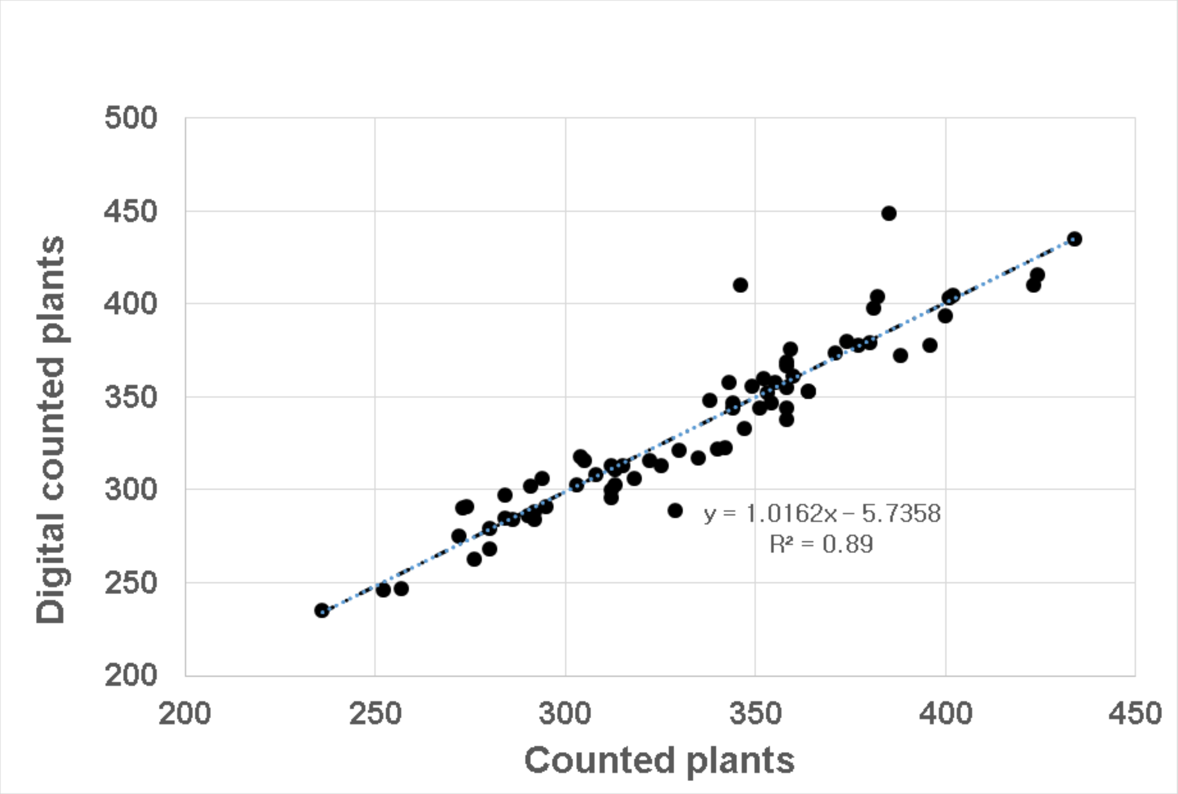

Figure 8. Correlation of visually counted plants serving as reference and the digitally recorded plant number. The ground cover indicated by the green pixel percentage ranged for all cultivars between 76% and 87%. Significant differences in the nitrogen levels were not observed at the investigated growth stages.

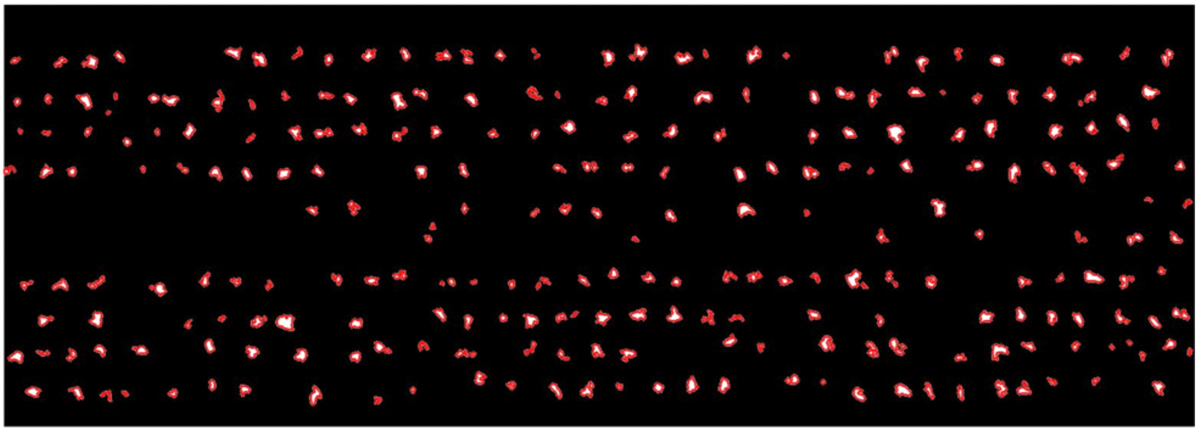

Figure 9. Image after using the Color Thresholder App of MATLAB. Selecting the yellow and lime green pixels of the image with the decorrstretch contrast enhancement procedure as shown for plot number 12.

The pixel size, which minimizes the difference between manually and digitally counted plant numbers, can be defined with the command area opening: bwareaopen (BW, p) as described in the M & M section. The operation removes all clusters in the binary image that are smaller than p (the defined area). This is illustrated in Figure 10a-B for p = 5, resulting in the smallest range of percentage differences between the digitally counted plant number and the visually field-counted plant number serving as a reference. In contrast, p = 10 and p = 3 (Fig.10a A and C) result in a higher spread, shown in box plots in Figure 10a, which is explained by larger differences in actually and digitally counted plants. For p = 3, more clusters were built and counted and the plant number was overestimated in contrast to p = 10, where the plant number was underestimated due to higher cluster extinction. The percentage difference between in situ and image-based counted plants was quite small (Figure 10b). The range of the percentage difference, including outliers, ranged between ±15% for all cultivars. The digital plant-counting model worked best for the cultivar Cannavaro, where the percentage difference was less than ±5% and with only one outlier over −5%. The cultivar Saludo and Vitallo showed the highest percentage differences between digitally and visually counted plants, exceeding slightly the ±5% range. The cultivar Vitallo included two outliers that extended to the −15% limit. Outliers from the cultivars Vitallo and Cannavaro are due to their fast and enhanced development in the seedling stage. Plants became too big and younger light-green leaves could not be separated sufficiently from older dark green leaves. The outlier of Lapriora is due to a higher illumination caused by the sun position since plants in the original image were very bright.

The image processing script can be used at the early leaf development stages within both planting systems, enabling successful segmentation of young plants. A good and clear segmentation depends on the type of object and/or the region.

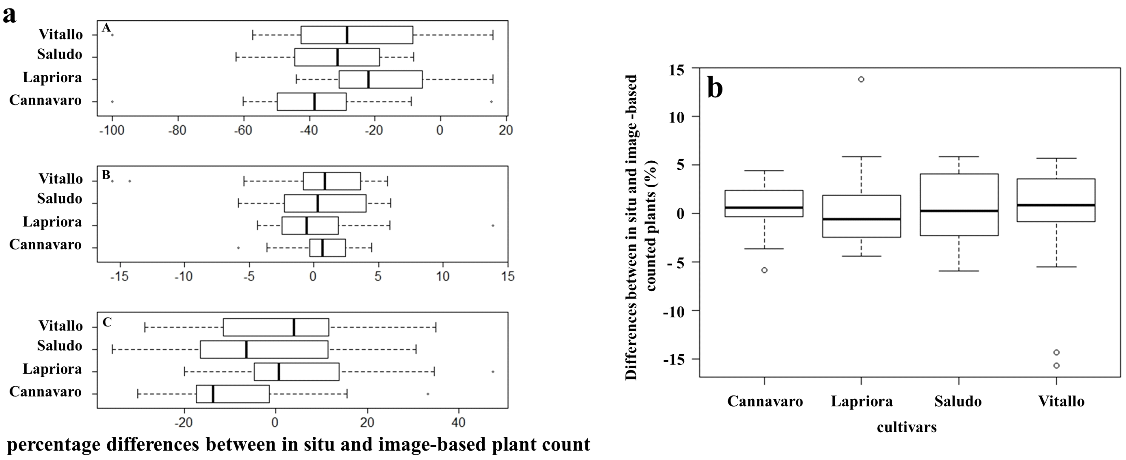

Figure 10. (a) Box plots illustrating the percentage differences between in situ and image-based counted plant numbers for all plots, depending on the command area opening bwareaopen (BW, p), which allows plants to be counted in a standardized way. A has an open area of p = 3; B shows the range for p = 5 and C for p = 10. The open area is defined through the pixel area entering a limit for counted or not counted combined components being below the limit. The percentage difference is calculated as difference (%) = (digitally measured plant number—actually counted plant number)/actually counted plant number x 100. The bold line inside the box shows the median, with the upper and lower lines of the box plot representing the 75th and 25th percentiles. The circles outside the boxes are outliers; (b) Box plots representing the distribution of the percentage differences between the actually and digitally counted plants number from all plots. The bold line inside the box shows the median, with the upper and lower lines of the box plot representing the 75th and 25th percentiles. The circles outside the boxes represent outliers.

A clear differentiation of two neighboring pixels or a pixel group depends on sharp color edges, which define a cluster (Solomon and Breckon, 2011). Therefore, the triangular planting systems could be slightly better assessed than the row planting system because the intra-row distances between the plants were larger (Figure 11). Plants did not overlap too much; thus plant counting for both plant systems was possible (She et al., 2014). The resolution and image sharpness may enhance digital plant counting but is not relevant for the detection of plant numbers on an image. Blurry pictures did not represent significant error in differentiating visually and digitally counted plants.

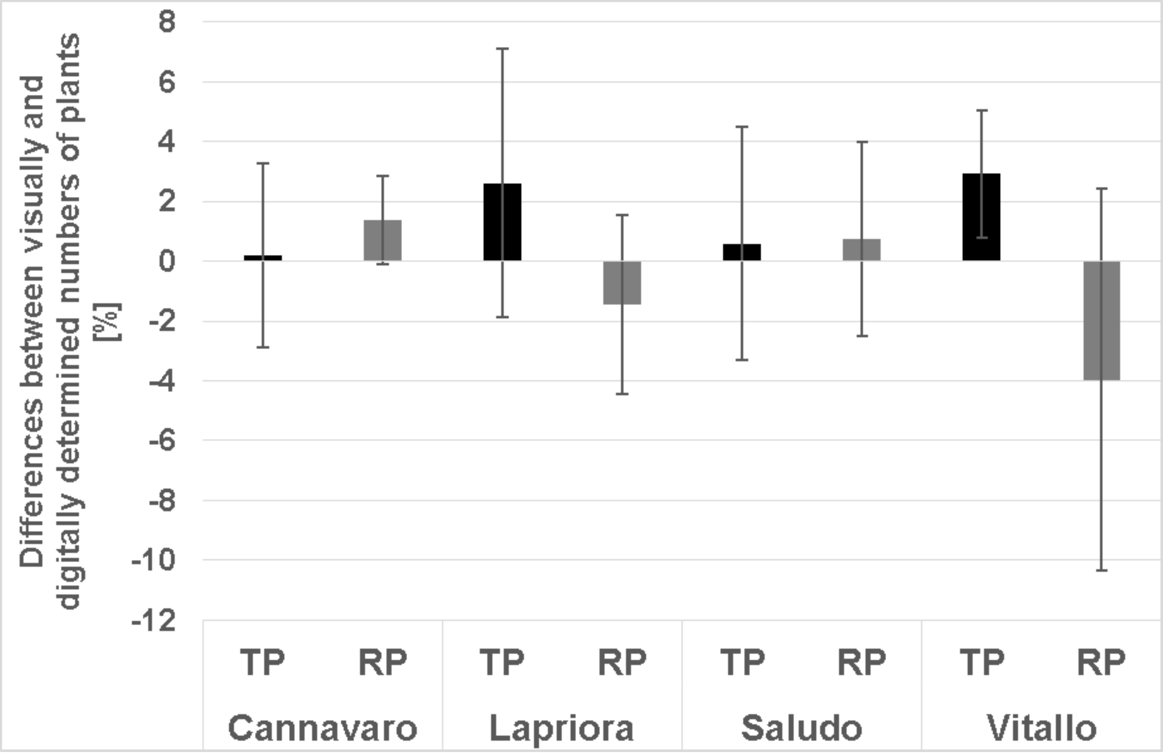

Figure 11. Bar chart illustrating the mean of the percentage differences between visually and digitally determined numbers of four cultivars in triangular planting (TP) and row planting (RP) systems. The percentage difference is calculated as: (digitally measured plant number—visually counted plant number)/visually counted plant number x 100.

Another source of error could result from the presence of weeds; they can have the same spectral reflectance in the visible spectrum. This would result in an increased number of digitally counted plants and a higher difference compared with the visually counted plants. Yang, et al. (2000) used fuzzy logic to differentiate the greenness of wheat plants and weeds, defined by three clusters chosen by their position in the field. Another solution to decrease errors is to increase p in the command bwareaopen (BW, p), which will erase smaller clusters (Figure 10a). The spread of differences between digitally and visually counted plants was less than 10% for all cultivars. There were only three outliers that exceeded the 10% range (Figure 10b). The differences between visually and digitally counted plants can be due to various factors. Too-late imaging of plant growth may not allow for the separation of younger from older leaves. Plants standing too close together, with enhanced overlapping effects, could result in counting fewer plants. This effect appears more often in row planting systems, where there is less regular spacing between plants. A good example of this is the cultivar Vitallo, which exhibited the largest deviation as a result of enhanced plant growth and thus increased overlapping of plants (Figure 11). Additionally, young, pale and green plant leaves could not be adequately distinguished from older leaves using the decorrstrech contrast enhancement procedure when plants were ahead of the plant stage. However, the median values were close to zero for all cultivars, which indicates a close relationship between digitally and visually counted plant numbers. After obtaining images and image processing, a field map can be created illustrating the post-emergence of plants. This allows researchers to judge the success and accuracy of seeding management and to judge the uniformity of the plant distribution, depicting irregularities and gaps between or within the rows caused by soil erosion, soil compaction or soil fertility (Blackmore, 2000).Equally important is the potential yield prediction calculated by the digitally counted plants. For post-emergence breeding purposes, the seed quality could be detected cheaply and quickly. The use of UAVs and image processing in agriculture is a promising tool to answer farm management questions, allowing researchers to optimize management and to support field experimentation in agronomy and breeding activities.

2.4 Conclusion

The use of UAVs provides time- and cost-saving data for further processing and allows for flexible and weather-independent data collection. The results of this study demonstrate the capability of image processing in agricultural fields to detect plant post-emergence. Ground cover detection did not correlate with the plant number on a plot level. It became possible to count plants only by introducing the decorrstretch command from MATLAB. Blurry effects and weed detection in images could lead to miscounting, which can be avoided by manually selecting thresholds and clustering of pixels. Plant number assessment is only possible during a specific window of early leaf development stages, when young, light-green leaves differ from older, dark-green leaves. If overlapping of the plants occurs, green pixel segmentation of young leaves is difficult or no longer feasible. Using an optimized time window enables image analysis in a batch procedure. The use of UAVs and image processing has the potential to optimize farm management and to support field experimentation for agronomic and breeding purposes.

2.5 Acknowledgement

The authors wish to thank Stefan Huber from the Chair of Agricultural Systems Engineering at the Technical University of Munich (TUM) for his technical support and providing the drone. This research was partially supported by the DFG (German Research Foundation) funded project SCHM 1456/6-1. We appreciate the pertinent comments by the reviewers which allowed us to improve the precision of the manuscript.

2.6 References

Abdin, O. A., Zhou, X. M., Cloutier, D., Coulman, D. C., Faris, M. A., and Smith, D. L. (2000). Cover crops and interrow tillage for weed control in short season maize (Zea mays). European Journal of Agronomy 12, 93-102.

Assefa, Y., Vara Prasad, P. V., Carter, P., Hinds, M., Bhalla, G., Schon, R., Jeschke, M., Paszkiewicz, S., and Ciampitti, I. A. (2016). Yield Responses to Planting Density for US Modern Corn Hybrids: A Synthesis-Analysis. Crop Science 56, 2802-2817.

Barmeier, G., and Schmidhalter, U. (2016). High-Throughput Phenotyping of Wheat and Barley Plants Grown in Single or Few Rows in Small Plots Using Active and Passive Spectral Proximal Sensing. Sensors 16, 1860.

Berge, T. W., René cederkvist, H., Aastveit, A. H., and Fykse, H. (2008). Simulating the effects of mapping and spraying resolution and threshold level on accuracy of patch spraying decisions and herbicide use based on mapped weed data. Acta Agriculturae Scandinavica, Section B — Soil & Plant Science 58, 216-229.

Blackmore, S. (2000). The interpretation of trends from multiple yield maps. Computers and Electronics in Agriculture 26, 37-51.

Bullock, D. G., Nielsen, R. L., and Nyquist, W. E. (1988). A Growth Analysis Comparison of Corn Grown in Conventional and Equidistant Plant Spacing. Crop Science 28, 254-258.

Burgos-Artizzu, X. P., Ribeiro, A., Guijarro, M., and Pajares, G. (2011). Real-time image processing for crop/weed discrimination in maize fields. Computers and Electronics in Agriculture 75, 337-346.

Dharani, T.; Aroquiaraj, I.L.; Mageshwari, V. (2016). Diverse image investigation using image metrics for content based image retrieval system. In Proceedings of the 2016 International Conference on Inventive Computation Technologies (ICICT), Tamilnadu, India, 26–27 August; pp. 1–8.

Floreano, D., and Wood, R. J. (2015). Science, technology and the future of small autonomous drones. Nature 521, 460-466.

Gautam, R., and Panigrahi, S. (2007). Leaf nitrogen determination of corn plant using aerial images and artificial neural networks. Canadian Biosystems Engineering 49, 7.

Geesing, D., Diacono, M., and Schmidhalter, U. (2014). Site-specific effects of variable water supply and nitrogen fertilisation on winter wheat. Journal of Plant Nutrition and Soil Science 177, 509-523.

Goetz, S. B. (2010). Produktionsvergleich von Gleichstandsaat und Normalsaat bei Silomais. Pflanze und Technik Landtechnik 65, 107-110.

Hoff, D. J., and Mederski, H. J. (1960). Effect of Equidistant Corn Plant Spacing on Yield. Agronomy Journal 52, 295-297.

Kipp, S., Mistele, B., Baresel, P., and Schmidhalter, U. (2014). High-throughput phenotyping early plant vigour of winter wheat. European Journal of Agronomy 52, 271-278.

Lelong, C. C. D., Burger, P., Jubelin, G., Roux, B., Labbe, S., and Baret, F. (2008). Assessment of unmanned aerial vehicles imagery for quantitative monitoring of wheat crop in small plots. Sensors 8, 3557-3585.

Maddonni, G. A., Chelle, M., Drouet, J. L., and Andrieu, B. (2001a). Light interception of contrasting azimuth canopies under square and rectangular plant spatial distributions: simulations and crop measurements. Field Crops Research 70, 1-13.

Maddonni, G. A., Otegui, M. E., and Cirilo, A. G. (2001b). Plant population density, row spacing and hybrid effects on maize canopy architecture and light attenuation. Field Crops Research 71, 183-193.

Martin, J., Edwards, H. H., Burgess, M. A., Percival, H. F., Fagan, D. E., Gardner, B. E., Ortega-Ortiz, J. G., Ifju, P. G., Evers, B. S., and Rambo, T. J. (2012). Estimating Distribution of Hidden Objects with Drones: From Tennis Balls to Manatees. Plos One 7, doi:10.1371/journal.pone.0038882.

MathWorks (2016). "Image Processing Toolbox™ User's Guide, Matlab," The MathWorks, Inc.

Pena, J. M., Torres-Sanchez, J., de Castro, A. I., Kelly, M., and Lopez-Granados, F. (2013). Weed Mapping in Early-Season Maize Fields Using Object-Based Analysis of Unmanned Aerial Vehicle (UAV) Images. Plos One 8, doi:10.1371/journal.pone.0077151.

Pérez-Ortiz, M., Peña, J. M., Gutiérrez, P. A., Torres-Sánchez, J., Hervás-Martínez, C., and López-Granados, F. (2016). Selecting patterns and features for between- and within- crop-row weed mapping using UAV-imagery. Expert Systems with Applications 47, 85-94.

Rasmussen, J., Ntakos, G., Nielsen, J., Svensgaard, J., Poulsen, R. N., and Christensen, S. (2016). Are vegetation indices derived from consumer-grade cameras mounted on UAVs sufficiently reliable for assessing experimental plots? European Journal of Agronomy 74, 75-92.

Recky, M.; Leberl, F. (2010) Windows detection using k-means in cie-lab color space. In Proceedings of the 2010 20th International Conference on Pattern Recognition (ICPR), Istanbul, Turkey, 23–26 August; pp. 356–359.

Romeo, J., Pajares, G., Montalvo, M., Guerrero, J. M., Guijarro, M., and Ribeiro, A. (2012). Crop Row Detection in Maize Fields Inspired on the Human Visual Perception. Scientific World Journal, doi:10.1100/2012/484390.

Sankaran, S., Khot, L.R., Espinoza, C.Z., Jarolmasjed, S., Sathuvalli, V.R., Vandemark, G.J., Miklas, P.N., Carter, A.H., Pumphrey, M.O., Knowles, N.R.; (2015). Low-altitude, high-resolution aerial imaging systems for row and field crop phenotyping: A review. European Journal of Agronomy, 70, 112–123.

She, T., Ehsani, R., Robbins, J., Leiva, J.N., Owen, J. (2014). Applications of Small UAV Systems for Tree and Nursery Inventory Management. In Proceedings of the 12th International Conference on Precision Agriculture, Sacramento, CA, USA.

Solomon, C., and Breckon, T. (2011). "Fundamentals of Digital Image Processing: A Practical Approach with Examples in Matlab," Wiley, Hoboken, New Jersey, United States.

Sural, S., Gang, Q., and Pramanik, S. (2002). Segmentation and histogram generation using the HSV color space for image retrieval. In "Proceedings. International Conference on Image Processing", Vol. 2, pp. II-589-II-592 vol.2.

Testa, G., Reyneri, A., and Blandino, M. (2016). Maize grain yield enhancement through high plant density cultivation with different inter-row and intra-row spacings. European Journal of Agronomy 72, 28-37.

Tripicchio, P., Satler, M., Dabisias, G., Ruffaldi, E., and Avizzano, C. A. (2015). Towards Smart Farming and Sustainable Agriculture with Drones. 2015 International Conference on Intelligent Environments Ie 2015, 140-143.

Turgut, I., Duman, A., Bilgili, U., and Acikgoz, E. (2005). Alternate Row Spacing and Plant Density Effects on Forage and Dry Matter Yield of Corn Hybrids (*Zea mays* L.). Journal of Agronomy and Crop Science 191, 146-151.

Weiner, J., Andersen, S. B., Wille, W. K. M., Griepentrog, H. W., and Olsen, J. M. (2010). Evolutionary Agroecology: the potential for cooperative, high density, weed-suppressing cereals. Evolutionary Applications 3, 473-479.

Winterhalter, L., Mistele, B., and Schmidhalter, U. (2013). Evaluation of active and passive sensor systems in the field to phenotype maize hybrids with high-throughput. Field Crops Research 154, 236-245.

Yang, C., Prasher, S., Landry, J., Perret, J., and Ramaswamy, H. (2000). Recognition of weeds with image processing and their use with fuzzy logic for precision farming. Canadian Agricultural Engineering 42, 195-200.

Zhang, C., and Kovacs, J. M. (2012). The application of small unmanned aerial systems for precision agriculture: a review. Precision Agriculture 13, 693-712.

3 Biomass accumulation and nitrogen use efficiency differences among cultivars for improved variety selection

3.1 Abstract

Understanding the nitrogen and carbon balance for enhanced nitrogen uptake and nitrogen use efficiency in cropping systems is important for appropriately adjusting agronomic recommendations to minimize unnecessary costs and to avoid nitrate pollution in the hydrosphere. Optimal fertilizer application needs to be adjusted to temporal variations in N uptake throughout the growing season. This study was conducted to examine the performance of different maize (*Zea mays* L.) hybrids in their above-ground biomass accumulation and nitrogen use efficiency (NUE) for a better understanding of the dynamics in the generative stages and therefore to enhance and improve further breeding selection and targets. The motivation for this study was the limited knowledge regarding differences in cultivars' ability to take up nitrogen and to remobilize it from the plant organs leaves and stems into the corns, especially under shortened growing seasons and with different utilization. This should answer the question of whether differences in biomass dry weight and N dynamics among cultivars could be used to improve NUE in breeding and to optimize the targeted use as corn, silage or biogas maize.

Therefore, a three-year field experiment was carried out with different cultivars and their various forms of use as corn, silage, and biogas maize in the years 2014, 2015, and 2016. In 2014, in the first year of the experiment, 12 different cultivars were grown under a given fertilization level of 150 kg N ha^{-1} and assessed regarding the above-ground biomass dry weight (BDW) and nitrogen dynamics. Additionally, the same dynamics of 8 different maize cultivars, grown at low (50 kg N ha^{-1}), medium (150 kg N ha^{-1}) and high (250 kg N ha^{-1}) fertilization levels were monitored in the years 2015 and 2016. Biomass samplings were only taken from the agricultural relevant biomass parameters at anthesis (flowering), silage and grain maturity, and the biomass was separated into leaves, stems and grains. Further, the N content of all organs was determined.

The plant above-ground biomass and nitrogen uptake responded positively to increased N fertilization. At flowering an average biomass production of 35% was observed. Contrary, the percentage biomass production at silage maturity varied among the years with 50% in 2014, 92% in 2015, and with 130% in 2016 which indicated a decrease in total above-ground biomass at grain maturity. The total

above-ground nitrogen uptake achieved 50% at flowering/silking (NU_{silk}) and increased further to 70-90% at silage maturity. From flowering to grain maturity, the leaf biomass dry weight (LDW) decreased from 33% to 11%. The stem biomass dry weight (SDW) also decreased from 61% to 22.3%, whereas the grain biomass dry weight (GDW) increased from 2% to 55%. The nitrogen distribution within the plant was similar to the biomass distribution with a reduction observed in stem nitrogen uptake (SNU) from 36% to 9.7%, a decrease in leaf nitrogen uptake (LNU) from 33% to 15% and an increase in grain N uptake (GNU) from 7% to 72%. Remobilized N (Nrem) was primarily associated with vegetative N and indicated a source driven process, influenced by nitrogen uptake at flowering. Reproductive N (Nrep) ranged between 25-59% between flowering and corn maturity and was not affected by the fertilization level. Also Nrep seemed to be driven by the ear biomass demand and was related to the final corn yield at maturity. The antagonistic relationship between Nrem and Nrep during the reproductive phase is the product of the final corn yield and indicates the complex sink and source driven processes in the plant. The strengths of Nrem and Nrep depend primarily on the stage of ripening among different hybrids and could therefore be important as NUE trait for breeding goals and for an optimized selection of maize cultivars regarding the production goals.

3.2 Introduction

Maize is one of the most important food crops in the world and with rice and wheat provides 30% of the worldwide food calories. Also maize covers a large portion of animal feed and plays an important role in the production of biofuels (Shiferaw et al., 2011). Since the early ‘60s crop production has strongly increased and needs to be further augmented due to the rising world population and the increasing demand for food and fodder. One of the reasons for higher yield was the utilization of industrially produced nitrogen fertilizers. But the use of nitrogen fertilizers not only increases yield but also influences the economic performance and the environment. Increasing nitrogen fertilization can lead to higher N losses and negatively impact the soil, water and air quality. Another aspect to improve food production effectively is the limitation of cereal production expansion by the preservation of remnant ecosystems (Lambin and Meyfroidt, 2011) and by losses of arable land towards urban land use (Duvick and Cassman, 1999). Also changing weather conditions and increasing extreme weather events could lead to drastic reductions in yield. In order to maintain increasing yield productivity per unit, arable land needs to be maximized sustainably (Ciampitti and Vyn, 2014) which can only partly be achieved by higher inputs. Yield losses due to extreme weather events can at least partly be decreased by choosing the optimal temporally, spatially and quantitatively optimized N utilization and improved variety selection (Ciampitti and Vyn, 2011).

The interaction of climate and field management causes year to year changes in yield and nitrogen requirement (Chen et al., 2015). Based on these concerns, the interaction between genome, environment and management (G*E*M) to improve productivity has to be fully explored because the complexity of these three factors is still not sufficiently understood (Ciampitti and Vyn, 2012). Therefore a three-year study was conducted to examine the performance of different maize hybrids in their biomass accumulation and NUE. The conscious choice of a broad range of cultivars with different targets in their usage and maturity stage was done, to enhance the chance of divergent carbon and nitrogen dynamics and to understand the process of optimal yield performance.

As maize could assimilate a high amount of nitrogen without influencing yield profitably, a targeted, optimized nitrogen application helps to improve the effective use of nitrogen. This also requires a better understanding of the remobilized nitrogen from vegetative organs and post flowering nitrogen uptake to maize kernel N or to total aboveground N. Differences in morphological and physiological properties should be explained in order to explain the reproductive and remobilized N within the genotypes and thus achieve an increased selection. Both nitrogen allocations – reproductive nitrogen (Nrep), taken up by the plants after flowering and remobilized nitrogen (Nrem) translocated from vegetative plant organs (leaves and stem) to the reproductive organ corn, are the result of many interactions and therefore relevant processes in relation to the final yield (Ciampitti and Vyn, 2013a).

Two methods are well established to measure C and N allocation and translocation processes such as remobilization and post flowering uptake. Firstly, differences between biomass at different phenological plant growth stages are used to estimate the nitrogen and carbon remobilization capacity in the above-ground plant parameters (Pommel et al., 2006; Rajcan and Tollenaar, 1999a, b; Uhart and Andrade, 1995). This method does not consider any biomass losses during harvest and sample preparation and is therefore only an approach on C and N allocation. Moreover, the root, which is an essential plant parameter, is not included in this calculation. This established method therefore only provides information about the plant parameters that are agronomical relevant and important for breeders and farmers.

The N uptake into the root as well as the remobilization from the root into other above-ground plant compartments are regarded as equal in this model and will be defined as reproductive N (Nrep).

Secondly, stable isotopes are used to trace C and N allocation and their recovery into different plant tissues and metabolites (Blessing et al., 2015; Gallais et al., 2007; Ma and Dwyer, 1998). These metabolism studies conducted with isotopes are more precise but it is difficult to establish a closed system under field conditions, which avoids losses. For example heavy rainfall can wash out a nitrogen tag applied in the form of ^{15}N enriched nitrate or ammonium, which heavily affects recovery levels in the plants. Therefore in this study, we concentrated on the first mentioned method which considers only the C and N accumulation and translocations within the above-ground plant parameters such as leaves, stem and corn.

A strong dependency of nitrogen and carbon allocation was already previously demonstrated (Ciampitti and Vyn, 2011). Chen et al. (2014) described a strong relationship between grain dry weight with biomass accumulation after silking. Acciaresi et al. (2014) explained that hybrids did not differ in their post-silking dry matter accumulation and additionally no differences in grain yield between earlier and late-senescing hybrids were discovered. The only significant differences were found in the lower kernel N concentration of late senescing cultivars. Regarding nitrogen allocation Chen et al. (2014) also found that 60-85% nitrogen, derived from nitrogen remobilization from silking to maturity can be found in the corn which explains the high importance of nitrogen remobilization within the plants. In the last years a steady increase in the contribution of post flowering nitrogen uptake to total nitrogen uptake of maize plants was achieved in new breeding lines compared to old era hybrids together with an increase in yield, thus post flowering nitrogen uptake – also called reproductive N - plays an elementary role in the nitrogen and carbon cycle of maize. Based on the following literature, the reproductive N is defined as the sum of remobilized N from the roots and the nitrogen which was taken up from the plants after flowering. In the time period before 1999, the percentage of vegetative nitrogen uptake (NUsilk) at flowering was, on average, 75% of the total corn N (Ciampitti and Vyn, 2012; Ciampitti and Vyn, 2013a), whereas after 1990 in the “new era” NUsilk only reached an average of 63%. In contrast Dharmakeerthi et al. (2006) found NUsilk of only 46% - but in general the total nitrogen uptake was slightly higher (Woli et al., 2016) for “new era” cultivars which implies a higher post silking nitrogen uptake. Moreover, increasing nitrogen fertilization influences NUsilk (Ciampitti et al., 2013c). Corn is the major N sink during the generative phase. About 60% of nitrogen uptake during the entire generative phase was shown to contribute to corn N (Ciampitti et al., 2013b; Ciampitti and Vyn, 2012; DeBruin et al., 2013).

But how remobilized and reproductive N influence the nitrogen use efficiency (NUE) has to be investigated more intensively. On one hand, a more efficient use of nitrogen helps to decrease production costs, thus implying economic benefits, and on the other hand it reduces the impact of agriculture on the environment as nitrate leaching to the hydrosphere is prevented (Moll et al., 1982). Nitrogen use efficiency plays an important role and therefore various definitions and interpretations exist. According to Moll et al. (1982) NUE is the product of nitrogen utilization efficiency (NUtE) which defines the ratio between nitrogen corn yield and the nitrogen bound in the aboveground biomass and the nitrogen uptake efficiency (NUpfE) which is the ratio of nitrogen uptake to the available nitrogen. In the formula of the NUtE the nitrogen harvest index (NHI) is an elementary factor which, besides the nitrogen contained in the grain (yield), also describes the quality of the corn (Moll et al., 1982). By increasing nitrogen remobilization, NUE is increased which is accompanied by a lower N concentration in the grain and a decreased NHI (Ciampitti and Vyn, 2012). Thus, nitrogen allocation is a very complex system including a variety of different processes, which work together and affect the yield stability of maize cultivars.

In this chapter, the nitrogen and carbon allocation of cultivars representing different maturity grades is addressed. There is also a focus on the factors which are influencing NUE and how breeders could use this information for further breeding, regarding effective N utilization. The following questions should be answered: Are the parameters remobilized nitrogen, reproductive nitrogen, nitrogen uptake, N content in above-ground plant organs (leaves, stem and corn) and carbon accumulation related to final yield - especially grain yield and how do they differ among cultivars? Is the interaction between remobilized N and reproductive N more driven by genetic traits of the cultivars or influenced by abiotic environmental impacts (e.g. drought stress and nitrogen fertilization limitation)? Lastly, the study of biomass and nitrogen partitioning of all plant organs of different cultivars with different maturity grades and different usage goals was evaluated to answer the question if cultivars differ in their C and N allocation and how these traits could be used to improve NUE in further breeding purposes. The NUE could be improved through higher NUpfE at lower nitrogen supply or through higher NUtE at higher nitrogen supply which may result in an increased NHI, lower grain N concentration, and therefore to lower grain quality. Additionally this information could be used for future field management in regard to targeted cultivar selection and their adaptation to environmental changes.

3.3 Material and Methods

In south Bavaria, over a period of three years (2014 to 2016), maize hybrids were planted on different field sites representing different soil conditions, at the research station from the Chair of Plant Nutrition belonging to the Technical University of Munich in Dürnast (48°24'15.6"N 11°41'34.0"E) (Fig.1). All experiments were conducted in a hilly tertiary landscape, with loess as the predominant soil material. Dominant soil types in this area are fine-silty Dystric Eutrochrept and fine-loamy Typic Udifluvent (Heil and Schmidhalter, 2017). In the first year of the experiment in 2014 the distribution of nitrogen and carbon content of hybrids with different maturity classes (Table 1) receiving 150 kg N ha^{-1} was assessed, while in the subsequent two years, there was an additional focus on the nitrogen use efficiency (NUE) applying fertilizer at 50, 150 and 250 kg N ha^{-1}. In all 3 years the experiments were organized in complete randomized block designs.

In 2014, 15 hybrids (n=4) were sown on 24 April on a loamy Cambisol soil at the field site Dürnast 48°40'N 11°70'E with 150 kg N ha^{-1} fertilizer applied at sowing. A combination of Cardo Gold and Callisto was applied at the ratio of 3.5 L and 0.5 L ha$^{- 1}$ between May and June to prevent weed infestation.

In 2015 and 2016, 8 different hybrids (Table 1) (n=4) were grown at three different fertilization levels of 50, 150 and 250 kg N ha^{-1} broadcast at sowing at the field sites Thalhausen 48°43'N 11°66'E and Allershausen 48°43'N 11°68', respectively. Sowing was done on April 27 and May 5 in 2015 and 2016, respectively. In 2015, weed management was done with Clio Super at 1.5 L ha^{-1} and Zeagran Ultimate at 1.5 L ha$^{- 1}$, while in 2016 Round Up Power Flex with 3 L ha^{-1} and Gardo Gold and Callisto at 3.75 L ha^{-1} were used.

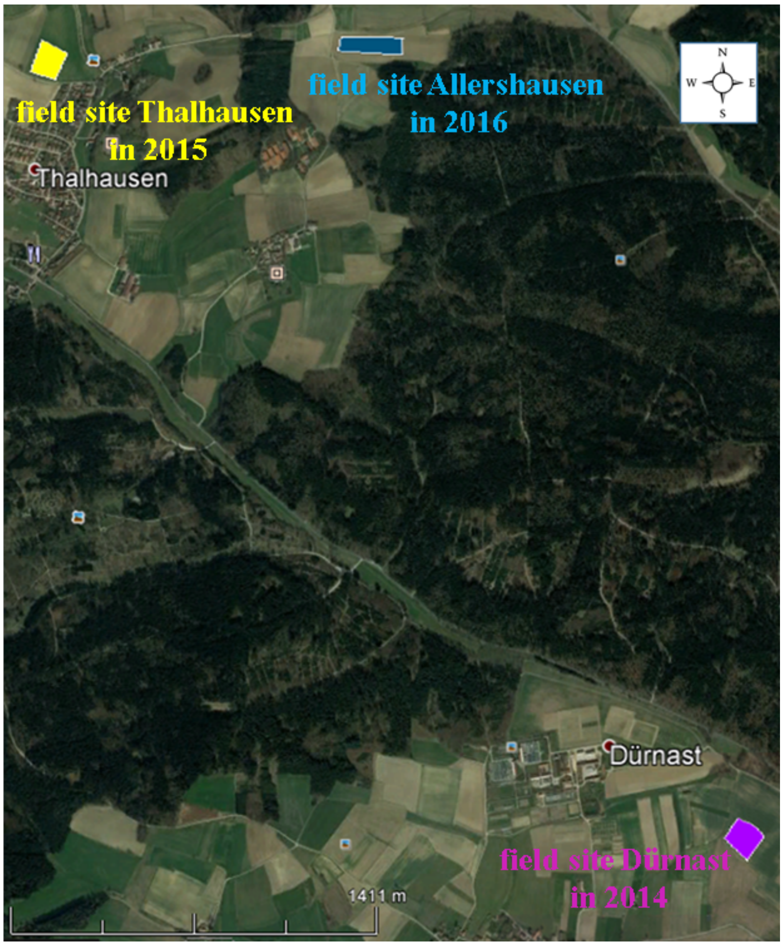

Fig. 1: Overview of the field experimental locations Dürnast (pink), Thalhausen (yellow), and Allershausen (blue) marked with colored rectangles from 2014 to 2016 in Bavaria close to Freising. Image taken from Google Earth (Google Inc., Mountain View, USA).

Table1: Usage, maturity class and FAO number of the maize cultivars used.

Cultivar	**Usage**	**Maturity class**	**FAO number**	**Year**
Lapriora	corn	very early	K190	2014, 2015, 2016
P 8400	corn	middle early	K 240	2014
Severus	corn, silage	early	S190, K190	2015, 2016
Saludo	corn, silage	early	S210, K210	2014, 2015, 2016
Amagrano	corn, silage	early	S210, K210	2014
Fabregas	corn, silage	early	S210, K220	2014
LG 30222	corn, silage	early	S210, K220	2014
P 8105	corn, silage	early	S180, K 220	2015, 2016
Amadeo	corn, silage	early, middle	S220, K230	2014
Colisee	corn, silage	early, middle	S220, K220	2014
Ricardinio	corn, silage	early, middle	S230, K220	2014
KWS 9361	corn, silage	middle, late	S290, K280	2014, 2015, 2016
Grosso	corn, silage	middle, late	S250, K250	2014
LG 32.58	corn, silage	middle, late	S250, K250	2014
Ronaldinio	silage	middle, late	S240	2014
Barros	silage	middle, late	S250	2014, 2015, 2016
Torres	corn, silage	late	S250, K260	2014
Vitallo	silage	late	S270	2015, 2016
Cannavaro	biogas	very late	S 310	2015, 2016

3.3.1 Sampling and harvest procedures in the years 2014 to 2016

Biomass samplings were done three times during the growing season at flowering, silage maturity and grain maturity and plants were separated into leaves, stem and corn. In the year 2014 the sampling was done in 7 m long rows alternately from the front and back of the plots, while the first and last border rows were omitted to avoid boundary effects. In the years 2015 and 2016, 10 plants were removed from the inner rows and were randomly sampled to avoid boundary effects.

The sampling times were synchronized with the flowering and maturity dates of the individual maize hybrids. Differences in the climatic conditions among the experimental years were recorded. The fresh weight of the whole crop and of each plant organ was measured immediately after harvest. After drying the samples for about one week at 60 °C, the dry matter was determined to determine as well the water content. Additionally, the corn number was counted with the grain counter Cantador (Pfeuffer GmbH, Kitzingen, Germany) and the corn weight was determined. All samples were ground using a Brabender rotor mill (Brabender® GmbH & Co.KG, Duisburg, Germany) with a 1 mm sieve. The nitrogen content was determined by near infrared spectroscopy (Bruker Vector 22/N, Bruker, Billerica, MA, USA). Organ-specific NIRS-models were developed by using the Unscrambler software (CAMO Software AS, Oslo, Norway). For establishing the calibration 1/3 of the samples were chemically analyzed by isotope ratio mass spectrometry (ANCA SL 20-20 preparation unit, Europe Scientific, Crewe, UK).

Visual data inspection indicated that the whole data of 2014 to 2016 were not normally distributed and normal distribution could not be achieved by transformation. Based on this observation, data separate from each year were evaluated using a linear mixed model calculated as an ANOVA with R (R Core Team, Boston, MA 02210, USA).

3.3.2 Calculations

Nitrogen and carbon remobilization within the above-ground biomass

Total nitrogen and carbon remobilization was calculated as follows:

$$N_{rem} = TNU_{silk} - TNU_{stover} \tag{1}$$

$$C_{rem} = BDW_{vegetative} - BDW_{stover} \tag{2}$$

Where TNU_{silk} or $BDW_{vegetative}$ defines the whole plant at silk emergence, and TNU and BDW of the stover is the total above-ground biomass or nitrogen uptake of the whole plant except the grain at maturity (Ciampitti and Vyn, 2013a). Nitrogen and carbon remobilization was also calculated for the plant organs, leaves (LNrem, LCrem) and stem (SNrem, SCrem).

The percentage share was calculated referring to vegetative TNU and BDW as 100%.

Post flowering nitrogen uptake

Nitrogen and carbon reproduction (Nrep, Crep) was calculated after Ciampitti and Vyn (2013a) as follows

$$N_{rep} = TNU_{grain\ maturity} - TNU_{silk\ emergency} \tag{3}$$

$$C_{rep} = BDW_{grain\ maturity} - BDW_{silk\ emergency} \tag{4}$$

where the percentage share of Nrep is calculated from the total nitrogen uptake of the above-ground biomass (TNU) at grain maturity as 100%.

3.4 Results

3.4.1 Climatic conditions

Annual rainfall was highest in the year 2016 (809 mm) and lowest in 2015 (642 mm). However, the distribution of the rainfall within the growing season varied over the years. In 2014, precipitation exceeded the average during May (96 mm), but hot peaks during June caused drought stress, despite existing water reserves. August and September were relatively wet, followed by a sunny October, resulting in high maize yield. In 2015, rainfall in April and May favorably enhanced maize growth till June. After some heavy rain fall in June a record heat wave caused drought stress for the rest of the growing season. This led to earlier and rapid maturity. In 2016, rainfall was relatively evenly distributed throughout the growing season. A sunny autumn allowed extended maturity, leading to above average maize yield (Fig. 2).

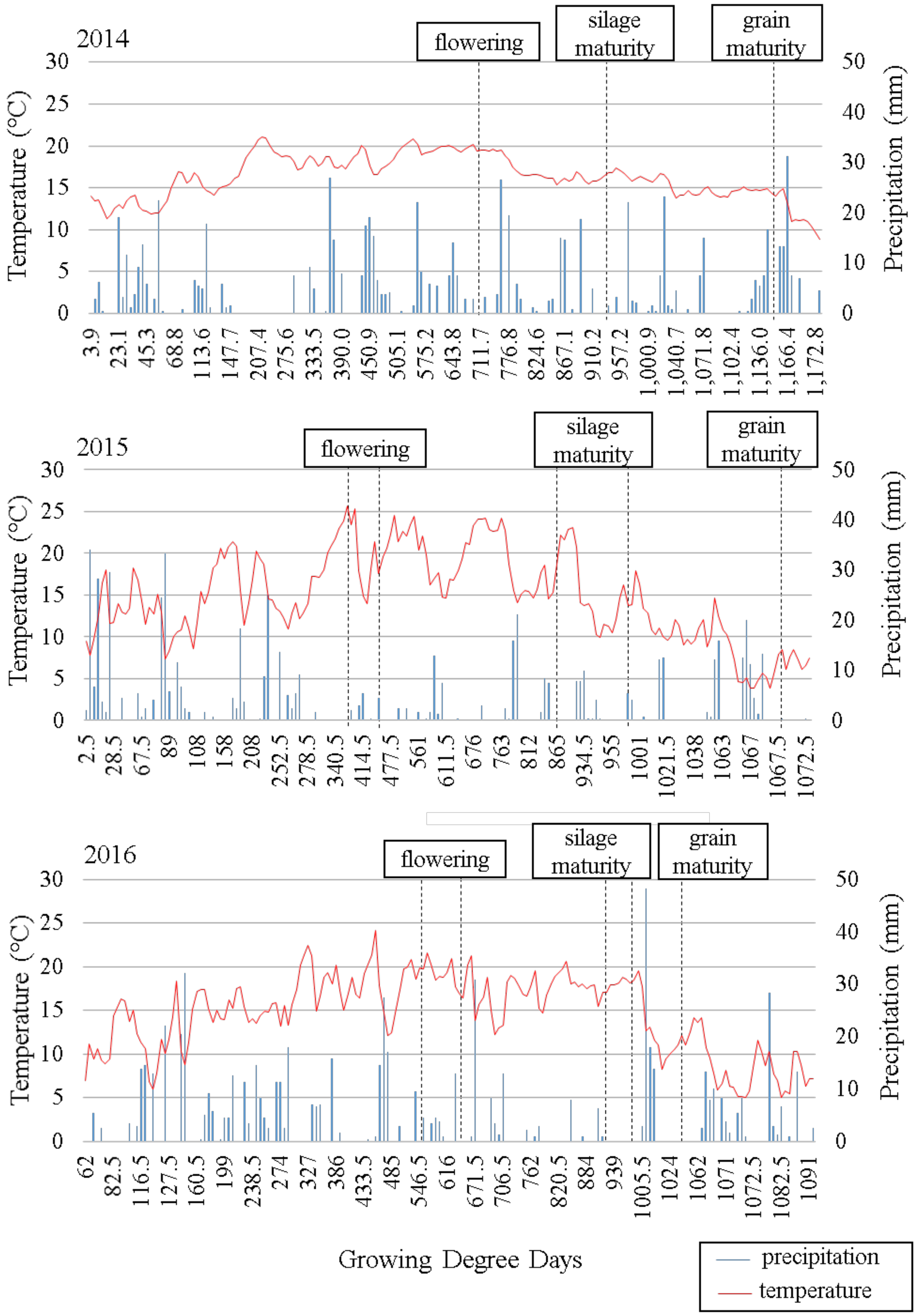

Fig.2: Daily mean temperature and precipitation at Freising in 2014-2016. Dashed lines indicate flowering, silage and grain maturity. Growing Degree Days with baseline 10°C is recorded on the X-axis.

3.4.2 Biomass and yield parameters

Biomass accumulation (BA) across the growing season measured at flowering, silage and grain maturity varied over the years. Generally an increase in total above-ground biomass plant dry weight (BDW) from flowering to grain maturity was observed in all years. Above-ground biomass dry weight at flowering yield was 7.2 t ha^{-1} in 2014 7.1 t ha^{-1} in 2015 and 9.2 t ha^{-1} in 2016. The maximum final yield was achieved at silage maturity with 34.3 t ha^{-1} in 2016 followed however by a decreased yield of 26 t ha^{-1} at grain maturity. In contrast until grain maturity, a steady increase in yield was observed in 2015 and 2014 with a moderate final yield of 18.5 t ha^{-1} in 2015 and increased yield amounting to 23 t ha^{-1} in 2014 (Table 2).

Table 2: Average above-ground biomass plant dry weight (t ha^{-1}) with standard deviation of maize hybrids at flowering, silage and grain maturity of all cultivars and given nitrogen fertilization levels.

year	**Flowering (t ha^{-1})**			**Silage maturity (t ha^{-1})**			**Grain maturity (t ha^{-1})**		
	50 $\left(\frac{\text{kg N}}{\text{ha}}\right)$	150 $\left(\frac{\text{kg N}}{\text{ha}}\right)$	250 $\left(\frac{\text{kg N}}{\text{ha}}\right)$	50 $\left(\frac{\text{kg N}}{\text{ha}}\right)$	150 $\left(\frac{\text{kg N}}{\text{ha}}\right)$	250 $\left(\frac{\text{kg N}}{\text{ha}}\right)$	50 $\left(\frac{\text{kg N}}{\text{ha}}\right)$	150 $\left(\frac{\text{kg N}}{\text{ha}}\right)$	250 $\left(\frac{\text{kg N}}{\text{ha}}\right)$
2014		7.2 ± 0.8			14.3 ± 1.3			23.7 ± 2.5	
2015	6.4 ± 1.3	7.1± 1.7	7.3 ± 2.1	15.5 ± 2.5	16.8 ± 2.8	18 ± 3.9	16.6 ± 3.7	18.5 ± 2.9	19.7 ± 4.2
2016	8.4 ± 1.8	9.2 ± 2.2	9.8 ± 2	30.9 ± 7.8	34.3 ± 8.3	38 ± 10.9	22.8 ± 4.2	26 ± 5.5	28.1 ± 4.6

In 2014 there were no significant differences in BDW observed among cultivars at flowering, silage and grain maturity (Table 3). Only at grain maturity, the cultivar Saludo showed a significantly increased leaf dry weight (LDW) ($p < 0.001$) compared to the other cultivars (Fig. 3).

In 2015 and 2016, the late maturing cultivars Cannavaro, Barros and Vitallo showed significantly higher BDW at flowering compared to the early maturing cultivars Lapriora, Severus and P8105 (Table 3, Figs. 4, 5). During silage maturity and grain maturity significant differences in biomass accumulation between cultivars were only observed in 2016 (Table 3).

Additionally, nitrogen fertilization exerted a significant effect on BDW at flowering, silage and grain maturity in 2015 (Fig. 4, Tables 2 and 3). During flowering BDW increases of only 0.9 t ha $^{-1}$ could be observed between the lowest and the highest nitrogen fertilization level, whereas BDW differed more at silage maturity with a difference of 2.8 t ha^{-1} and 3.1 t ha^{-1} at grain maturity between the lowest and highest nitrogen fertilization level. Nitrogen fertilization influenced significantly leaf biomass dry weight (LDW) and significant differences were also observed among cultivars with higher LDW values for the late maturing cultivars Cannavaro with the highest LDW (3.2 t ha^{-1}), Barros (2.7 t ha^{-1}) and Vitallo (2.5 t ha^{-1}) compared to early maturing cultivars Lapriora with the lowest LDW (1.6 t ha $^{-1}$), Saludo (1.9 t ha^{-1}), and Severus (2.1 t ha^{-1}). A significant effect on LDW regarding the fertilization level could also be observed at all sampling times ($p < 0.001$) with higher values being found for late maturing cultivars compared to early maturing cultivars, contrasting to corn yield with significantly increased yield for early maturing cultivars ($p < 0.001$) being observed at flowering (Fig. 4).

The fertilization level showed only significant effects on stem biomass dry weight (SDW) at grain maturity ($p < 0.001$), while significant differences among cultivars were observed at flowering ($p < 0.001$) and grain maturity ($p < 0.001$) where Vitallo and Cannavaro reached the highest values and Lapriora and Saludo reached lower values.

The fertilization level exerted a significant effect on grain yield (GDW) at silage and grain maturity ($p < 0.001$) and cultivars differed significantly in the corn yield at all sampling times. Early maturing cultivars such as Lapriora (10 t ha^{-1}) and Severus (9.8 t ha^{-1}) performed better compared to late maturing cultivars such as KWS 9361 (9 t ha^{-1}) and Vitallo (7.7 t ha^{-1}). In contrast, Cannavaro, a very late maturing cultivar, and the cultivar Barros, with stay green traits, reached GDW values of 9 t ha^{-1} and were similar to the early maturing cultivars. An interaction between the fertilization level and cultivars could be observed for all plant organs (Table 3, Fig. 4). Especially the interaction between nitrogen fertilization and cultivars exerted a significant effect on GDW where the cultivar Barros performed better at enhanced N fertilization compared to the cultivar Saludo with indicating the highest final kernel yield at the lowest N fertilization dose.

In contrast, differences in above-ground biomass between nitrogen fertilization levels were only present at silage and grain maturity, but not at flowering in 2016 (Fig. 5, Table 3). Nitrogen fertilization caused a significant effect on LDW at flowering ($p < 0.001$) and grain maturity ($p < 0.001$) where late maturing cultivars achieved higher LDW values compared to early maturing cultivars ($p <0.001$). The fertilization levels showed no significant effect on SDW but late maturing cultivars reached significantly higher SDW compared to early maturing cultivars ($p < 0.001$) at grain maturity. Additionally nitrogen fertilization increased GDW at silage ($p = 0.04$) and grain maturity ($p = 0.03$) but not at flowering. Also significant differences among cultivars could be distinguished at flowering, silage and grain maturity ($p<0.001$) where the cultivar Cannavaro always performed best and the cultivars Severus, Lapriora and P8105 were ranking lowest. In contrast to 2015, no interaction between cultivars and the fertilization level was observed for organs and all sampling times (Table 3, Fig. 5).

Table 3: Statistical overview of the plant parameters total above ground biomass dry weight (BDW) (t ha^{-1}) and total nitrogen uptake (TNU) (kg ha^{-1}) at flowering (H1), silage maturity (H2) and grain maturity (H3), nitrogen and carbon remobilization (Nrem, Crem) of the organs leaves (LNrem, LCrem) and stems (SNrem, SCrem) and nitrogen reproduction (Nrep). Statistically significant differences ($P<0.05$) are indicated in bold.

	BDW H1 (t ha^{-1})	BDW H2 (t ha^{-1})	BDW H3 (t ha^{-1})	TNU H1 $\left(\frac{kg}{ha}\right)$	TNU H2 $\left(\frac{kg}{ha}\right)$	TNU H3 $\left(\frac{kg}{ha}\right)$	LNrem $\left(\frac{kg}{ha}\right)$	SNrem $\left(\frac{kg}{ha}\right)$	TNrem $\left(\frac{kg}{ha}\right)$	Nrep. $\left(\frac{kg}{ha}\right)$	LCrem (t ha^{-1})	SCrem (t ha^{-1})	Kernel yield (t ha^{-1})
2014													
cultivars	0.403	0.354	0.197	0.088	**0.024**	**0.047**	**0.003**	**0.042**	**0.003**	**0.004**	0.259	0.226	0.5
2015													
N	**0.007**	**0.003**	**0.002**	**<0.001**	**<0.001**	**<0.001**	0.96	0.74	0.40	0.044	0.47	0.7	**<0.001**
cultivars	**<0.001**	0.208	0.069	**<0.001**	**0.04**	0.194	**0.001**	0.122	**<0.001**	**<0.001**	0.125	**0.004**	**0.01**
cultivars x N	0.089	**0.021**	0.129	**0.02**	**0.036**	0.252	0.84	0.682	0.756	0.808	0.754	0.792	0.32
2016													
N	0.135	**0.02**	**<0.001**	**<0.001**	**0.01**	**<0.001**	0.351	**0.021**	**<0.001**	0.174	0.779	0.963	**<0.001**
cultivars	**<0.001**	**0.001**	**<0.001**	**<0.001**	**0.047**	0.240	**<0.001**	**0.002**	0.180	0.277	**<0.001**	0.104	**0.015**
cultivars x N	0.617	0.427	0.297	0.057	0.620	0.520	0.359	0.186	0.196	0.576	0.051	0.786	0.183

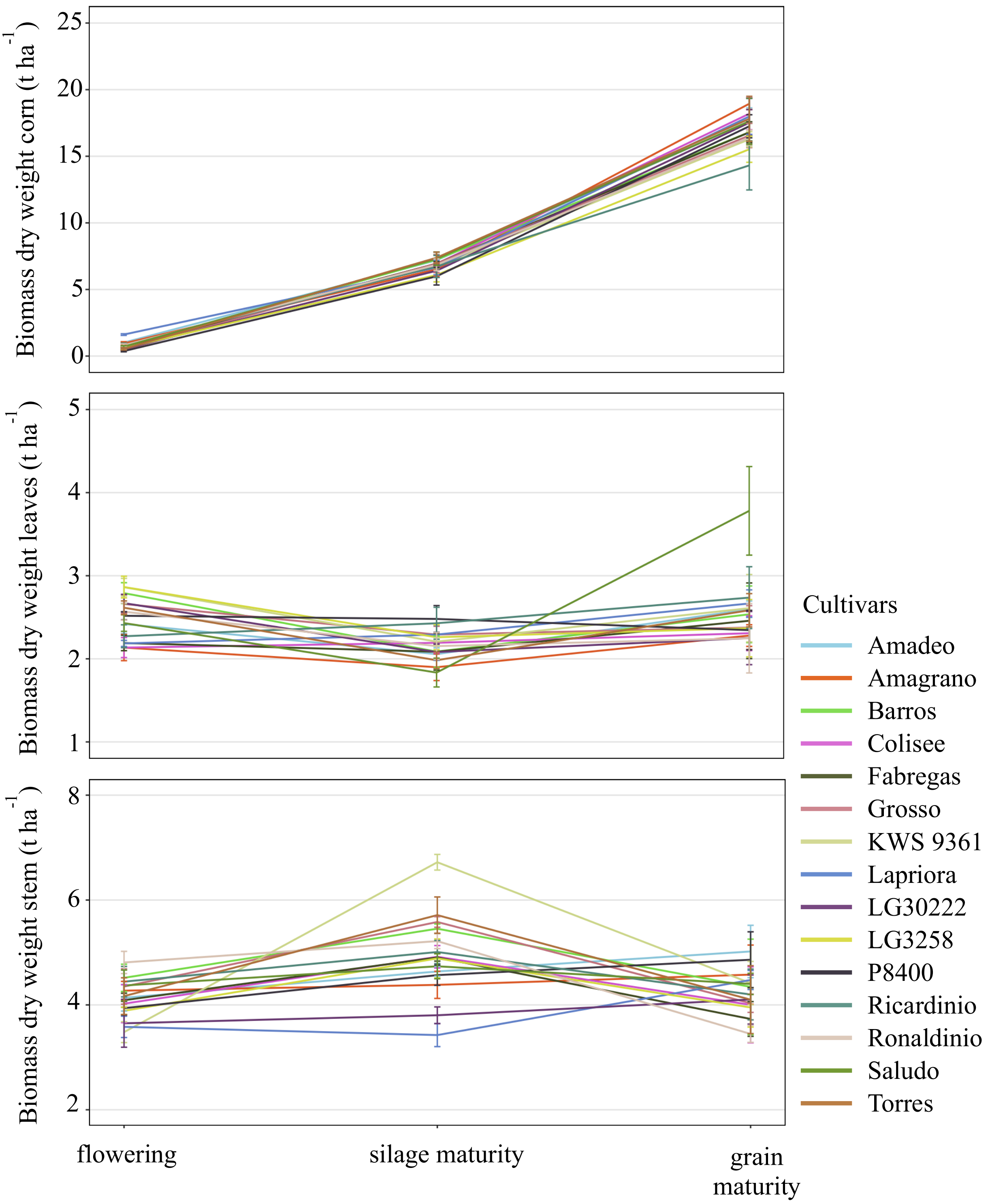

Fig. 3: Above-ground biomass of corn, leaves and stem (t ha^{-1}) at flowering, silage, and grain maturity of 15 cultivars at 150 kg N ha^{-1} in 2014. Standard deviations are indicated as error bars.

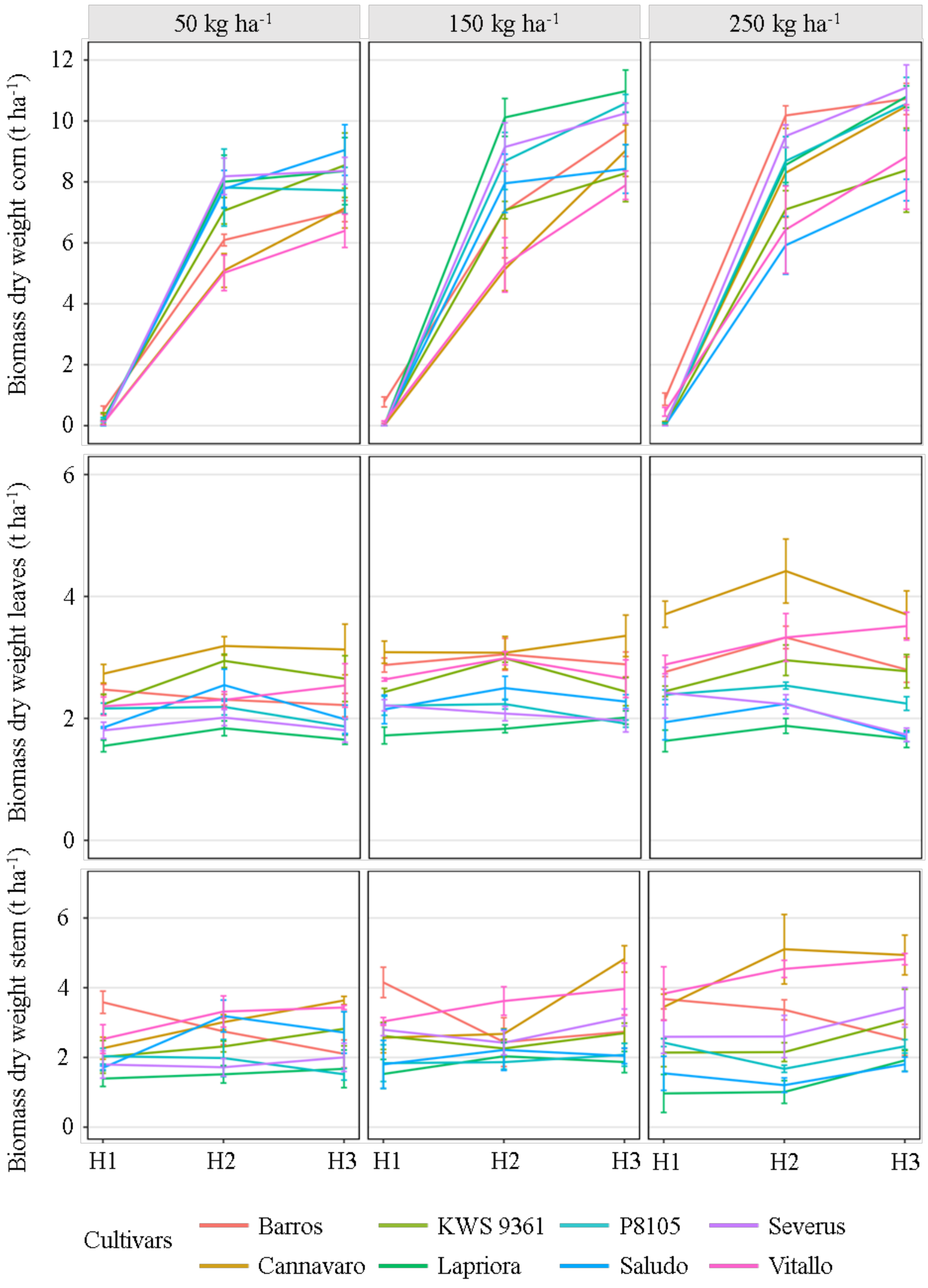

Fig. 4: Above-ground biomass of corn, leaves and stem (t ha^{-1}) at flowering (H1), silage maturity (H2), and grain maturity (H3) of eight cultivars as obtained for three different nitrogen levels of 50, 150 and 250 kg N ha^{-}1 in 2015. Standard deviations are indicated as error bars.

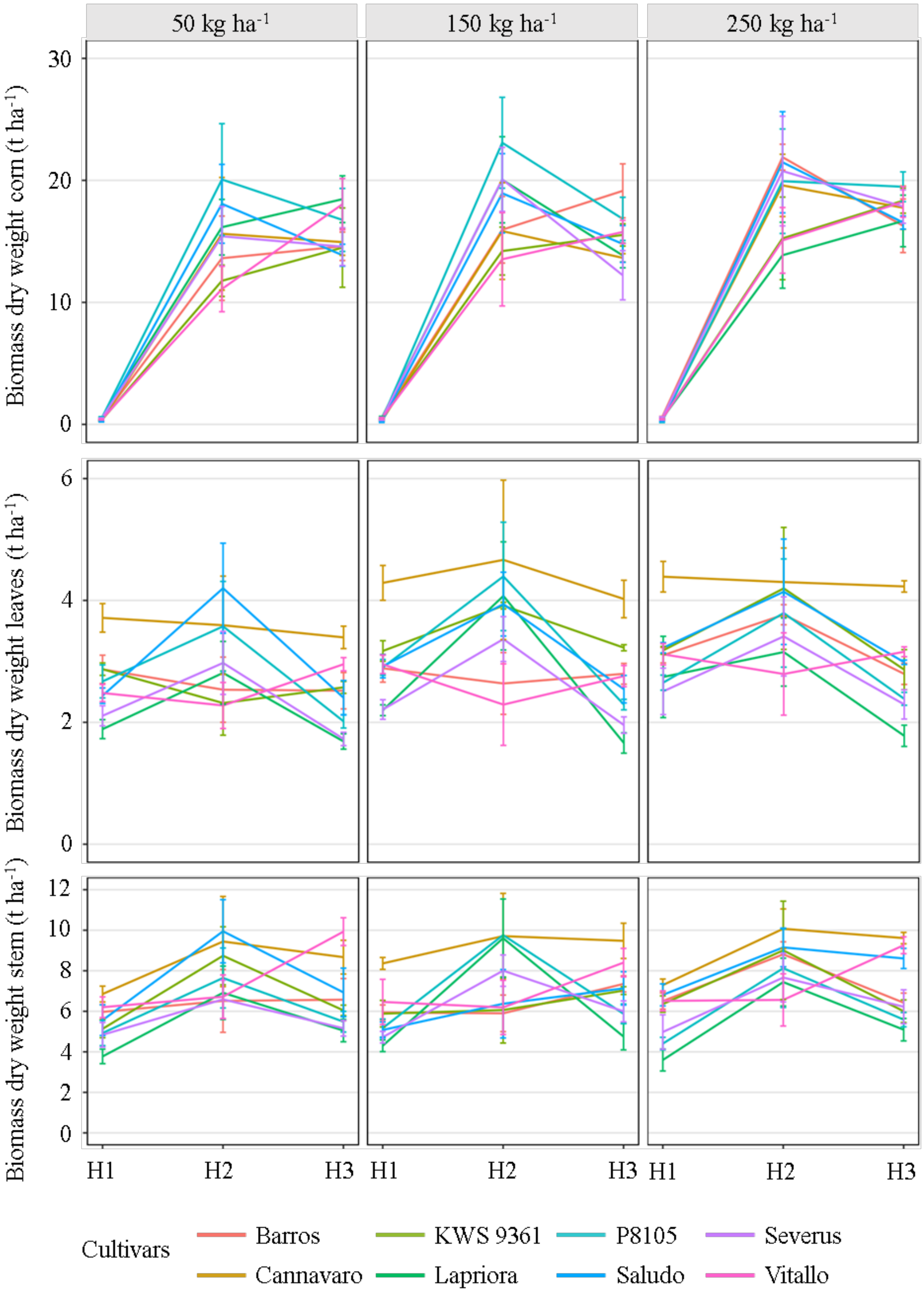

Fig. 5: Above-ground biomass of corn, leaves and stem (t ha^{-1}) at flowering (H1), silage maturity (H2), and grain maturity (H3) of eight cultivars as obtained for three different nitrogen levels of 50, 150 and 250 kg N ha^{-1} in 2016. Standard deviations are indicated as error bars.

The distribution of BDW over the years was very similar. During flowering, the share of LDW from total above ground biomass was 22-32%, SDW represented 45-64% and grain yield 4-8%. At silage maturity grain yield assumed the highest proportion of total biomass (45-50%). The stem biomass dry weight totaled 21-22% and the leaf biomass dry weight decreased to 10-15% of the total above-ground biomass. Until grain maturity the proportion of grain yield further increased to 50-64 %. In contrast, the stem biomass dry weight and the leaf biomass dry weight decreased to 18-25% and 8-13%, respectively (Table 4).

Table 4: Percentage biomass distribution of stem biomass dry weight (SDW), leaf biomass dry weight (LDW) and grain yield (GDW) at different sampling times in the years 2014, 2015 and 2016.

Year	**Total biomass dry weight at flowering (%)**			**Total biomass dry weight at silage maturity (%)**			**Total biomass dry weight at grain maturity (%)**		
	SDW	LDW	GDW	SDW	LDW	GDW	SDW	LDW	GDW
2014	57	34	-	32	14	45	18	11	64
2015	64	34	2	27	15	45	26	13	49
2016	63	32	5	23	10	50	23	9	54

Nitrogen uptake was closely linked to dry weight and its distribution within the plants. Nitrogen uptake into the above-ground plant compartments steadily increased from flowering (NU_{silk}) to corn maturity in all years, except in 2016 where the average total nitrogen uptake (TNU) was slightly higher at silage maturity compared to corn maturity (Table 5 and Figs. 6, 7 and 8). The maximum nitrogen uptake at flowering was achieved with 171 kg N ha^{-1} in 2016, whereas a decreased nitrogen uptake was observed with only 69 kg ha^{-1} in 2015, and a moderate nitrogen uptake of 151 kg ha^{-1} was achieved in 2014. Further, the final nitrogen uptake differed over the years and showed an above average nitrogen uptake of 309 kg ha^{-1} in 2016, an average value of 246 kg ha^{-1} in 2014, and a decreased nitrogen uptake of 185.4 kg ha^{-1} in 2015 (Table 5).

In 2014 significant differences in nitrogen uptake at silage and grain maturity between cultivars were observed, while the early maturing cultivars Colisee, Lapriora and Saludo performed better compared to the late maturing LG 3258 and KWS 9361. At grain maturity the cultivar Lapriora showed significant differences in TNU with the highest nitrogen uptake value of 303 kg ha^{-1} ($p < 0.001$) compared to the other cultivars (Fig. 6).

In 2015 and 2016, nitrogen fertilization exerted a significant effect on TNU at flowering, silage and corn maturity ($p < 0.001$) and significant differences among cultivars at flowering and silage maturity ($p < 0.001$) were observed with Cannavaro always performing best. In 2015 Severus and Barros also showed consistently higher nitrogen uptakes whereas Saludo was less well performing. The nitrogen uptake of Lapriora, a very early cultivar, increased constantly and reached with 187 kg ha^{-1} the level of the best performing cultivar Cannavaro with 189 kg ha^{-1}. During flowering, TNU differences of only 27 kg ha^{-1} were observed between the lowest and the highest fertilization level, whereas TNU differed more in the later growth phase with exactly the same differences of 77 kg ha^{-1} being observed at silage and grain maturity between the lowest and highest nitrogen fertilization level (Fig. 7).

In 2016, cultivars showed significant differences in nitrogen uptake. At flowering, highly significant differences between the better performing late maturing cultivars Cannavaro, Vitallo, Barros and the early maturing cultivars Lapriora, Severus and P 8105 were found. In contrast, at silage and corn maturity, differences in TNU between late and early maturing cultivars were smaller, but the two groups could still be distinguished based on TNU. In contrast to 2015, Lapriora and Severus also showed a decreased TNU. The effect of the nitrogen fertilizer level on plant nitrogen content was highly significant among all sampling dates, and was strongly influenced by the cultivars´ performance (Table 3). During flowering and silage maturity TNU increases of 61 kg ha^{-1} could be observed from the lowest to the highest nitrogen fertilization level. However, TNU differed more in the later growth phase differing by 89 kg ha^{-1} at silage maturity between the lowest and highest nitrogen fertilization level (Fig. 8).

Table 5: Average total above-ground nitrogen uptake (kg ha^{-1}) at flowering, silage and grain maturity of all cultivars with included standard deviations at all three fertilization levels.

year	**Flowering (kg ha^{-1})**			**Silage maturity (kg ha^{-1})**			**Grain maturity (kg ha^{-1})**		
	50 $\left(\frac{\text{kg N}}{\text{ha}}\right)$	150 $\left(\frac{\text{kg N}}{\text{ha}}\right)$	250 $\left(\frac{\text{kg N}}{\text{ha}}\right)$	50 $\left(\frac{\text{kg N}}{\text{ha}}\right)$	150 $\left(\frac{\text{kg N}}{\text{ha}}\right)$	250 $\left(\frac{\text{kg N}}{\text{ha}}\right)$	50 $\left(\frac{\text{kg N}}{\text{ha}}\right)$	150 $\left(\frac{\text{kg N}}{\text{ha}}\right)$	250 $\left(\frac{\text{kg N}}{\text{ha}}\right)$
2014		151± 26.5			166.3± 22.03			246.7± 45	
2015	56.7 ± 14.3	69.± 20.4	83.5± 26.6	115± 26.5	156.7± 31.4	192± 40.4	131.2± 26.4	185.4± 31.2	208.2± 39.1
2016	130.3± 28.8	171± 45.5	191.4± 40.4	278.8± 68.2	369.5± 118.9	339± 110.6	243.7± 47.12	309.7± 74.47	332.1± 50.57

At flowering more than half of the nitrogen contained in the above-ground part of the plants was allocated to the leaves (LNU) (55-58%) whereas the stem (SNU) reached 32-40% and the cob 5-7% of the total plant nitrogen contained across all years. At silage maturity, the leaves translocated around half of the nitrogen and the nitrogen content dropped to 17-28% and was similar in the stems with 7-13%. In contrast, grain nitrogen (GNU) made up more than half of TNU within the plant (54-74%). Until corn maturity the relative proportion of nitrogen in the grains increased only slightly to 70-73% and the share of leaf nitrogen reflected 14-17%, while the proportion of N contained in the stem was slightly lower with 8-12% of the total plant nitrogen uptake (Table 6).

Table 6: Percentage nitrogen uptake distribution within the organs stem, leaves and corn. Husks and rachis represent the remaining percentages.

year	**Total N uptake at flowering (%)**			**Total N uptake at silage maturity (%)**			**Total N uptake at grain maturity (%)**		
	SNU	LNU	GNU	SNU	LNU	GNU	SNU	LNU	GNU
2014	32	58	10	29	29	55	8	14	73
2015	37	55	7	8	17	70	9	15	72
2016	41	54	6	8	21	69	12	17	71

Indeed, the temporal pattern of nitrogen allocation appeared to be quite typical, as the distribution of nitrogen within the plant was very similar among cultivars representing different maturity grades and different fertilization levels in 2015 and 2016. A strong dependency (R^2= 0.9) between grain nitrogen uptake (GNU) and TNU at maturity was observed in all years. The more nitrogen plants took up during the growing season the more nitrogen was found at the final harvest in the corn.

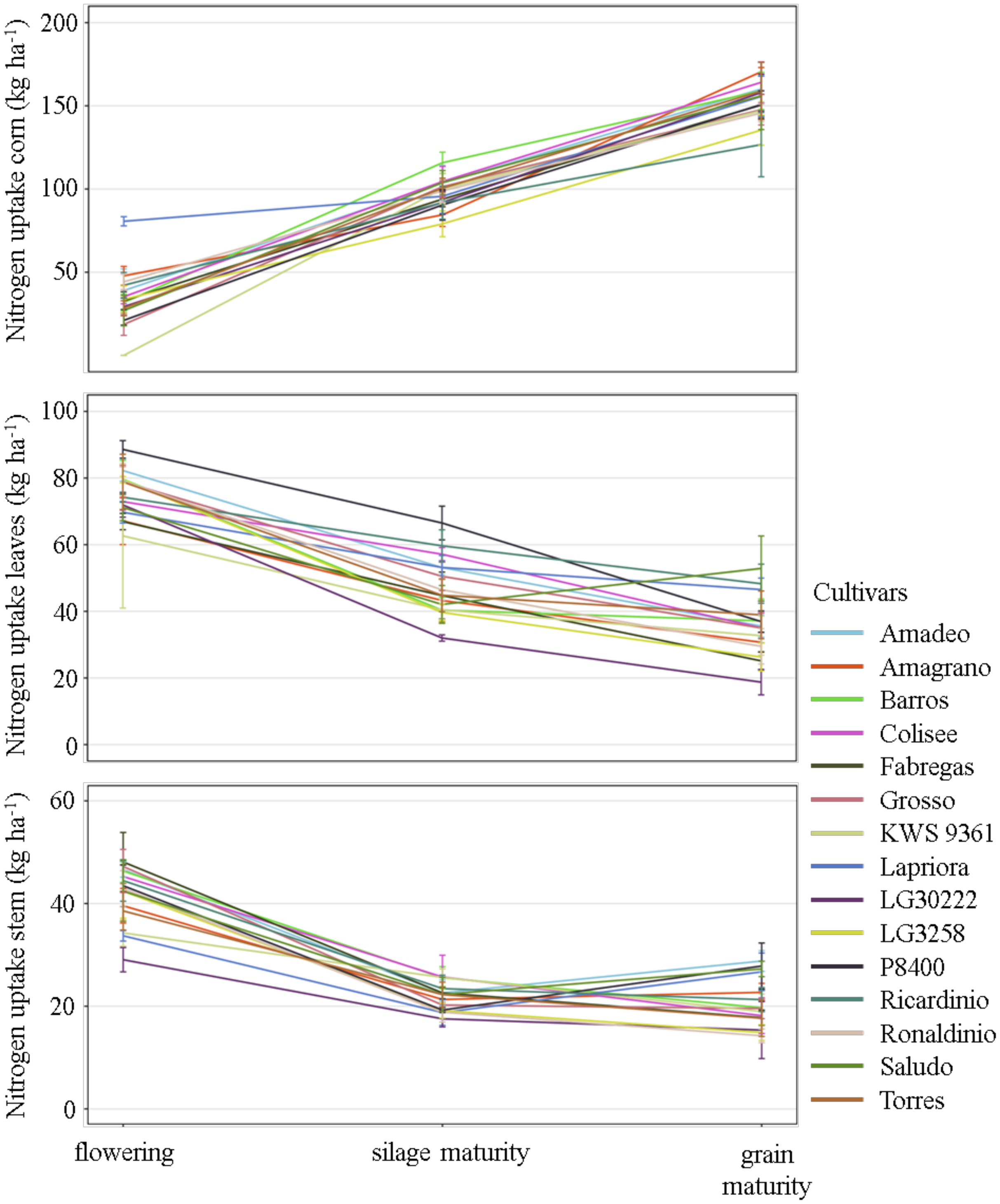

Fig. 6: Total above-ground nitrogen uptake (kg ha^{-1}) for the organs stem, leaves and corn at flowering, silage maturity and grain maturity at the nitrogen level 150 kg N ha^{-1} in 2014. Standard deviations are indicated as error bars.

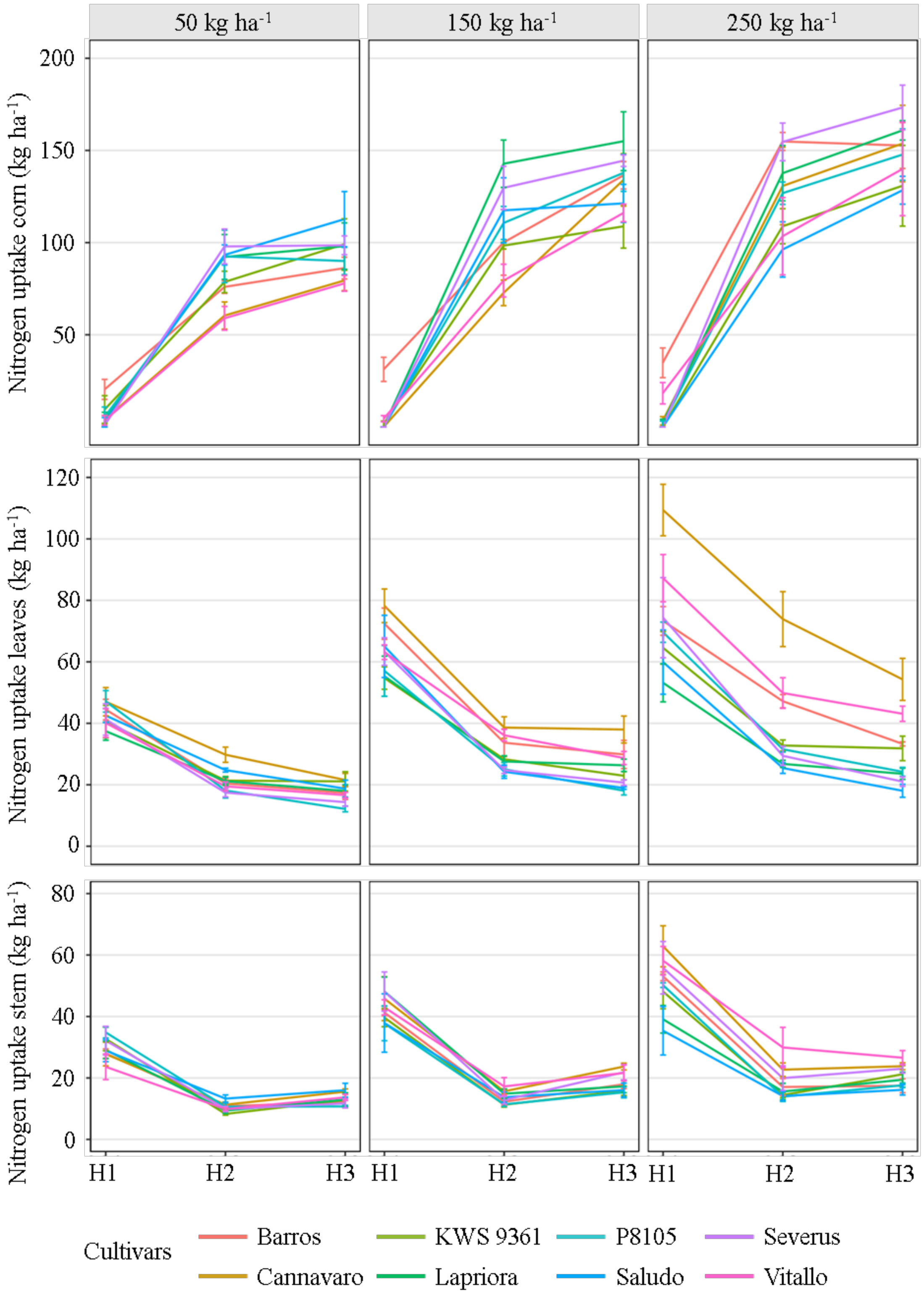

Fig. 7: Total above-ground nitrogen uptake (kg ha^{-1}) found in 2015 in the stem, leaves and corn at flowering (H1), silage maturity (H2) and grain maturity (H3) at the three different nitrogen levels of 50, 150 and 250 kg N ha^{-1}. Standard deviations are indicated as error bars.

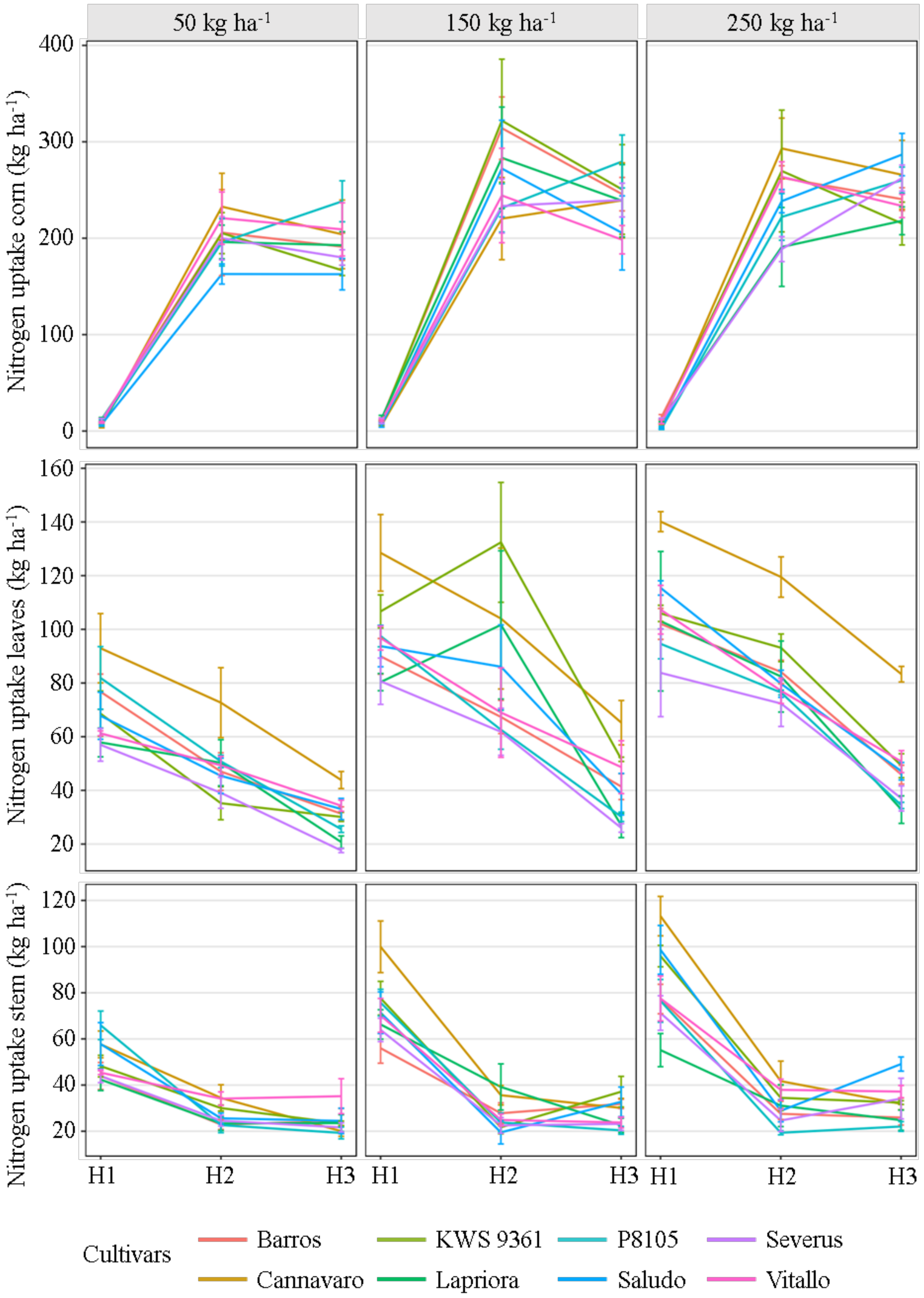

Fig. 8: Total above-ground nitrogen uptake (kg ha^{-1}) found in 2016 in the stem, leaves and corn at flowering (H1), silage maturity (H2) and grain maturity (H3) at the three different nitrogen levels of 50, 150 and 250 kg N ha^{-1}. Standard deviations are indicated as error bars.

3.4.3 Temporal development of total biomass nitrogen uptake

Until flowering, around half of the nitrogen was taken up by the plants. Between anthesis and maturity the plants still took up nitrogen. Even between silage and corn maturity the plants still accumulated nitrogen in the above-ground plant compartments, transported from the roots or soil of about 10-30% (Table 7).

Table 7: Plant nitrogen uptake in percentage of the total aboveground N at grain maturity from flowering to grain maturity in the years 2014 to 2016. For 2015 and 2016 the different fertilization levels of 50, 150 and 250 kg N ha^{-1} are indicated separately.

year	Total N uptake at flowering (%)			Total N uptake at silage maturity (%)			Total N uptake at grain maturity (%)		
	50 $\left(\frac{\text{kg N}}{\text{ha}}\right)$	150 $\left(\frac{\text{kg N}}{\text{ha}}\right)$	250 $\left(\frac{\text{kg N}}{\text{ha}}\right)$	50 $\left(\frac{\text{kg N}}{\text{ha}}\right)$	150 $\left(\frac{\text{kg N}}{\text{ha}}\right)$	250 $\left(\frac{\text{kg N}}{\text{ha}}\right)$	50 $\left(\frac{\text{kg N}}{\text{ha}}\right)$	150 $\left(\frac{\text{kg N}}{\text{ha}}\right)$	250 $\left(\frac{\text{kg N}}{\text{ha}}\right)$
2014		52			67			100	
2015	43	37.6	39	90	85	92	100	100	100
2016	53.4	55.1	57.6	114.3	119.3	102	100	100	100

Regarding the nitrogen fertilization levels no difference in the temporal nitrogen uptake was observed. Plants took comparatively up at different fertilization levels (Table 7). Considering the absolute amounts significantly more nitrogen was taken up at the two highest nitrogen levels.

In the year 2015 the total N uptake reached a maximum of 320 kg ha^{-1} at 250 kg N ha^{-1} fertilizer application in contrast to 220 kg ha^{-1} at the lowest fertilization level of 50 kg N ha^{-1} (Fig. 9). Total N uptake differed between cultivars among the nitrogen fertilization levels. At the lowest nitrogen fertilization level, the cultivar Saludo showed the highest N uptake being comparable to the medium and highest fertilization level. The cultivar Cannavaro took up most from flowering to grain maturity at the highest N fertilization level. The cultivars showed significant differences in their nitrogen uptake and differed in the uptake patterns (Fig. 9). The interaction of N and cultivars was significant at all sampling times. For example the cultivars Cannavaro, Lapriora, and Severus showed an increased uptake particularly at the later growing stages whereas Vitallo and Barros were less well performing.

Between the fertilization levels, the late maturing cultivars performed better at the highest fertilization level compared to some early maturing cultivars showing a good adaptation to the lower nitrogen level (Fig. 9).

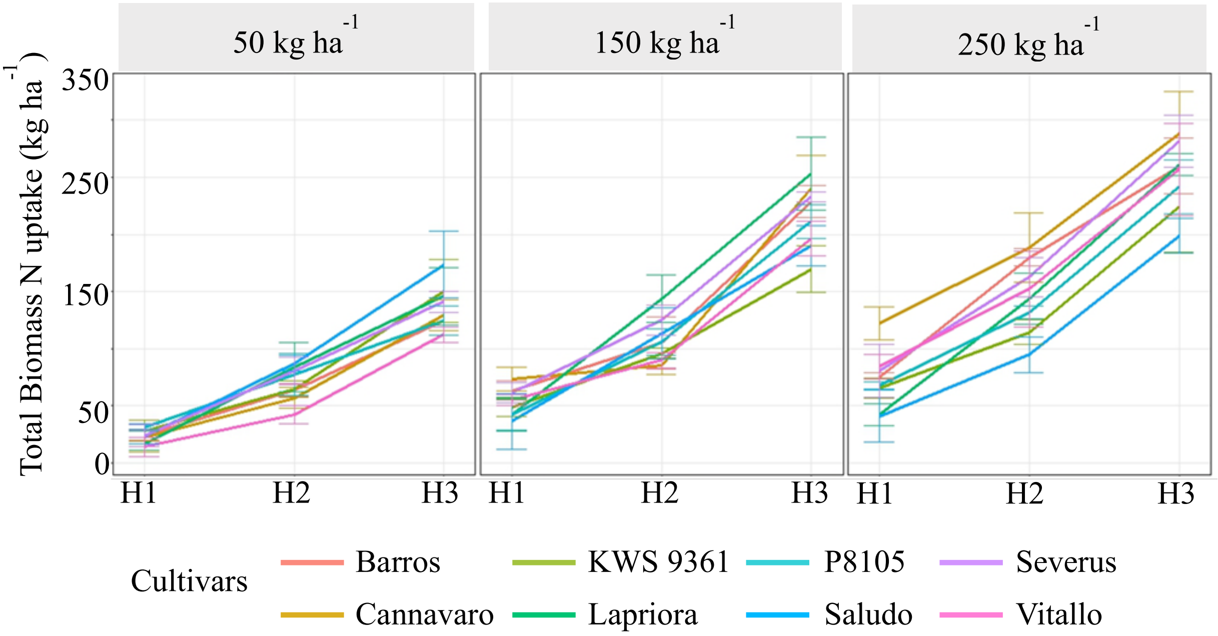

Fig. 9: Total above-ground biomass nitrogen uptake (kg ha^{-1}) during the season 2015 at flowering, silage, and grain maturity at 50, 150 and 250 kg N ha^{-1}. Error bars indicating standard deviations.

In 2016 TNU$_{silk}$ ranged between 46% and 56% for the lowest and the highest nitrogen fertilization level. The percentage TNU did not differ between nitrogen fertilization levels compared to the year 2015 and there was also no steady increase in TNU from flowering till grain maturity. The highest nitrogen uptake rate was observed at silage maturity and further decreased by about 5-10% until grain maturity (Table 7). The nitrogen uptake increased with increasing nitrogen dose and the cultivar Cannavaro was best performing at the highest N fertilization rate. Nitrogen uptake differed mostly among the cultivars at the highest nitrogen fertilization level. The cultivar Cannavaro showed the highest nitrogen uptake followed by the cultivars Barros and KWS 9361 with 360 - 450 kg ha^{-1}. The remaining cultivars ranged between 220 and 260 kg ha^{-1} in TNU at silage maturity. In contrast, the nitrogen uptake from flowering till corn maturity was for all cultivars very similar at the low and medium fertilization level depicting values of 220 to 350 kg ha^{-1} and 300 to 450 kg ha^{-1} for the lowest fertilization level and the medium fertilization level, respectively, at silage maturity (Fig.10).

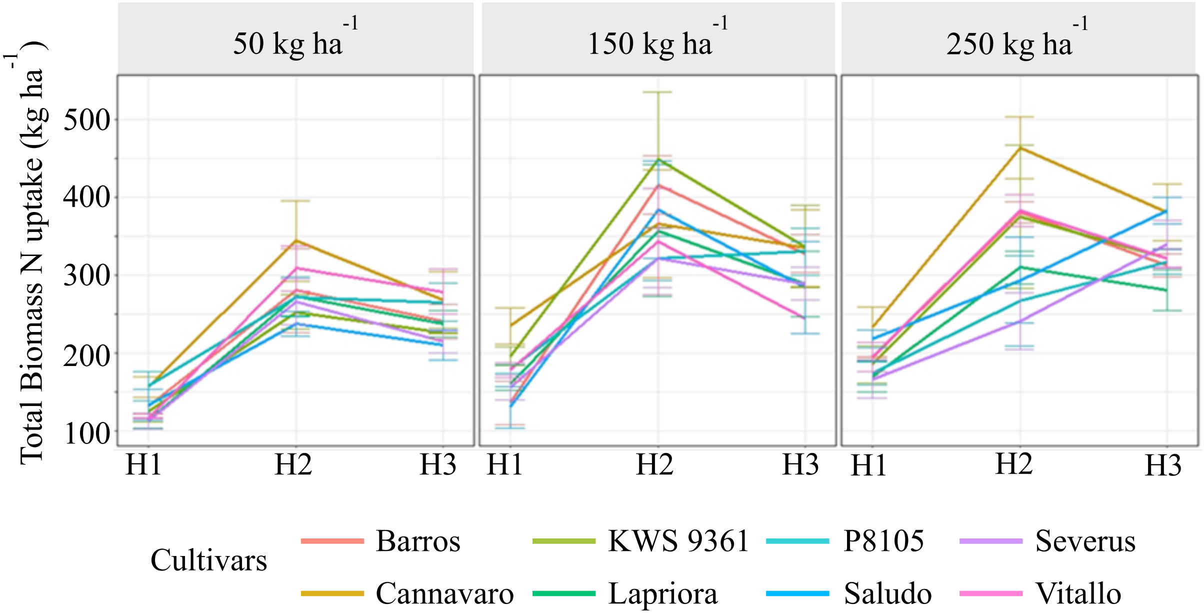

Fig. 10: Total above-ground biomass nitrogen uptake (kg ha^{-1}) during the season 2016 at flowering, silage and grain maturity at 50, 150 and 250 kg N ha^{-1}. Error bars indicating standard deviations and different columns demonstrate the different fertilization levels.

The Nitrogen Harvest Index (NHI) is an essential factor for determining the NUE and is defined as the ratio of grain nitrogen uptake to the total nitrogen uptake. In 2014, there were significant differences in the NHI between silage and grain maturity ($p < 0.001$). In contrast, no significant differences were discernible among cultivars. This observation was also confirmed in 2015 and 2016, when there were no significant differences in the NHI at silage and grain maturity and among cultivars. In addition, the different nitrogen fertilization levels did not have any effect on the NHI (Table 8, Fig. 11 and 12).

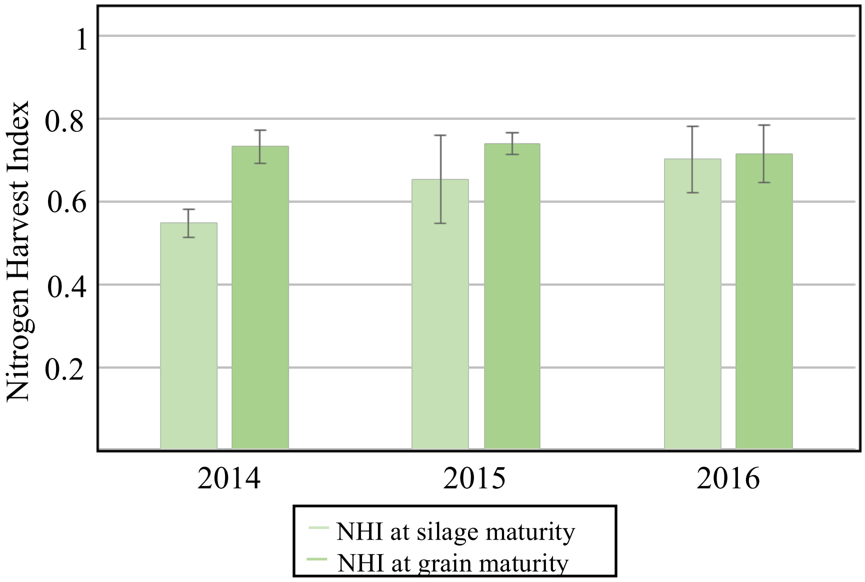

Fig. 11: The average Nitrogen Harvest Index (NHI) at silage and grain maturity in 2014, 2015 and 2016. Error bars indicating standard deviations over all cultivars and fertilization levels.

Table 8: Nitrogen Harvest Index with standard deviations at the fertilization levels 50, 150 and 250 kg N ha^{-1} in the years 2014 to 2016.

year	**Nitrogen Harvest Index at silage maturity**			**Nitrogen Harvest Index at grain maturity**		
	50 $\left(\frac{\text{kg N}}{\text{ha}}\right)$	150 $\left(\frac{\text{kg N}}{\text{ha}}\right)$	250 $\left(\frac{\text{kg N}}{\text{ha}}\right)$	50 $\left(\frac{\text{kg N}}{\text{ha}}\right)$	150 $\left(\frac{\text{kg N}}{\text{ha}}\right)$	250 $\left(\frac{\text{kg N}}{\text{ha}}\right)$
2014		0.55 ± 0.03			0.73 ± 0.04	
2015	0.65 ± 0.13	0.66 ± 0.09	0.65 ± 0.10	0.70 ± 0.04	0.71 ± 0.05	0.70 ± 0.07
2016	0.68 ± 0.04	0.66 ± 0.05	0.63 ± 0.10	0.73 ± 0.02	0.74 ± 0.04	0.75 ± 0.02

3.4.4 Remobilization of carbon

Between flowering and grain maturity carbon remobilization (Crem) and reproduction (Crep) in stems and leaves differed between the years. In 2014, Crem showed the lowest value with -3.3 t ha^{-1}, whereas in 2016 a value of -0.86 t ha^{-1} and in 2015 a value of - 0.78 t ha^{-1} was obtained. Stem Crem (SCrem) differed significantly between cultivars ($p = 0.003$) in 2015, whereas leaf Crem (LCrem) showed significant differences between cultivars ($p < 0.001$) in 2016. In all three years hardly any SCrem was observed, however more accumulation of C in the stem (-0.69% to -25.58%) was observed. In contrast to stems, leaves remobilized up to 34% C (LCrem) especially under favorable conditions in 2014 and 2016. Leaf accumulation or remobilization ranged on average between -4.2 and +9% in 2015. Furthermore, no significant differences between C remobilization and accumulation between nitrogen fertilization levels for both organs were observed.

3.4.5 Remobilization of nitrogen

Nitrogen remobilization was particularly increased in 2016 where LNrem reached 51 kg ha^{-1} and SNrem 40.6 kg ha^{-1}. In 2015 LNrem was slightly lower being 34 kg ha^{-1} and also SNrem was lower with 25 kg ha^{-1}. In contrast in the year 2014 LNrem was ranging in between the values of the later years with 41.5 kg ha^{-1} and showed the lowest SNrem of 20.9 kg ha^{-1}. Remobilization from stems (SNrem) and leaves (LNrem) ranged on average between +47% and +57% while the remobilization percentage of both organs paralleled each other across the years. During all years significant differences in LNrem were found among cultivars (Table 3). Remobilization from the leaves was higher for early maturing cultivars compared to late maturing cultivars due to the shorter reproductive phase. In 2015 and 2014 no significant difference in SNrem was observed among cultivars, but at the same time remobilization was generally very low due to abiotic stress. Furthermore, the nitrogen fertilization level showed no significant influence on the remobilization capacity of both plant organs among cultivars. However in 2016 the higher fertilization level among cultivars resulted in a significant effect on SNrem ($p = 0.027$). Carbon allocation was correlated with nitrogen allocation and showed a strong relationship between LCrem and LNrem across all years (R^2= 0.4-0.7).

Total N remobilization (TNrem) ranged between 60 and 100 kg ha^{-1} with the lowest nitrogen remobilization being observed in 2015 (20.5 kg ha^{-1}) probably caused by drought stress during the growing season. Most of the cultivars showed lower remobilization in 2015 compared to the years 2014 and 2016 characterized by more favorable weather and growing conditions (Table 9). Significant differences in TNrem among cultivars were only found in the years 2015 and 2014 (Table 3). In 2014 the early maturing cultivar Lapriora depicted the highest remobilization whereas the late maturing cultivars indicated lower remobilization. Overall, the highest TNrem of 110 kg ha^{-1} was observed for the cultivar Barros, a stay green cultivar, in the year 2015 characterized by drought stress. In comparison, the cultivar Barros remobilized only 55- 80 N kg ha^{-1} under favorable conditions in 2014 and 2016. Lapriora, a very early maturing cultivar, showed the lowest nitrogen remobilization of 50 N kg ha^{-1} in 2015. In 2016 no significant difference in the remobilization between early and late maturing cultivars was observed and also no significant difference between the nitrogen fertilization levels.

The Nrep ranged between 47-105 kg N ha^{-1}, whereas Nrep was most increased with values of 59% in the drought affected year in 2015. Nrep in early maturing cultivars ($p = < 0.001$) was significantly higher compared to late maturing cultivars in 2015, whereas the opposite was observed in 2014. Nrep was lower under favorable weather conditions in the years 2014 and 2016 compared to the less favorable year in 2015. Generally, Nrep (30%) contributed less to N at corn maturity than TNrem (70%). However, under drought stress Nrep became more important (59%) allowing to achieve a high nitrogen capacity/concentration in the grain at corn maturity. The Nrep capacity was independent of the N fertilization levels in 2015 and 2016. The percentage share of Nrep (26%) in 2016 was low due to sufficient remobilization in earlier growing periods (Tables 3 and 9).

Table 9: Total nitrogen remobilization and N reproduction capacity, and their contribution to total N (in percent) as an average of all cultivars in the years 2014 to 2016.

Year	**TNrem** $\left(\frac{kg}{ha}\right)$	**TNrem (%)**	**Nrep** $\left(\frac{kg}{ha}\right)$	**Nrep (%)**	**Percentage of total Nrem in grain (%)**
2014	84.5	62.2	96	37.8	49.4
2015	60.4	40.6	105	59.4	17.7
2016	100	73.8	65	26.2	60.0

This was also evident in the final distribution of nitrogen contained in the grain at corn maturity. Most of the remobilized N was found in the corn and represented about 60% of the total corn nitrogen. Under favorable growing conditions the contribution of TNrem to total N at grain maturity reached on average 50-60%. In contrast, the remobilization capacity was lower at 20% when drought occurred.

The nitrogen fertilization had no influence on the contribution of TNrem to total N at grain maturity.

Commonalities were also noticed between Crem and Nrem. The more nitrogen was remobilized, the more carbon was remobilized, too. Best correlations were found in the year 2015 where remobilization contributed more to the final yield (R^2 = 0.6). Close antagonistic correlations were also found in Nrem and Nrep with R^2 = 0.36 in 2014, R^2 = 0.8 in 2015, and R^2 = 0.52 in 2016 (Fig. 13). Good relationships were as well found between Nrem and anthesis N, with an R^2 = 0.8 and between Nrep and final corn yield with R^2 of 0.6.

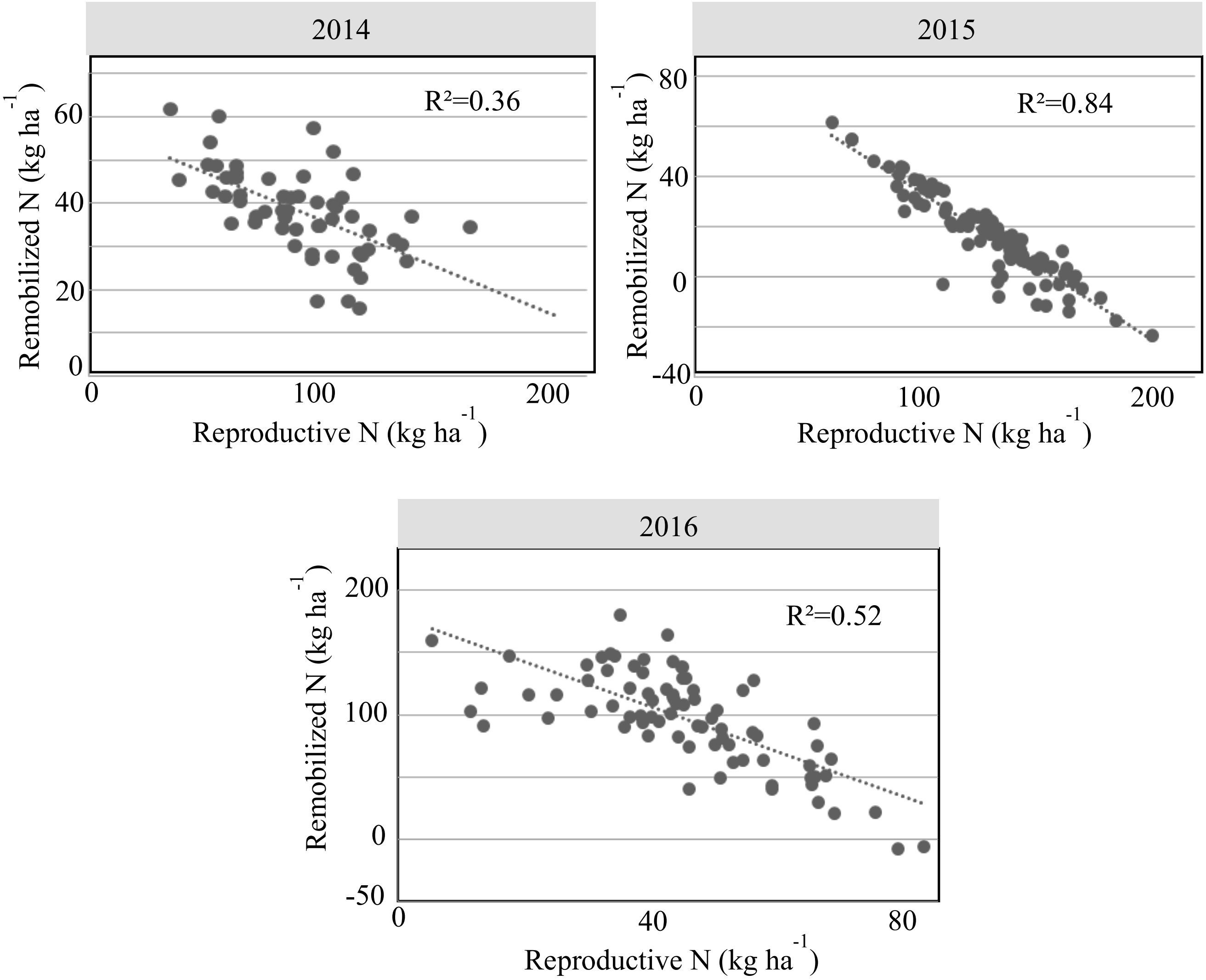

Fig. 13: Correlations between remobilized N (kg ha^{-1}) and reproductive N (kg ha^{-1}) in the years 2014, 2015 and 2016.

3.5 Discussion

Final yield, nitrogen and carbon allocation were strongly influenced by climatic conditions. In 2014, a rainy spring and a sunny autumn resulted in an average maize yield of 23.7 t ha^{-1}. In contrast, heat and drought stress occurring during flowering in 2015 impaired nitrogen and carbon accumulation, which caused reduced yields of 18 t ha^{-1}. Increased global radiation (Fig. 2) and above-average rainfall (Fig. 2) resulted in a final, average Bavarian maize yield of 37 t ha^{-1} in 2016.

Already at flowering, differences in biomass accumulation were obvious throughout these three contrasting years**,** with 7.2 t ha^{-1} in **2014**, 6.9 t ha^{-1} in **2015** and 8.7 t ha^{-1} in **2016**. These differences in biomass yield increased until silage maturity, where the biomass in **2015** with 17 t ha^{-1} reached only half of the biomass in **2016** with 34 t ha^{-1}. Also in **2014**, the year with a medium yield of 19 t ha^{-1}, biomass at silage maturity was much lower with 14 t ha^{-1} compared to **2016**. Across all years late maturing cultivars achieved higher biomass accumulation at flowering compared to earlier flowering cultivars which could be explained through genetics and their breeding targets, to produce high amounts of biomass in agreement with Duvick (2005). Under suboptimal growing conditions characterized by drought and heat stress the performance of the cultivars, evidenced by the reduced dry weight biomass, was affected from flowering till late maturity, a finding which is in agreement with observations by Efeoğlu et al. (2009). Only late maturing cultivars were able to better withstand drought stress and did benefit from the late senescence allowing to accumulate biomass until grain maturity, but nevertheless corn yield was still impaired. Similar to Pommel et al. (2006), Yan et al. (2014) and Chen et al. (2014) even under optimal climatic conditions, higher biomass accumulation especially in the generative phase was observed for late maturing cultivars compared to early maturing cultivars as, due to a shift in senescence, they could exploit their whole growing potential till the later generative phase. This observation stays in contrast to Acciaresi et al. (2014) who described no differences in post-silking dry matter accumulation between early and late maturing cultivars.

Not only the final biomass, but also the final kernel yield significantly dropped due to unfavorable climatic conditions in **2015** to 9.77 t ha^{-1} compared to **2016** with 16.6 t ha^{-1} and **2014** with 15.2 t ha^{-1}. These kernel yields and differences between seasons are in accordance with Chen et al. (2015). Under very favorable climatic conditions late maturing cultivars, which are used for higher biomass production, were comparable in the final kernel yield with early maturing cultivars characterized by a harvest index of 0.6. However this was not the case under drought stress, characterized by a harvest index of 0.44. This observation is opposite to the total dry weight accumulation and implies a higher focus on kernel filling for early maturing cultivars and a higher focus on biomass production for late maturing cultivars.

3.5.1 Influence of nitrogen fertilization

Nitrogen fertilization exerted a significant influence on the performance of all cultivars. Biomass and kernel yield increased with increased nitrogen rates in all years. Even at the highest fertilization rates of 150 and 250 kg N ha^{-1}, an increase in yield was still observed. Therefore fertilization supply positively influenced biomass production and could not be compensated by genetic improvement (Yan et al., 2014). At the lowest N fertilization level, yield losses of around 10 t ha^{-1} possibly resulted from N shortage. The final kernel yield also showed significant decreases at 50 kg N ha$^{- 1}$, whereas an increased rate of 250 kg N ha^{-1} did not differently influence the final kernel yield compared to 150 kg N ha^{-1}. This could be explained through saturation of nitrogen uptake as shown as well by Chen et al. (2015) and Yan et al. (2014).

3.5.2 Carbon accumulation

Across all years, during the generative phase, plants accumulated preferably C into the stem instead of remobilizing C to other plant tissues, primarily the corn. This is in contrast to observations by Chen et al. (2015) who reported a SCrem of around 20%. The accumulation of C in the stem could strengthen the plant´s architecture. During the generative phase 6% more carbon was bound in the stem tissue compared to flowering in the year 2014, whereas in 2015 the accumulation into the stem increased to 14.4% from flowering to grain maturity and was highest with 25.5% in 2016. Carbon is transformed into immobilized starch and stored in the stem in order to support a healthy and powerful plant architecture until senescence. Also remobilization of C from the leaves was very low or even negative which resulted in an accumulation of C of -4.2% in 2014 and of -1.2% in 2015. This was opposite in 2016 where positive values were found and therefore a remobilization of 9.1% was observed. This means that the photosynthetic activity can be maintained to guarantee plant growth and this became particularly obvious in 2016 when the highest C accumulation into the stems was observed as plants were temporarily lodged by a heavy thunderstorm. Consistent with previous studies (Ciampitti and Vyn, 2012; Pommel et al., 2006), significantly more carbon accumulated in the stems in late maturing cultivars as observed in 2015, which can be ascribed to an enhanced overall biomass accumulation, extended generative phase and longer photosynthetic activity – a source driven process. Additionally in 2015, accelerated senescence due to drought and heat waves during flowering, reduced C accumulation of almost all early maturing cultivars and interrupted "early" remobilization, which occurs in the grain filling period till R3 (Ciampitti et al., 2013b). The significantly higher SCrem in the cultivar Barros could be an effect of the "stay green character" – type B – explained by Thomas and Howarth (2000) where senescence started on schedule but was very slow, while remobilization time was extended and "late" remobilization (R3-R6), was favored (Ciampitti et al., 2013b). The extended senescence also explained the relatively high remobilization rate from leaves and reduced accumulation in the stems of the cultivar Barros in 2016. The increased C accumulation in leaves and stems during the generative phase found in the very early maturing cultivar Lapriora during the drought period might be explained by the interruption or possibly even cessation of the Crem process. Carbon accumulation in the stem during non-stress conditions could be compensated through the significantly higher carbon remobilization from leaves. Contrarily a lower carbon transport from leaves due to a shorter senescence period was observed in very late maturing cultivars.

3.5.3 Nitrogen uptake capacity

From flowering to corn maturity, nitrogen uptake increased constantly and no saturation of the nitrogen uptake capacity after silking could be observed which stays in contrast to Ciampitti and Vyn (2013b) and Pommel et al. (2006) who described that after silking the nitrogen uptake slowly reaches a saturation level. However climatic conditions influenced nitrogen allocation as well as carbon allocation and explained discrepancies in nitrogen uptake over years. In 2014, the nitrogen uptake reached 246 kg N ha^{-1} on average. Higher nitrogen application significantly increased nitrogen uptake from flowering till grain maturity in 2015 and 2016. A similar pattern of nitrogen uptake was found in previous studies (Ciampitti and Vyn, 2012). The TNU at grain maturity increased by 100 kg ha^{-1} between the lowest fertilization (50 kg N ha^{-1}) and the highest fertilization (250 kg N ha^{-1}). Corn maize accumulated only 26% of the total biomass dry weight and 36% N during one-fourth of the entire growing season which is expressed as the bracketing silking period and does not agree with Ciampitti et al.(2013c) who described an increased biomass dry weight accumulation of 42% but the same nitrogen uptake capacity. Cultivars which are used for silage and biogas production, on the other hand, accumulated 29% of the total biomass dry weight, and even 45% N till flowering. At the generative phase, remobilization or N uptake from the roots was significantly higher for late maturing cultivars compared to early maturing cultivars which was also described by Martin et al. (2005) and Rajcan and Tollenaar (1999b). Until corn maturity, this difference between early and late maturing cultivars became consistently more pronounced due to later senescence of late maturing cultivars. This observation was confirmed by Wang et al. (2014) who discovered that N uptake was strongly driven by photosynthetic C assimilation. Additionally, late maturing cultivars accumulated higher root biomass (unpublished data) which makes it possible to maintain N uptake and remobilization from the roots during grain filling by supplying the roots before with carbohydrates and therefore reduce mobilization of N from other plant organs such as leaves which may result in a longer maintained leaf area (Rajcan and Tollenaar, 1999a). In 2015, there was a strong interaction between cultivars and nitrogen fertilization, as flowering was strongly affected by drought stress. At the two lowest nitrogen fertilization levels 50 and 150 kg N ha^{-1} at flowering, late maturing cultivars performed better, whereas at silage and grain maturity the early maturing cultivars, Lapriora and Severus, exceeded late maturing cultivars in their nitrogen uptake and showed a higher tolerance towards nitrogen shortage. It seems that early maturing cultivars have more effective nitrogen uptake and reproductive capacity. In contrast to the highest nitrogen fertilization level, where late maturing cultivars performed best and could exploit their full potential through the high nitrogen supply. This can be also explained by a sufficiently developed root system of the late maturing cultivars, which allows an increased outspread nitrogen uptake and may enhanced N remobilization from the roots into aboveground biomass during generative phase.

The capacity to remobilize nitrogen from leaves was 25% higher than for carbon but a strong correlation between Crem and Nrem from leaves ($R^2 = 0.4$-0.7) was observed which leads to a close relation between both patterns of allocation (Hanway, 1962; Swank et al., 1982). TNrem differed over years and exhibited the highest percentage (73.8%) in 2016, as opposed to the lowest TNrem (40.6 %) in 2015 and an average TNrem of 62 % in 2014. Remobilization of nitrogen from leaves and stems seemed to be co-regulated as LNrem and SNrem were always very similar; LNrem was 47 % N and SNrem was 48 % in 2014, and LNrem was 56.5 % and SLrem was 55.5 % in 2015 and 2016. Overall, around half of the stored nitrogen in leaves and stems was remobilized throughout the generative phase; similar remobilization rates were also found by DeBruin et al. (2013). Similar to C, in 2015 the N remobilization was significantly higher in late maturing cultivars (Barros) due to increased vegetative BDW and therefore a higher remobilization capacity which indicates a source driven process. Early growing corn cobs showed a close relation between early senescence in leaves and increased sink strength (Rajcan and Tollenaar, 1999b). Contrarily, late maturing cultivars with delayed and shorter senescence maintained photosynthetic activity later in the season and therefore extended the nitrogen uptake from soil, thus not relying on remobilization since they could exploit Nrep and Nrem from the roots (Martin et al., 2005). Additionally increased Nrep is supported through enhanced assimilate transport from shoots to roots of late maturing cultivars and therefore increased N uptake during the grain filling period (Rajcan and Tollenaar, 1999b). Despite the systematic remobilization depending on the grade of maturity of cultivars, abiotic and biotic stress at the end of the vegetative phase and during the generative phase could disrupt remobilization from leaves. In particular, very early maturing cultivars could experience substantial losses in their remobilization efficiency, which can be offset by an elevated Nrep. Late maturing cultivars could compensate drought periods better due to an extended generative phase and can thus maintain Nrem. Delayed senescence and extended photosynthetic activity allowed more carbon and nitrogen to be allocated to roots which increase root size and therefore could maintain a higher capacity to extract nitrogen and water from the soil (Borrell et al., 2001).

In 2015, we observed that the very early maturing cultivar, Lapriora and Saludo, compensated for low Nrem with increased Nrep when early senescence decreased the photosynthetic activity along with less nitrogen uptake from soil. Photosynthetic activity and nitrogen allocation processes within the plant were suspended by drought and heat stress during flowering, and at the beginning of the grain filling/development. Due to suspended allocation processes a full remobilization capacity from leaves was not achieved. This resulted in higher amounts of N remaining in leaves. On top of that any **remaining nitrogen** could reactivate the photosynthetic activity again (Efeoğlu et al., 2009) and could increase Nrep. On the other hand senescence might even be accelerated due to abiotic stress as drought or lack of nitrogen (Rajcan and Tollenaar, 1999a, b), which drastically reduce the period of active C and N uptake in early maturing cultivars and lead to an interruption of N remobilization. In follow-up studies close negative correlations between root mass and soil water content were observed (unpublished data). Lower root mass of early maturing cultivars led to higher soil water contents during drought stress and could facilitate assimilation of soluble and mobilized nitrogen in the plants during the generative phase (D'Andrea et al., 2008).

Based on steady remobilization rates for securing the nitrogen supply to the reproductive organ – corn, nitrogen fertilization supply did not influence Nrem. In spite of this, nitrogen remobilization capacity is a source driven process due to its close association with N uptake in the vegetative stage of the whole plant which significantly affected the available N and is in accordance with the observations of studies by Ciampitti et al. (2013b), Ciampitti and Vyn (2012) and Ciampitti and Vyn (2013a). Therefore nitrogen remobilization from leaves is strongly influenced by vegetative N uptake and heavily driven by the source (Ciampitti and Vyn, 2013a). SNrem was strongest in the absence of climatic stress as there was a lesser need to keep N in the stem to support plant architecture and optimal conditions delayed senescence and allowed more time for remobilization. It is possible that cultivars with a thicker shoot diameter remobilized more N from the stem based on higher N reserves compared to thin stems. Nrem and Nrep were affected by different drivers – as Nrem is a source driven process, influenced by vegetative nitrogen uptake as opposed to Nrep, which is a sink driven process (Ciampitti and Vyn, 2012). The strong negative correlations ($R^2=0.8$) between Nrem and Nrep could also be observed in various other studies (Ciampitti et al., 2013a; Ciampitti and Vyn, 2011; Gallais et al., 2007; He et al., 2004; Mi et al., 2003; Pommel et al., 2006). Nevertheless no relation between these **nitrogen transportation systems** has been found so far (Mueller and Vyn, 2016). A drought period during the season could reduce the Nrem proportion in corn to 18% whereas under optimal conditions the share of Nrem achieved an amount of 60%, thereby providing more than half of the nitrogen found in the corn. Hence, the target of optimal field management should address climatic conditions and include the choice of adapted cultivars. In summary, corn N is the outcome of various complex interrelations (Ciampitti and Vyn, 2012) especially as Nrem and Nrep are both affected by abiotic stress and genetic variability among cultivars.

N availability primarily affected the pattern of the N allocation between vegetative and reproductive organs (D'Andrea et al., 2008). Under N deficiency, the reproductive N became an important source for maintaining kernel nitrogen content (D'Andrea et al., 2008). While enhanced reproductive N was achieved in early maturing cultivars under drought stress to preserve N content in the reproductive organ – the corn (Borrell et al., 2001; Ciampitti and Vyn, 2012), late maturing cultivars can only compensate drought stress to a limited extent and experience losses in N uptake in the grain.

3.6 Conclusions

The most noteworthy results are the steady accumulation and greater growing profit of late maturing cultivars. Carbon uptake after flowering has priority compared to the remobilization process. But nitrogen remobilization and reproduction have an antagonistic relationship. Abiotic and biotic stress at flowering could disrupt remobilization process and cultivars could experience substantial losses, which can be, however, compensated by, enhance reproduction. Under optimal seasonal conditions allocation processes among cultivars do not differ. Nevertheless, with changing nitrogen fertilization level, the total nitrogen uptake differs among cultivars and shows a better performance of Saludo and Lapriora under lower nitrogen level in contrast to the late maturing cultivar Cannavaro, Vitallo and Barros that only achieved fully potential under highest fertilization level. In further investigations, the root should be taken into account as a plant parameter and should be considered in the translocation processes, since in this assumption the remobilization from the root and Nrep cannot be differentiated. Also the possible remobilized N from the leaves and stem into the root cannot be proven.

To improve breeding purposes with regard to higher nitrogen content in the corn, the interaction of Nrem and Nrep should be increased. Apart from these observations the imprecise definition of Nrem due to above-ground biomass deduction could lead to overestimation of Nrem, especially in the grain. Biomass losses on the basis of plant respiration are not considered and could lead to imprecise estimates of nitrogen and carbon allocations. Field experiments using tracers like ^{15}N and ^{13}C could detect Nrep more exactly and allocation processes could be more precisely calculated and studied. However, these methods have their weakness in tracer losses due to strong precipitation and this has to be considered during field experimentation as well.

3.7 References

Acciaresi, H. A., Tambussi, E. A., Antonietta, M., Zuluaga, M. S., Andrade, F. H., and Guiamet, J. J. (2014). Carbon assimilation, leaf area dynamics, and grain yield in contemporary earlier- and later-senescing maize hybrids. European Journal of Agronomy 59, 29-38.

Blessing, C. H., Werner, R. A., Siegwolf, R., and Buchmann, N. (2015). Allocation dynamics of recently fixed carbon in beech saplings in response to increased temperatures and drought. Tree Physiology 35, 585-598.

Borrell, A., Hammer, G., and Oosterom, E. (2001). Stay-green: A consequence of the balance between supply and demand for nitrogen during grain filling? Annals of Applied Biology 138, 91-95.

Chen, Y. L., Xiao, C. X., Chen, X. C., Li, Q., Zhang, J., Chen, F. J., Yuan, L. X., and Mi, G. H. (2014). Characterization of the plant traits contributed to high grain yield and high grain nitrogen concentration in maize. Field Crops Research 159, 19.

Chen, Y. L., Xiao, C. X., Wu, D. L., Xia, T. T., Chen, Q. W., Chen, F. J., Yuan, L. X., and Mi, G. H. (2015). Effects of nitrogen application rate on grain yield and grain nitrogen concentration in two maize hybrids with contrasting nitrogen remobilization efficiency. European Journal of Agronomy 62, 79-89.

Ciampitti, I. A., Camberato, J. J., Murrell, S. T., & Vyn, T. J. (2013a). Maize nutrient accumulation and partitioning in response to plant density and nitrogen rate: I. Macronutrients. Agronomy Journal, 105(3), 783-795.

Ciampitti, I. A., Murrell, S. T., Camberato, J. J., Tuinstra, M., Xia, Y., Friedemann, P., and Vyn, T. J. (2013b). Physiological dynamics of maize nitrogen uptake and partitioning in response to plant density and nitrogen stress factors: II. Reproductive phase. Crop Science 53, 2588-2602.

Ciampitti, I. A., Murrell, S. T., Camberato, J. J., Tuinstra, M., Xia, Y. B., Friedemann, P., and Vyn, T. J. (2013c). Physiological Dynamics of Maize Nitrogen Uptake and Partitioning in Response to Plant Density and N Stress Factors: I. Vegetative Phase. Crop Science 53, 2105-2119.

Ciampitti, I. A., and Vyn, T. J. (2011). A comprehensive study of plant density consequences on nitrogen uptake dynamics of maize plants from vegetative to reproductive stages. Field Crops Research 121, 2-18.

Ciampitti, I. A., and Vyn, T. J. (2012). Physiological perspectives of changes over time in maize yield dependency on nitrogen uptake and associated nitrogen efficiencies: A review. Field Crops Research 133, 48-67.

Ciampitti, I. A., & Vyn, T. J. (2013a). Grain nitrogen source changes over time in maize: a review. Crop Science, 53(2), 366-377.

Ciampitti, I. A., and Vyn, T. J. (2013b). Maize nutrient accumulation and partitioning in response to plant density and nitrogen rate: II. Calcium, Magnesium, and Micronutrients. Agronomy Journal 105(6), 1645-1657.

Ciampitti, I. A., and Vyn, T. J. (2014). Understanding Global and Historical Nutrient Use Efficiencies for Closing Maize Yield Gaps. Agronomy Journal 106, 2107-2117.

D'Andrea, K. E., Otegui, M. E., and Cirilo, A. G. (2008). Kernel number determination differs among maize hybrids in response to nitrogen. Field Crops Research 105, 228-239.

DeBruin, J., Messina, C. D., Munaro, E., Thompson, K., Conlon-Beckner, C., Fallis, L., Sevenich, D. M., Gupta, R., and Dhugga, K. S. (2013). N distribution in maize plant as a marker for grain yield and limits on its remobilization after flowering. Plant Breeding 132, 500-505.

Dharmakeerthi, R. S., Kay, B. D., and Beauchamp, E. G. (2006). Spatial variability of in-season nitrogen uptake by corn across a variable landscape as affected by management. Agronomy Journal 98, 255-264.

Duvick, D. N. (2005). The contribution of breeding to yield advances in maize (Zea mays L.). Advances in Agronomy, 86, 83-145.

Duvick, D. N., and Cassman, K. G. (1999). Post–green revolution trends in yield potential of temperate maize in the North-Central United States. Crop Science 39, 1622-1630.

Efeoğlu, B., Ekmekci, Y., and Cicek, N. (2009). Physiological responses of three maize cultivars to drought stress and recovery. South African Journal of Botany 75, 34-42.

Gallais, A., Coque, M., Le Gouis, J., Prioul, J., Hirel, B., and Quillere, I. (2007). Estimating the proportion of nitrogen remobilization and of postsilking nitrogen uptake allocated to maize kernels by nitrogen-15 labeling. Crop Science 47, 685-691.

Hanway, J. (1962). Corn growth and composition in relation to soil fertility: II. Uptake of N, P, and K and their distribution in different plant parts during the growing season. Agronomy Journal 54, 217-222.

He, P., Zhou, W., and Jin, J. (2004). Carbon and nitrogen metabolism related to grain formation in two different senescent types of maize. Journal of Plant Nutrition 27, 295-311.

Heil, K., and Schmidhalter, U. (2017). Improved evaluation of field experiments by accounting for inherent soil variability. European Journal of Agronomy 89, 1-15.

Lambin, E. F., and Meyfroidt, P. (2011). Global land use change, economic globalization, and the looming land scarcity. Proceedings of the National Academy of Sciences of the United States of America 108, 3465-3472.

Ma, B., and Dwyer, L. (1998). Nitrogen uptake and use of two contrasting maize hybrids differing in leaf senescence. Plant and Soil 199, 283-291.

Martin, A., Belastegui-Macadam, X., Quilleré, I., Floriot, M., Valadier, M. H., Pommel, B., Andrieu, B., Donnison, I., and Hirel, B. (2005). Nitrogen management and senescence in two maize hybrids differing in the persistence of leaf greenness: agronomic, physiological and molecular aspects. New Phytologist 167, 483-492.

Mi, G., Liu, J. a., Chen, F., Zhang, F., Cui, Z., and Liu, X. (2003). Nitrogen uptake and remobilization in maize hybrids differing in leaf senescence. Journal of Plant Nutrition 26, 237-247.

Moll, R. H., Kamprath, E. J., and Jackson, W. A. (1982). Analysis and interpretation of factors which contribute to efficiency of nitrogen utilization. Agronomy Journal 74(3), 562-564.

Mueller, S. M., & Vyn, T. J. (2016). Maize plant resilience to N stress and post-silking N capacity changes over time: A review. Frontiers in Plant Science, 7:53, doi: 10.3389/fpls.2016.00053.

Pommel, B., Gallais, A., Coque, M., Quillere, I., Hirel, B., Prioul, J. L., Andrieu, B., and Floriot, M. (2006). Carbon and nitrogen allocation and grain filling in three maize hybrids differing in leaf senescence. European Journal of Agronomy 24, 203-211.

Rajcan, I., and Tollenaar, M. (1999a). Source: sink ratio and leaf senescence in maize: I. Dry matter accumulation and partitioning during grain filling. Field Crops Research 60, 245-253.

Rajcan, I., and Tollenaar, M. (1999b). Source: sink ratio and leaf senescence in maize: II. Nitrogen metabolism during grain filling. Field Crops Research 60, 255-265.

Shiferaw, B., Prasanna, B. M., Hellin, J., and Bänziger, M. (2011). Crops that feed the world 6. Past successes and future challenges to the role played by maize in global food security. Food Security 3, 307.

Swank, J. C., Below, F. E., Lambert, R. J., and Hageman, R. H. (1982). Interaction of carbon and nitrogen metabolism in the productivity of maize. Plant Physiology 70(4), 1185-1190.

Thomas, H., and Howarth, C. J. (2000). Five ways to stay green. Journal of Experimental Botany 51, 329-337.

Uhart, S. A., & Andrade, F. H. (1995). Nitrogen and carbon accumulation and remobilization during grain filling in maize under different source/sink ratios. Crop Science, 35(1), 183-190.

Wang, Z. G., Gao, J. L., and Ma, B. L. (2014). Concurrent Improvement in Maize Yield and Nitrogen Use Efficiency with Integrated Agronomic Management Strategies. Agronomy Journal 106, 1243-1250.

Woli, K. P., Boyer, M. J., Elmore, R. W., Sawyer, J. E., Abendroth, L. J., and Barker, D. W. (2016). Corn Era Hybrid Response to Nitrogen Fertilization. Agronomy Journal 108, 473-486.

Yan, P., Yue, S. C., Qiu, M. L., Chen, X. P., Cui, Z. L., and Chen, F. J. (2014). Using maize hybrids and in-season nitrogen management to improve grain yield and grain nitrogen concentrations. Field Crops Research 166, 38-45.

4 Phenotyping nitrogen and carbon parameters of maize cultivars with high-throughput at the reproductive phase

4.1 Abstract

The opportunity to detect yield, nitrogen status parameters and maize traits by measuring spectral reflectance could accelerate breeding targets and could reduce time and cost intensive breeding processes. In a two-year study at three different field sites (Thalhausen, Allershausen and Dürnast), 8 different maize cultivars, with different production goals were grown at different fertilization levels (50, 150 and 250 kg N ha^{-1}) and varying annual environmental influences in the seasons 2015 and 2016. The goal of this work was to achieve an improved understanding of the performance of maize plants at the reproductive phase, depending on genetic or environmental factors, by means of non-destructive high-throughput sensing techniques. Best predictions of important breeding traits such as leaf dry weight (LDW), total aboveground biomass (BDW), leaf nitrogen uptake (LNU), total nitrogen uptake (BNU) were achieved using wavebands between 400 to 999 nm in the reproductive phase, at flowering and at silage maturity. Closet correlations between predicted and actual total aboveground biomass ($R^2 = 0.6\text{-}0.9$) were determined at flowering. Between the fertilization levels, the best correlation between calculated indices and destructive parameters were found at the lowest and highest nitrogen rate as a consequence of increased differentiation among the cultivars in nitrogen uptake. By combining the most predictive PLSR models across trials, the total nitrogen uptake was best predicted at flowering with $R^2 = 0.84$ to at the Dürnast site. Classification and grouping of cultivars regarding the previously mentioned parameters were possible within all field trials and could therefore be used as selection tool in enhanced selection processes. The most relevant wavelengths for predicting biomass production were in the waveband range around 500-600 nm which is associated with the photosynthetic capacity, whereas the nitrogen uptake was best predicted around the red inflection point at 680-780 nm.

4.2 Introduction

High-throughput phenotyping covers an elementary section of agricultural sciences and practices. The synergies of computer- and sensor technology, robotics and image analysis for a better understanding of environmental - genotyping interaction analysis, contributes to a considerable improvement in future farming (Furbank and Tester, 2011; Walter et al., 2015). The intensive research on plant - phenomes based on plant growth and – performance capability offers plant breeders the opportunity to merge genetics, physiology and phenotype with regard to abiotic and biotic stress factors and to discover not yet analyzed molecular genetic traits and processes within the plant. Winterhalter et al. (2013) and Singh et al. (2016) described the phenotyping screening of maize traits in the field as a bottleneck whereas genomic research is already experiencing substantial progress. Over the last 30 years the methods for characterizing phenomic plant traits have been developed considerably less compared to genotyping and DNA sequencing and therefore require special attention in further breeding research (White et al., 2012). The investigation of different phenotypic plant parameters is time consuming, tedious and cost intensive and is mostly influenced by subjective perception (Montes et al., 2007). Automated phenotyping methods could improve quantitative scoring of plant parameters without subjective human influences (Barmeier et al., 2017; Barmeier and Schmidhalter, 2016). Various studies found close relations between biomass production and grain yield and spectral reflectance indices among different cultivars (Erdle et al., 2011, 2013b; Kipp et al., 2014a; Mistele and Schmidhalter, 2008, 2010; Montes et al., 2011; Rischbeck et al., 2016; Weber et al., 2012; Winterhalter et al., 2011a; Winterhalter et al., 2012, 2013).

The potential of active and passive sensors within maize plants was examined to disentangle the contribution of upper and lower leaves as well as from the stem and cob (Winterhalter et al., 2013). Active sensors which use their own light source could only detect upper leaf layers in maize plants depending on the intensity of the light source (Winterhalter et al., 2013) which decreases quadratically with distance (Kipp et al., 2014b). In contrast, passive sensors enabled the detection of the contribution of all leaf layers within the plant canopy (Winterhalter et al., 2012).

Besides the nitrogen and biomass detection, sensors could also detect further characteristics such as the chlorophyll content, drought stress, and senescence characteristics (Christensen et al., 2005; Schlemmer et al., 2005; Winterhalter et al., 2011b)

In future visions, phenotyping techniques should detect proximal spectral reflection and the temperature of the plant stock. They should simultaneously screen plant architecture and therefore need to be capable of recording and evaluating big data during the whole cycle of plant growth including the vegetative and generative phase (White et al., 2012). **In various studies the vegetative phase of maize plant growth has already been studied (Behmann et al., 2014; Mistele and Schmidhalter, 2010; Montes et al., 2011; Winterhalter et al., 2011b) but the utilization of high throughput phenotyping during the generative phase is still little explored**. The generative phase is very important, in relation to final yield, since this is when translocation of nitrogen starts and the grain filling period begins. At flowering and silage maturity, spectral reflection measurements were conducted in field trials with 8 differently maturing cultivars and with different breeding targets to detect the uptake of C and N in several plant organs. Spectral measurements including passive and active sensors, recording at wavelengths between 400-900 nm, were conducted during midday to avoid shadow effects. Additionally, 10 randomly collected maize plants were separated into leaves, stems and cobs, dried and used as reference samples. Data from spectral detection were prepared and evaluated by using linear regression models and by calculating Partial Least Square Regression (PLSR) models. Optimized reflection indices to assess the nitrogen uptake of different plant organs and total biomass dry weight could potentially improve the preliminary selection of more nitrogen efficient and more drought stress resistant cultivars exhibiting increased yield.

The goal of this work, was to achieve an improved understanding of the performance of maize plants at the reproductive phase, depending on genetic or environmental factors, by means of non-destructive high-throughput sensing techniques, in order to possibly enhance and shorten the breeding process, and to further improve the nitrogen management in an effective and sustainable way.

4.3 Material and Methods

Experimental field trials were conducted in the years 2015 and 2016 in Dürnast (11° 70'E, 48° 40'N, and 450 m asl), Thalhausen (11°39E, 48°25'N, 444 m asl) and Allershausen (11°39'E, 48°25'N, and 400 m asl). The field sites are approximately 7 km apart. Within this region the annual precipitation averages 800mm with an average temperature of 7.8 °C. The soils are characterized as homogeneous Cambisol with silty clay loam. The field experiments were managed conventionally and the experiments were performed as fully randomized block design with four replicates and three nitrogen fertilization levels, to simulate suboptimal, normal rates and over-supply of nitrogen (50, 150 and 250 kg N ha^{-1}). In the year 2015, 8 different hybrids with different breeding targets for corn, silage or biogas production were sown on April 27 and for the weed management Clio Super at 1.5L ha^{-1} and Zeagran Ultimate at 1.5L ha^{-1} were used. A detailed description of the cultivars is contained in Table 1. In 2016, the same hybrids with four replicates were sown on May 5 and the same fertilization rates were used. For weed control Round Up Power Flex With 3 L ha^{-1} and Gardo Gold and Callisto at 3.75 L ha^{-1} were used.

Table1: Cultivars used with their breeding targets and maturity grades grown in three field trials in Thalhausen 2015, Allershausen 2016 and Dürnast 2016.

Cultivar	Usage	Maturity Group	FAO Number
Lapriora	corn	very early	K190
Severus	corn, silage	early	S190, K190
Saludo	corn, silage	early	S210, K210
P 8105	corn, silage	early	S180, K 220
KWS 9361	corn, silage	middle, late	S290, K280
Barros	silage	middle, late	S250
Vitallo	silage	late	S270
Cannavaro	biogas	very late	S 310

In both years, biomass samples were taken at flowering and silage maturity, by randomly removing 10 plants from the second inner row to avoid boundary effects. The **plants were separated into leaves, stems and cobs**. The complete harvested plant material from the destructive biomass sampling was immediately weighed after removal and chopped. A representative subsample was weighed and oven-dried at 60°C for one week and reweighed to determine the dry matter content. The dried samples were milled and analyzed by near infrared spectroscopy (Bruker Vector 22/N, Bruker, Billerica, MA, USA). Organ-specific NIRS-models were developed by using the Unscrambler software (CAMO Software AS, Oslo, Norway). For establishing the calibration 1/3 of the samples were chemically analyzed by isotope ratio mass spectrometry (ANCA SL 20-20 preparation unit, Europe Scientific, Crewe, UK) for their N content.

High-throughput sensor measurements were conducted at flowering and silage maturity. Different active and passive sensors were mounted in a nadir position, on a frame positioned on a front loader with flexible height-distance regulation of the sensor system, to keep the distance to the top of the canopy constant (Winterhalter et al., 2013). To avoid border effects, the spectral measurements were recorded on the second and third row of the plots in sowing direction. For best passive reflection recording, measurements were conducted on clear days during midday, to use the full radiation spectrum of the sun. More detailed description about the timing of the measurements is given in Table 2.

Table 2: **Background** information including spectral reflection measurement days and timescales and mean global radiance RAD (kWh/m²) at flowering and silage maturity.

location	**Measurement days at flowering**	**Measurement days at silage maturity**	**Day time at flowering**	RAD flowering	**Day time at silage maturity**	RAD silage maturity
Thalhausen	22.07.2015	09.09.2015	2 pm-4 pm	76.60	2 pm-3 pm	118.40
Allershausen	03.08.2016	26.09.2016	1:30 pm-3 pm	171.24	11:30 am –1 pm	135.84
Dürnast	25.07.2016	13.09.2016	10:15 am-11am	105.64	10.40 am-12 am	106.93

Spectral indices which are listed in Table 3 were calculated from the reflectance wavelength information as obtained from the active and passive sensors. The sensor systems tested were a passive reflectance sensor and three active sensors, the GreenSeeker, the CropCircle and a modified ALS sensor. The custom-made, passive, bi-directional reflectance sensor system (tec5, Oberursel, Germany) contained two Zeiss MMS1 silicon diode array spectrometers that detect reflectance between 300 to 1000 nm with a bandwidth of 3.3 nm (Mistele and Schmidhalter, 2008). In contrast, the GreenseekerRT100 (NTech Industries, Ukiah, CA, USA) uses LEDs as a light source to detect reflectance in the VIS (656 nm) and NIR (774 nm) wavelength region. The CropCircle ACS470 (Holland Sientific, Inc, Lincoln, NE) instrument emits white light (~ 400- ~ 800 nm) and is equipped with an additional filter to detect spectral reflectance at 670, 730 and 760 nm. The third active sensor was a custom-made active flash sensor (AFS) which is similar to the N-Sensor ALS (YARA International, Oslo, Norway) which has a Xenon flash light as a light source providing multispectral light of high intensity and detects reflectance at 730, 760, 970 and 900 nm. All sensor data were fitted with the corresponding GPS coordinates from a Trimble RTK-GPS (real-time kinematic global positioning system) (Trimble, Sunnyvale, CA, USA). Spectral indices ascertained in previous work (Table 3) were calculated based on the reflectance of the passive sensors. Additionally, the following ratios HPS 780_740 (Erdle et al., 2011) and HPS 742_764 estimated from contour maps were also used. Contour maps are calculating a correlation matrix with all possible wavelengths to find the best indices and wavelength combinations.

Table 3: Calculated spectral indices of the reflectance of the passive sensor; formulas indicating the used wavelength combinations and targets are listed.

Spectral reflectance indices (SRI)	**Abbreviation**	**Formula**	**Target**	**Reference**
Normalized difference vegetation index	NDVI	$\frac{(780-670)}{(780+670)}$	Estimation of canopy photosynthetic area	(Raun et al., 2001)
Water band index	WI	$\frac{970}{900}$	Canopy water status	(Peñuelas et al., 1993)
Red edge inflection point	REIP	$700+40*\frac{\frac{670+780}{2}-700}{740-700}$	Nitrogen content	(Guyot et al., 1988)
Reflectance intensity ratio NIR/RR	NIR/RED	$\frac{780}{670}$		(Mistele and Schmidhalter, 2010)
Reflectance intensity ratio NIR/G	NIR/GEEN	$\frac{780}{550}$		(Mistele and Schmidhalter, 2010)
Simple ratio	SR	$\frac{900}{680}$	Estimation of canopy photosynthetic area	(Aparicio et al., 2000)
Photochemical reflectance index	PRI	$\frac{531-570}{531+570}$	Estimation of Xanthophyll pigment cycle changes	(Gamon et al., 1992)

4.3.1 Partial least square regression analysis

To estimate and to test relations between various parameters, a statistical model with partial least square regression (PLSR) was developed. The PLSR model was calculated with the program Unscambler®X10.3 (Camo Software AS, Oslo, Norway) to find 'latent' structures in the wavelength spectra (X) that best predict the measured parameter (Y). For detailed information see also Esbensen et al. (2002) and Wold et al. (2001). In this study, the parameter X defined the recorded wavelengths from 400 to 999 nm. For the parameter Y, destructive data collected at flowering and silage maturity, such as total above ground biomass, leaf biomass, and nitrogen uptake of the latter mentioned parameters were chosen. Before calculating the model, spectra of the wavebands were smoothed with the Savitzky-Golay smoothing algorithm and light scattering was corrected with a standard normal variate transformation (SNV). By evaluating the model a cross validation was conducted.

4.3.2 Statistics

An analysis of variance (ANOVA) was done to distinguish differences ($P<0.05$) among the cultivars and calculated with RStudio, Inc. 2011 (Boston, MA 02210, USA). Statistical analysis for obtaining relationships between the sensors´ and destructive measurements on the basis of linear models were conducted in Microsoft Excel 2013 (Microsoft Inc., Seattle, WA, USA) and MATLAB (the Mathworks, Inc., Natick, Massachusetts, USA). Additionally, a contour map analysis was conducted by estimating relationships between all destructive parameters, total aboveground biomass dry weight (BDW), leaf dry weight (LDW), stem dry weight (SDW) and grain dry weight (GDW) and the reflected wavelengths.

Heritability (5) was calculated as follows:

$$h^2(\text{hÂ}^2) = \frac{\sigma g^2}{(\sigma g^2+\sigma e^2)} \qquad (5)$$

Where the heritability of a trait is the ratio of the genetic variability (∂g^2) to phenotypic variability (σp^2) (Singh et al., 1993).

4.4 Results

4.4.1 Agronomic Parameters

For all sampling dates across the seasons 2015 and 2016 the mean values of the parameters leaf dry weight (LDW), stem dry weight (SDW), grain dry weight (GDW) and total aboveground biomass dry weight (BDW) as influenced by the three nitrogen fertilization rates are indicated in Tables 4, 5 & 6. Leaf nitrogen uptake (LNU), stem nitrogen uptake (SNU), grain nitrogen uptake (GNU) and total nitrogen contained in the above-ground biomass dry weight (BNU), nitrogen content (N%) and the nitrogen nutrition index (NNI) separately indicated among the nitrogen fertilization levels are shown in Tables 11, 12 & 13.

During flowering, the highest yield was achieved with 9.2 t ha^{-1} in the year 2016 in Allershausen, whereas decreased biomass dry weights were observed in 2015 in Thalhausen with 7.06 t ha^{-1} and 8.5 t ha^{-1} in Dürnast. A maximum yield of 34.3 t ha^{-1} at silage maturity was obtained in Allershausen in 2016. However, a reduced yield of 24.7 t ha^{-1} in Thalhausen and 16.8 t ha^{-1} in Dürnast at silage maturity was detected. At grain maturity, compared to anthesis, a decrease in biomass dry weight was observed in the experimental trials in Allershausen with 26 t ha^{-1} in 2016 and in Thalhausen with 18.5 t ha^{-1} in 2015. In the Dürnast experiment no final yield measurements at grain maturity were done (Tables 4, 5, 6).

In 2015 in Thalhausen, at flowering all agronomic parameters showed significant differences among cultivars ($p < 0.001$), where late maturing cultivars such as Cannavaro and Barros performed best for biomass dry weight (8- 9 t ha^{-1}), stem dry weight (4.8-4.8 t ha^{-1}) and leaf dry weight (2.7-3.2 t ha^{-1}). In contrast, early maturing cultivars such as Lapriora and Saludo reached lower biomass dry weight (5-6 t ha^{-1}), stem dry weight (3.2-3.6 t ha^{-1}) and leaf dry weight (1.6-1.9 t ha^{-1}). At silage maturity, significant differences among cultivars could also be observed in nearly all parameters except for biomass dry weight. The highest leaf dry weight values were again reached by the late maturing cultivars for example Cannavaro (3.6 t ha^{-1}) and KWS 9361 (3.0 t ha^{-1}), whereas for the early maturing cultivars, decreased leaf dry weights were observed such as for Lapriora with 1.8 t ha^{-1} and Severus with 2.1 t ha^{-1}. The stem dry weights showed the same pattern as the leaf dry weight with increased stem dry weight observed for the late maturing cultivars such as Vitallo and Cannavaro (5.8- 5.7 t ha^{-1}) and decreased stem dry weight values observed for Lapriora and P 8105 (3.5- 3.8 t ha^{-1}) (Tables 4, 7).

Additionally, the fertilization rates also exerted a significant effect on almost all destructive parameters ($p < 0.001$) except on stem dry weight at flowering and silage maturity. At flowering the difference in biomass dry weight between the highest and lowest N fertilization level accounted for only 0.9 t ha^{-1} which increased rapidly to 2.8 t ha^{-1} at silage and grain maturity. Differences in the leaf dry weight were almost the same between the lowest and the highest N fertilization level with 0.4 t ha^{-1} at all sampling dates (Tables 4 and 7).

In the field trial Allershausen in 2016, the cultivars showed significant differences in the agronomic parameters at flowering, and for almost all parameters at silage maturity ($p < 0.001$). Only for the grain dry weight the cultivars did not show significant differences at silage maturity. Until flowering, the late maturing cultivars Cannavaro (11 t ha^{-1}) and Vitallo (9 t ha^{-1}) accumulated more biomass compared to the early maturing cultivars Lapriora and Severus which showed lower values with 6.6 - 7.5 t ha^{-1}. At silage maturity, they were similarly ranked with significantly higher BDW values observed for Cannavaro (24 t ha^{-1}) and Barros (36 t ha^{-1}) and decreased values for Severus (26 t ha^{-1}) and P 8105 (29 t ha^{-1}). As already indicated the biomass dry weight and the leaf dry weight reached higher values for the late maturing cultivars Cannavaro and Barros (3.0- 3.9 t ha^{-1}) compared to the early maturing cultivars Lapriora and Severus (1.7- 2.0 t ha^{-1}). In Allershausen during the growing season in 2016, the N fertilization levels always exerted a significant effect on almost all parameters ($p < 0.001$) except for the grain dry weight at flowering and the stem dry weight at silage maturity. The differences in biomass dry weight between the highest and the lowest fertilization level accounted for only 1.5 t ha^{-1} at flowering, increased to 7 t ha^{-1} at silage maturity and to 5 t ha^{-1} at grain maturity. Slight differences could be observed in leaf dry weight, which differed between the sampling dates by 0.4-0.6 t ha^{-1}, and in the stem dry weight with differences between 0.3-0.4 t ha^{-1}. Also in grain yield no large differences were observed for the fertilization levels and they ranged at all sampling dates between 1.6- 2.8 t ha^{-1} (Tables 5 and 7).

In Dürnast, in the year 2016, significant differences were observed among the cultivars in their biomass dry weight at flowering and silage maturity. At flowering, again the late maturing cultivars, e.g. Cannavaro and Vitallo showed higher biomass dry weight values (8.5-9.2 t ha^{-1}), whereas the early maturing cultivars such as Lapriora and Saludo displayed decreased biomass dry weights (6.9 t ha^{-1}). In contrast, at silage maturity Saludo performed better compared to Vitallo and reached a higher biomass dry weight. However, significant differences were only observed for the increased biomass dry weight of Cannavaro (24.7 t ha^{-1}) and the decreased biomass dry weight of Lapriora (21.3 t ha^{-1}). At silage maturity, significant differences in leaf dry weight and stem dry weight were also observed, demonstrating the same pattern with increased values for Cannavaro and decreased values for Lapriora (Tables 6 and 7).

Table 4: Average aboveground biomass (t ha^{-1}) of eight different maize hybrids at flowering, silage and grain maturity at three fertilization levels in the field trial Thalhausen in 2015.

	Flowering (t ha^{-1})			**Silage maturity (t ha^{-1})**			**Grain maturity (t ha^{-1})**		
	50 $\left(\frac{\text{kg N}}{\text{ha}}\right)$	150 $\left(\frac{\text{kg N}}{\text{ha}}\right)$	250 $\left(\frac{\text{kg N}}{\text{ha}}\right)$	50 $\left(\frac{\text{kg N}}{\text{ha}}\right)$	150 $\left(\frac{\text{kg N}}{\text{ha}}\right)$	250 $\left(\frac{\text{kg N}}{\text{ha}}\right)$	50 $\left(\frac{\text{kg N}}{\text{ha}}\right)$	150 $\left(\frac{\text{kg N}}{\text{ha}}\right)$	250 $\left(\frac{\text{kg N}}{\text{ha}}\right)$
BDW (t ha^{-1})	6.4 ± 1.3	7.1± 1.7	7.3± 2.1	15.5± 2.5	16.8± 2.8	18.3± 3.9	16.6± 3.7	18.5± 2.9	19.7± 4.2
LDW (t ha^{-1})	2.1± 0.42	2.4 ± 0.94	2.5± 0.7	2.4± 0.5	2.6 ± 0.6	2.8± 0.8	2.2± 0.7	2.4± 0.6	2.6± 0.9
SDW (t ha^{-1})	4.1± 0.9	4.5± 0.1	4.6± 0.1	4.5± 0.9	4.5± 1	4.8± 1.7	4.5± 1.0	5.9± 1.2	5.2± 1.5
Grain (t ha^{-1})				6.7± 2.1	7.5± 2.3	8.1± 2.2	7.8± 1.6	9.4± 1.6	9.7± 2.2

Table 5: Average aboveground biomass (t ha^{-1}) of eight different maize hybrids at flowering, silage and grain maturity at three fertilization levels in the field trial Allershausen in 2016.

	Flowering (t ha^{-1})			**Silage maturity (t ha^{-1})**			**Grain maturity (t ha^{-1})**		
	50 $\left(\frac{\text{kg N}}{\text{ha}}\right)$	150 $\left(\frac{\text{kg N}}{\text{ha}}\right)$	250 $\left(\frac{\text{kg N}}{\text{ha}}\right)$	50 $\left(\frac{\text{kg N}}{\text{ha}}\right)$	150 $\left(\frac{\text{kg N}}{\text{ha}}\right)$	250 $\left(\frac{\text{kg N}}{\text{ha}}\right)$	50 $\left(\frac{\text{kg N}}{\text{ha}}\right)$	150 $\left(\frac{\text{kg N}}{\text{ha}}\right)$	250 $\left(\frac{\text{kg N}}{\text{ha}}\right)$
BDW (t ha^{-1})	8.4± 1.8	9.2± 2.2	9.8± 2	30.9± 7.8	34.3± 8.3	38± 10.9	22.8± 4.2	26± 5.5	28. ± 4.6
LDW (t ha^{-1})	2.6± 0.6	2.9± 0.7	3.1± 0.8	3.1± 0.9	4.1± 0.2	3.7± 1.0	2.4± 0.6	2.7± 0.8	2.8± 0.7
SDW (t ha^{-1})	5.4± 1.3	5.7± 1.6	5.7± 1.5	8.5± 4.0	8.4± 3.4	8.5± 2.4	6.7± 2.1	7± 1.8	7.1± 1.9
Grain (t ha^{-1})	0.4± 0.2	0.4± 0.2	0.4± 0.2	15.6± 4.1	19.1± 5.6	18.4± 4.6	13.9± 2.0	14.9± 2.9	15.5± 2.8

Table 6: Average aboveground biomass (t ha^{-1}) of 4 different maize hybrids at flowering, silage and grain maturity at three fertilization levels in the field trial Dürnast in 2016.

	Flowering (t ha^{-1})			**Silage maturity (t ha^{-1})**			**Grain maturity (t ha^{-1})**		
	50 $\left(\frac{\text{kg N}}{\text{ha}}\right)$	150 $\left(\frac{\text{kg N}}{\text{ha}}\right)$	250 $\left(\frac{\text{kg N}}{\text{ha}}\right)$	50 $\left(\frac{\text{kg N}}{\text{ha}}\right)$	150 $\left(\frac{\text{kg N}}{\text{ha}}\right)$	250 $\left(\frac{\text{kg N}}{\text{ha}}\right)$	50 $\left(\frac{\text{kg N}}{\text{ha}}\right)$	150 $\left(\frac{\text{kg N}}{\text{ha}}\right)$	250 $\left(\frac{\text{kg N}}{\text{ha}}\right)$
BDW (t ha^{-1})	6.1± 1.8	8.5± 1.8	9.25± 1.9	16.5± 5.3	24.7± 3.4	28.5± 4.4			
LDW (t ha^{-1})				2.1± 0.5	2.8± 0.5	3.0± 0.6			
SDW (t ha^{-1})				4.9± 1.6	7.5± 1.5	8.1± 1.2			
Grain (t ha^{-1})				7.4± 2.7	11.2± 1.7	13.3± 3.0			

Table 7: Statistical overview of the variables total, stem, grain and leaf above-ground biomass (BDW, SDW, GDW, LDW) at flowering and silage maturity for all experimental sites, indicating differences among cultivars and N treatments. Statistically significant differences ($P < 0.05$) are indicated in bold.

	Flowering				**Silage maturity**			
	BDW $\left(\frac{\text{t}}{\text{ha}}\right)$	LDW $\left(\frac{\text{t}}{\text{ha}}\right)$	SDW $\left(\frac{\text{t}}{\text{ha}}\right)$	GDW $\left(\frac{\text{t}}{\text{ha}}\right)$	BDW $\left(\frac{\text{t}}{\text{ha}}\right)$	LDW $\left(\frac{\text{t}}{\text{ha}}\right)$	SDW $\left(\frac{\text{t}}{\text{ha}}\right)$	GDW $\left(\frac{\text{t}}{\text{ha}}\right)$
2015_TH								
N	**0.004**	**<0.001**	0.06		**<0.001**	**<0.001**	0.11	**0.008**
cultivars	**<0.001**	**<0.001**	**<0.001**		0.16	**<0.001**	**<0.001**	**<0.001**
cultivars x N	0.278	0.185	0.48		**0.006**	**0.006**	**<0.001**	0.193
2016_AL								
N	**0.002**	**<0.001**	0.321	0.822	**0.002**	**0.001**	0.991	**0.012**
cultivars	**<0.001**	**<0.001**	**<0.001**	**0.001**	**0.003**	**<0.001**	**<0.001**	0.21
cultivars x N	0.089	0.763	0.623	0.794	0.768	0.089	0.947	0.416
2016_DU								
N	**<0.001**				**<0.001**	**<0.001**	**<0.001**	**<0.001**
cultivars	**<0.001**				**0.028**	**<0.001**	**<0.001**	0.52
cultivars x N	**0.001**				0.156	0.689	1.36	**0.013**

The highest heritability of the total biomass dry weight parameters was observed at flowering across all years with values of 0.9 in Dürnast in 2016, 0.87 in Thalhausen in 2015 and 0.85 in Allershausen in 2016. In contrast to flowering, the heritability decreased at silage maturity to 0.49 in Dürnast, 0.76 in Thalhausen and 0.8 in Allershausen at the highest N fertilization level. At the middle fertilization level of 150 kg N ha^{-1} the heritability was 0.70 in Dürnast, whereas low heritabilities were observed in Thalhausen in 2015 and in Allershausen in 2016 (Tables 8, 9, 10). At the lowest N fertilization level, at silage maturity, there was no heritability observed across all three experimental years.

In contrast to the total biomass dry weight, which decreased steadily from flowering till grain maturity, the leaf dry weight, the stem dry weight and the grain dry weight showed no tendencies in the heritability in 2015 in Thalhausen. The heritability of the leaf dry weight ranged between 0.64 and 0.98 in all nitrogen fertilization levels and from flowering till grain maturity except at silage maturity, where the heritability decreased to zero. From flowering till grain maturity, a slight increase in the heritability of the stem dry weight was observed at all N fertilization levels, whereas the heritability of grain dry weight decreased steadily from flowering to grain maturity for all fertilization levels (Table 8).

Table 8: Broad sense heritability (hÂ^2) of total, leaf, stem, and grain biomass dry weight (t ha^{-1}) of different maize hybrids at flowering, silage, and grain maturity of all cultivars and fertilization levels in Thalhausen in the year 2015.

Year 2015	**Flowering** (hÂ^2)			**Silage maturity** (hÂ^2)			**Grain maturity** (hÂ^2)		
	50 $\left(\frac{\text{kg N}}{\text{ha}}\right)$	150 $\left(\frac{\text{kg N}}{\text{ha}}\right)$	250 $\left(\frac{\text{kg N}}{\text{ha}}\right)$	50 $\left(\frac{\text{kg N}}{\text{ha}}\right)$	150 $\left(\frac{\text{kg N}}{\text{ha}}\right)$	250 $\left(\frac{\text{kg N}}{\text{ha}}\right)$	50 $\left(\frac{\text{kg N}}{\text{ha}}\right)$	150 $\left(\frac{\text{kg N}}{\text{ha}}\right)$	250 $\left(\frac{\text{kg N}}{\text{ha}}\right)$
BDW (t ha^{-1})	0.28	0.68	0.78	0.00	0.00	0.66	0.14	0.63	0.42
LDW (t ha^{-1})	0.92	0.91	0.88	0.00	0.90	0.64	0.76	0.83	0.98
SDW (t ha^{-1})	0.61	0.78	0.80	0.77	0.44	0.92	0.80	0.92	0.89
Grain (t ha^{-1})	0.68	0.96	0.90	0.55	0.79	0.64	0.00	0.92	0.35

In the year 2016 in Allershausen, the same pattern as for 2015 could be observed with a decrease in the heritability of the grain dry weight, an increase in the heritability of the stem dry weight, and a steady outcome of the heritability of leaf dry weight from flowering to grain maturity. However the weakest heritability was found at silage maturity for all fertilization levels and parameters. The highest heritability was detected at flowering and grain maturity (Table 9).

In the year 2016 at the field site Dürnast, the highest heritability could be observed at flowering for the middle and highest N fertilization level. At silage maturity, the heritability of the leaf dry weight ranged between 0.59-0.79 within the fertilization levels, with the highest heritability found at the middle fertilization level. Also the heritability of the stem dry weight showed highest values at the middle fertilization level with almost 0.89. In contrast, the grain dry weight depcited the lowest heritability at the middle N fertilization level (0.00) and increased values at the lowest N fertilization level (0.52) and the highest fertilization level (0.73) (Table 10).

Table 9: Broad sense heritability (hÂ²) of total, leaf, stem and grain biomass dry weight (t ha^{-1}) of different maize hybrids at flowering, silage and grain maturity for all cultivars and fertilization levels in Allershausen in 2016.

Year 2016	**Flowering** (hÂ²)			**Silage maturity** (hÂ²)			**Grain maturity** (hÂ²)		
	50 $\left(\frac{\text{kg N}}{\text{ha}}\right)$	150 $\left(\frac{\text{kg N}}{\text{ha}}\right)$	250 $\left(\frac{\text{kg N}}{\text{ha}}\right)$	50 $\left(\frac{\text{kg N}}{\text{ha}}\right)$	150 $\left(\frac{\text{kg N}}{\text{ha}}\right)$	250 $\left(\frac{\text{kg N}}{\text{ha}}\right)$	50 $\left(\frac{\text{kg N}}{\text{ha}}\right)$	150 $\left(\frac{\text{kg N}}{\text{ha}}\right)$	250 $\left(\frac{\text{kg N}}{\text{ha}}\right)$
BDW (t ha^{-1})	0.83	0.85	0.68	0.00	0.14	0.78	0.67	0.49	0.80
LDW (t ha^{-1})	0.90	0.93	0.76	0.00	0.75	0.78	0.92	0.97	0.96
SDW (t ha^{-1})	0.80	0.82	0.51	0.54	0.03	0.74	0.90	0.88	0.93
Grain (t ha^{-1})	0.20	0.50	0.74	0.00	0.00	0.62	0.27	0.00	0.67

Table 10: Broad sense heritability (hÂ²) of total, leaf, stem and grain biomass dry weight (t ha^{-1}) of different maize hybrids at flowering and silage maturity for all cultivars and fertilization levels in Dürnast in 2016.

Year 2016	**Flowering** (hÂ²)			**Silage maturity** (hÂ²)			**Grain maturity** (hÂ²)		
	50 $\left(\frac{\text{kg N}}{\text{ha}}\right)$	150 $\left(\frac{\text{kg N}}{\text{ha}}\right)$	250 $\left(\frac{\text{kg N}}{\text{ha}}\right)$	50 $\left(\frac{\text{kg N}}{\text{ha}}\right)$	150 $\left(\frac{\text{kg N}}{\text{ha}}\right)$	250 $\left(\frac{\text{kg N}}{\text{ha}}\right)$	50 $\left(\frac{\text{kg N}}{\text{ha}}\right)$	150 $\left(\frac{\text{kg N}}{\text{ha}}\right)$	250 $\left(\frac{\text{kg N}}{\text{ha}}\right)$
BDW (t ha^{-1})	0.45	0.91	0.90	0.12	0.70	0.49			
LDW (t ha^{-1})				0.59	0.81	0.79			
SDW (t ha^{-1})				0.42	0.89	0.50			
Grain (t ha^{-1})				0.52	0.00	0.73			

Nitrogen uptake behaved similarly to the biomass accumulation across the growth period. At flowering, an above-average N-uptake of 170 kg ha^{-1} in the year 2016 in Allershausen and a moderate biomass nitrogen uptake of 117 kg ha^{-1} in Dürnast could be observed. The biomass nitrogen uptake in the year 2015 in Thalhausen reached only 70 kg ha^{-1} at flowering. The biomass nitrogen uptake pattern at flowering was similar at silage maturity with a maximum biomass nitrogen uptake of 370 kg ha^{-1} in Allershausen in 2016, an average biomass nitrogen uptake of 128 kg ha^{-1} in the same year in Dürnast, and a below-average biomass nitrogen uptake of 185 kg ha^{-1} in 2015 in Thalhausen (Tables 11, 12, 13).

In the year 2015 in Thalhausen at flowering almost all agronomic parameters showed significant differences among the cultivars ($p < 0.001$) except the stem nitrogen uptake where the late maturing cultivar Cannavaro performed best for biomass nitrogen uptake (96 kg ha^{-1}) and leaf nitrogen uptake (80 kg ha^{-1}). In contrast, the early maturing cultivars Lapriora and Saludo showed a lower biomass nitrogen uptake (73-80 kg ha^{-1}) and leaf nitrogen uptake (53-54 kg ha^{-1}). At silage maturity significant differences among cultivars could also be observed for all parameters. The highest leaf nitrogen uptake values were reached by the late maturing cultivars Cannavaro (49.9 kg ha^{-1}) and Vitallo (35.3 kg ha^{-1}), whereas for the early maturing cultivars a decreased leaf nitrogen uptake was observed, for Severus with 23.4 kg ha^{-1} and Saludo with 25 kg ha^{-1}. Additionally, the N fertilization levels also exerted significant effects on all destructive parameters ($p < 0.001$) at flowering and silage maturity. At flowering, the difference in biomass nitrogen uptake between the highest and the lowest fertilization level accounted for only 27 kg ha^{-1} which increased rapidly to 77 kg ha^{-1} at silage and grain maturity. This effect was also observed for the leaf nitrogen uptake, with a difference of 32 kg ha^{-1} at flowering and leaf nitrogen uptake difference of 17.6- 19.3 kg ha^{-1} at silage and grain maturity. The fertilization level also had an effect on grain nitrogen uptake which reached an amount of 45 kg ha^{-1} at flowering and at silage maturity, and led to differences of 55 kg ha^{-1} at grain maturity (Tables 12 and 14).

In 2016 in Allershausen, cultivars showed significant differences with regard to all destructive parameters at flowering, however only for stem nitrogen uptake and leaf nitrogen uptake at silage maturity ($p < 0.001$). Till flowering, the late maturing cultivar Cannavaro (207 kg ha^{-1}) took up more nitrogen compared to the early maturing cultivar Severus with values of 144 kg ha^{-1}. Also the nitrogen uptake in stems and leaves was significantly different for Cannavaro with a stem nitrogen uptake of 88 kg ha^{-1} and 120 kg ha^{-1} for the leaf nitrogen uptake. At silage maturity, cultivars behaved similarly with significantly higher biomass nitrogen uptake values observed for Cannavaro (415 kg ha^{-1}) and KWS 9361(428 kg ha^{-1}) and decreased values for Severus (300 kg ha^{-1}) and P 8105 (319 kg ha^{-1}). At silage maturity, as already shown for the biomass nitrogen uptake, the leaf nitrogen uptake also reached higher values for the late maturing cultivars KWS 9361 and Cannavaro (87- 98 kg ha^{-1}) compared to the early maturing cultivars Severus and P 8105 (58- 63 kg ha^{-1}). During the growing season in Allershausen in 2016, the N fertilization levels always exerted a significant effect on all parameters ($p < 0.001$) except for grain nitrogen uptake at flowering and stem nitrogen uptake at silage maturity. The differences in total nitrogen uptake between the highest and lowest fertilization levels accounted for only 1.5 t ha^{-1} at flowering and increased to 7 t ha^{-1} at silage maturity and to 5 t ha^{-1} at grain maturity. Also, the leaf nitrogen uptake difference between the highest and lowest fertilization level reached 61 kg ha^{-1} at flowering and silage maturity and increased to 89 kg ha^{-1} at grain maturity. The fertilization level also had an effect on stem nitrogen uptake, where from the lowest to the highest fertilization level an increase of 32 kg ha^{-1} was observed at flowering, whereas only a slight difference at silage maturity with 3.6 kg ha^{-1} and 1.6 kg ha^{-1} at grain maturity was found (Tables 12 and 14).

The effects of different N levels on total nitrogen uptake, stem nitrogen uptake, grain nitrogen uptake and leaf nitrogen uptake in the year 2016 in Dürnast were highly significant. In contrast, cultivars did not differ in total nitrogen uptake at both harvest times. At silage maturity, the highest grain nitrogen uptake was achieved by Saludo (148 kg ha^{-1}), whereas Cannavaro reached only a grain nitrogen uptake of 123 kg ha^{-1}. Saludo performed best regarding the stem nitrogen uptake compared to Cannavaro (25 kg ha^{-1}) which showed decreased nitrogen values of 17 kg ha^{-1}. However, despite the lower stem nitrogen uptake and grain nitrogen uptake values, Cannavaro achieved the highest leaf nitrogen uptake with 44.8 kg ha^{-1} compared to Lapriora with decreased leaf nitrogen uptake values of 30 kg ha^{-1} (Tables 13 and 14)

Table 11: Average nitrogen uptake of total above-ground biomass (TNU), leaf nitrogen uptake (LNU), stem nitrogen uptake (SNU) and grain nitrogen uptake (GNU) in kg ha^{-1} at flowering, silage and grain maturity of all cultivars and fertilization levels for Thalhausen in 2015.

Year 2015	**Flowering** $\left(\frac{kg}{ha}\right)$			**Silage maturity** $\left(\frac{kg}{ha}\right)$			**Grain maturity** $\left(\frac{kg}{ha}\right)$		
TH	50 $\left(\frac{kg\ N}{ha}\right)$	150 $\left(\frac{kg\ N}{ha}\right)$	250 $\left(\frac{kg\ N}{ha}\right)$	50 $\left(\frac{kg\ N}{ha}\right)$	150 $\left(\frac{kg\ N}{ha}\right)$	250 $\left(\frac{kg\ N}{ha}\right)^1$	50 $\left(\frac{kg\ N}{ha}\right)$	150 $\left(\frac{kg\ N}{ha}\right)$	250 $\left(\frac{kg\ N}{ha}\right)$
TNU	56.7± 4.3	77± 20.4	83.5± 26.6	115± 26.5	156.7± 31.4	192.1± 40.4	131.2± 26.4	185.4± 31.2	208.2± 39.1
LNU	42.6± 8	63.4± 13	75± 22.4	21.4± 4.8	29.8± 6.9	40.7± 18.2	14.4± 4.7	25.3± 7.8	31.9± 13.6
SNU	29.7± 7	42.3± 11	50.7± 13.5	10.2± 2	13.7± 3.5	18.6± 7.7	13.2± 3.3	18.7± 4.7	20.8± 4.9
GNU				81.4± 21.5	105.7± 30.7	126.8± 33	92.7± 20.2	132.4± 23.7	147.8± 32.4

Table 12: Average nitrogen uptake of total above-ground biomass (TNU), leaf nitrogen uptake (LNU), stem nitrogen uptake (SNU) and grain nitrogen uptake (GNU) in kg ha^{-1} at flowering, silage and grain maturity of all cultivars and fertilization levels for Allershausen in 2016.

Year 2016	**Flowering** $\left(\frac{kg}{ha}\right)$			**Silage maturity** $\left(\frac{kg}{ha}\right)$			**Grain maturity** $\left(\frac{kg}{ha}\right)$		
AL	50 $\left(\frac{kg\ N}{ha}\right)$	150 $\left(\frac{kg\ N}{ha}\right)$	250 $\left(\frac{kg\ N}{ha}\right)$	50 $\left(\frac{kg\ N}{ha}\right)$	150 $\left(\frac{kg\ N}{ha}\right)$	250 $\left(\frac{kg\ N}{ha}\right)$	50 $\left(\frac{kg\ N}{ha}\right)$	150 $\left(\frac{kg\ N}{ha}\right)$	250 $\left(\frac{kg\ N}{ha}\right)$
TNU	130.3 ± 8.8	170.8 ±45.5	191.4± 40.4	278.8± 68.2	369.5± 118.9	338.9± 110.6	243.7± 47.12	309.7± 74.47	332.1± 50.57
LNU	70.5± 19	97.1± 20.2	106.5± 26.5	49.2± 16.6	85.1± 38.9	85.4± 19.2	29.7± 9.4	40.6± 16.4	39.6± 16.5
SNU	50.6± 12.7	72.7± 18.1	82.2± 22	27± 7.4	27± 11.2	30.6± 12.2	27.8± 10.3	27.5± 8.9	32.2± 11.1
GNU	8.6± 4.9	9.7± 4.2	9.1±4.1	202.4± 51.6	264.5± 86.3	234.6± 75	193.2± 42.8	237.2± 61.2	246.5± 41.5

Table 13: Average nitrogen uptake of total above-ground biomass (TNU), leaf nitrogen uptake (LNU), stem nitrogen uptake (SNU) and grain nitrogen uptake (GNU) in kg ha^{-1} at flowering, silage and grain maturity of all cultivars and fertilization levels for Dürnast in 2016.

Year 2016	**Flowering** $\left(\frac{kg}{ha}\right)$			**Silage maturity** $\left(\frac{kg}{ha}\right)$			**Grain maturity** $\left(\frac{kg}{ha}\right)$		
DU	50 $\left(\frac{kg\ N}{ha}\right)$	150 $\left(\frac{kg\ N}{ha}\right)$	250 $\left(\frac{kg\ N}{ha}\right)$	50 $\left(\frac{kg\ N}{ha}\right)$	150 $\left(\frac{kg\ N}{ha}\right)$	250 $\left(\frac{kg\ N}{ha}\right)$	50 $\left(\frac{kg\ N}{ha}\right)$	150 $\left(\frac{kg\ N}{ha}\right)$	250 $\left(\frac{kg\ N}{ha}\right)$
TNU	70± 30.8	117.5± 32	149.1± 28.2	128.7± 63.8	204.2± 50	260.5± 68.3			
LNU				26.22± 13.35	41.2± 14.53	50.9± 19			
SNU				15.54± 6.72	22.04± 6.65	28.2± 8.7			
GNU				86.86± 46.25	141± 35.86	182± 51.58			

Table 14: Statistical overview for the variables total, stem, grain and leaf nitrogen uptake in kg ha^{-1} (TNU, SNU, GNU, LNU) at flowering and silage maturity, indicating differences between cultivars and the treatment N. Statistically significant differences ($P < 0.05$) are indicated in bold for all experimental sites.

	Flowering				**Silage maturity**			
	TNU $\left(\frac{kg}{ha}\right)$	SNU $\left(\frac{kg}{ha}\right)$	GNU $\left(\frac{kg}{ha}\right)$	LNU $\left(\frac{kg}{ha}\right)$	TNU $\left(\frac{kg}{ha}\right)$	SNU $\left(\frac{kg}{ha}\right)$	GNU $\left(\frac{kg}{ha}\right)$	LNU $\left(\frac{kg}{ha}\right)$
2015_TH								
N	**<0.001**	**<0.001**		**<0.001**	**<0.001**	**<0.001**	**<0.001**	**<0.001**
cultivars	**<0.001**	0.09		**<0.001**	**0.024**	**<0.001**	**<0.001**	**<0.001**
cultivars x N	**0.03**	0.1		**0.026**	**0.013**	**0.014**	**0.047**	**<0.001**
2016_AL								
N	**<0.001**	**<0.001**	0.461	**<0.001**	**<0.001**	0.187	**0.002**	**<0.001**
cultivars	**<0.001**	**<0.001**	**<0.001**	**<0.001**	0.047	**<0.001**	0.357	**0.002**
cultivars x N	0.057	**0.041**	0.55	0.684	**0.041**	0.3	0.71	0.244
2016_DU								
N	**<0.001**				**<0.001**	**<0.001**	**<0.001**	**<0.001**
cultivars	0.012				0.186	**<0.001**	**0.015**	**<0.001**
cultivars x N	0.076				0.399	**0.006**	0.043	0.583

The heritability of the biomass nitrogen uptake was comparable to the biomass dry weight and showed the highest values at flowering with a heritability of 0.9 in the year 2016 in Dürnast. Comparably, the heritability observed in Thalhausen in 2015 and 2016 in Allershasuen indicated values of 0.88 and 0.75 (Tables 15, 16, 17). In general the heritability of the total nitrogen uptake decreased steadily from flowering to grain maturity.

In the year 2015 at the field site Thalhausen the highest heritability of 0.88 was found at the highest fertilization level at flowering. At silage maturity, the heritability of the total nitrogen uptake decreased to 0.73 and reached low values of 0.20 in 2015 in Thalhausen at the highest fertilization level. In contrast the heritability of the total nitrogen uptake at the lowest fertilization level was always lower compared to the highest fertilization level. The parameter leaf nitrogen uptake also showed the highest heritability at the highest fertilization level ranging from 0.84 to

0.99 from flowering to grain maturity. The lowest heritability of the leaf nitrogen uptake was observed at the lowest fertilization level. From flowering to grain maturity, also for stem nitrogen uptake increased heritability values were observed (0.69-0.77) at the highest fertilization level and low heritabilities were found at the lowest fertilization level (0.03-0.36). However the heritability of the grain nitrogen uptake increased from flowering to silage maturity but the heritability was zero at grain maturity (Table 15).

Table 15: Broad sense heritability (hÂ²) of total, leaf, stem, and corn nitrogen uptake (kg ha^{-1}) of different maize hybrids at flowering, silage and grain maturity indicated for all cultivars and fertilization levels in Thalhausen in the year 2015.

Year 2016	**Flowering** (hÂ²)			**Silage maturity** (hÂ²)			**Grain maturity** (hÂ²)		
	50 $\left(\frac{\text{kg N}}{\text{ha}}\right)$	150 $\left(\frac{\text{kg N}}{\text{ha}}\right)$	250 $\left(\frac{\text{kg N}}{\text{ha}}\right)$	50 $\left(\frac{\text{kg N}}{\text{ha}}\right)$	150 $\left(\frac{\text{kg N}}{\text{ha}}\right)$	250 $\left(\frac{\text{kg N}}{\text{ha}}\right)$	50 $\left(\frac{\text{kg N}}{\text{ha}}\right)$	150 $\left(\frac{\text{kg N}}{\text{ha}}\right)$	250 $\left(\frac{\text{kg N}}{\text{ha}}\right)$
TNU (kg ha^{-1})	0.62	0.80	0.88	0.00	0.55	0.73	0.00	0.63	0.20
LNU (kg ha^{-1})	0.00	0.57	0.84	0.86	0.87	0.95	0.64	0.87	0.99
SNU (kg ha^{-1})	0.03	0.00	0.69	0.70	0.60	0.73	0.36	0.72	0.77
GNU (kg ha^{-1})	0.68	0.96	0.93	0.71	0.82	0.63	0.37	0.63	0.00

As already shown at the field site Thalhausen in 2015, in Allershausen in 2016 the heritability mostly increased with enhanced fertilization rate for all parameters at flowering, silage and grain maturity. However, at flowering, an increeased heritability at the highest fertilization level was not observed for the parameters total nitrogen uptake and leaf nitrogen uptake with the highest heritability being observed at the medium fertilization level amounting to 0.75 or 0.80 (Table 16).

In contrast to Thalhausen in 2015 and Allershausen in 2016, the field site Dürnast in 2016 revealed the highest heritability for total nitrogen uptake at the medium fertilization level at flowering. At silage maturity, a similar pattern as in the other two experimental fields was evident with increased heritability for the parameters total above-ground nitrogen uptake, leaf and stem nitrogen uptake at the highest fertilization level. Only for the parameter grain nitrogen uptake increased heritabilities were found at the lowest fertilization level at silage maturity (Table 17).

Table 16: Broad sense heritability (hÂ²) of the total above-ground nitrogen uptake, leaf nitrogen uptake, stem nitrogen uptake and corn nitrogen uptake (kg ha^{-1}) of different maize hybrids at flowering, silage and grain maturity indicated for all cultivars and fertilization levels in Allershausen in 2016.

Year 2016	**Flowering** (hÂ²)			**Silage maturity** (hÂ²)			**Grain maturity** (hÂ²)		
	50 $\left(\frac{\text{kg N}}{\text{ha}}\right)$	150 $\left(\frac{\text{kg N}}{\text{ha}}\right)$	250 $\left(\frac{\text{kg N}}{\text{ha}}\right)$	50 $\left(\frac{\text{kg N}}{\text{ha}}\right)$	150 $\left(\frac{\text{kg N}}{\text{ha}}\right)$	250 $\left(\frac{\text{kg N}}{\text{ha}}\right)$	50 $\left(\frac{\text{kg N}}{\text{ha}}\right)$	150 $\left(\frac{\text{kg N}}{\text{ha}}\right)$	250 $\left(\frac{\text{kg N}}{\text{ha}}\right)$
TNU (kg ha^{-1})	0.50	0.75	0.54	0.00	0.00	0.80	0.45	0.00	0.68
LNU (kg ha^{-1})	0.60	0.80	0.58	0.57	0.42	0.79	0.92	0.90	0.95
SNU (kg ha^{-1})	0.70	0.75	0.81	0.61	0.53	0.60	0.33	0.56	0.78
GNU (kg ha^{-1})	0.10	0.53	0.76	0.00	0.13	0.22	0.54	0.00	0.54

Table 17: Broad sense heritability (hÂ²) of total, leaf, stem, and grain nitrogen uptake (kg ha^{-1}) of different maize hybrids at flowering and silage maturity of all cultivars and fertilization levels in Dürnast in 2016.

Year 2016	**Flowering** (hÂ²)			**Silage maturity** (hÂ²)		
	50 $\left(\frac{\text{kg}}{\text{ha}}\right)$	150 $\left(\frac{\text{kg}}{\text{ha}}\right)$	250 $\left(\frac{\text{kg}}{\text{ha}}\right)$	50 $\left(\frac{\text{kg}}{\text{ha}}\right)$	150 $\left(\frac{\text{kg}}{\text{ha}}\right)$	250 $\left(\frac{\text{kg}}{\text{ha}}\right)$
TNU (kg ha^{-1})	0.00	0.93	0.06	0.17	0.29	0.57
LNU (kg ha^{-1})				0.23	0.63	0.84
SNU (kg ha^{-1})				0.00	0.00	0.84
GNU (kg ha^{-1})				0.92	0.26	0.64

4.4.2 Spectral Indices

In general, the correlations between spectral reflection indices/data and the maize organs stem and corn were very low. As well the evaluation of the correlation of all passive wavelengths calculated by contour map analysis is not outlined since only poor relationships were observed.

Correlations of active and passive sensors and additionally of indices calculated from the passive sensor by means of a contour map analysis are indicated across the three nitrogen fertilization levels for all three field experiments in Tables 13, 14, 15. No significant correlations could be observed for the active sensors Greenseeker and ALS and therefore the focus is placed more on results from the passive sensor.

In general, hyperspectral passive sensing (HPS) delievered an improved performance in assessing non-destructive parameters compared to active sensing systems. Leaf dry weight and nitrogen uptake of leaves were best assessed among the organs by non-destructive sensing.

In 2015 on the field site Thalhausen, only the active sensor CropCircle (Cc) exhibited weak correlations. The best correlations were obtained at wavebands around 700 nm at flowering and silage maturity with improved correlations being observed at silage maturity. In general, nitrogen uptake could be better detected than biomass at flowering and at silage maturity, with enhanced relationships found at silage maturity. During flowering, better relationships were found for total biomass compared to leaf biomass, however, this was reversed at silage maturity. Also good correlations (R^2 = 0.79) could be observed for the nitrogen nutrition index (NNI) where sensors performed best at silage maturity (Table 18).

Table 18: Correlations (R^2) between **the means from cultivars x N levels** and the non-destructively and destructively assessed parameters leaf and biomass dry weight, leaf and biomass nitrogen uptake at flowering and silage maturity abbreviated as LDW, BDW, LNU and BNU, respectively, for Thalhausen in the year 2015.

	Flowering					**Silage maturity**				
Sensors	LDW	BDW	LNU	BNU	NNI	LDW	BDW	LNU	BNU	NNI
Cc 730_670	0.35	0.34	0.09	0.07	0.00	0.25	0.040	0.07	0.02	0.01
Cc 670	**0.56**	**0.58**	0.02	0.24	0.03	**0.53**	0.19	0.05	0.07	0.01
HPS NDVI	0.45	0.47	0.27	0.21	0.03	**0.61**	0.01	0.42	0.00	0.06
HPS 730_670	0.39	0.47	0.14	0.09	0.00	**0.62**	0.28	0.41	0.00	0.05
HPS 760_670	0.45	**0.53**	0.31	0.25	0.06	**0.72**	0.40	0.59	0.01	0.16
HPS 760_730						0.49	**0.57**	**0.76**	0.37	**0.59**
HPS 742_764	0.35	0.32	**0.61**	**0.60**	**0.63**	**0.79**	**0.51**	**0.68**	**0.54**	**0.79**
HPS PRI	0.36	0.45	0.26	0.24	0.06	0.25	0.32	0.46	0.37	0.44
HPS 670	0.46	0.49	0.29	0.22	0.03	**0.6**	0.37	0.46	0.00	0.07
REIP	0.13	0.16	**0.56**	**0.56**	**0.68**	0.07	0.35	0.44	**0.62**	**0.76**
(700-555)/ (700+555)	0.35	0.32	0.13	0.09	0.00	**0.79**	0.41	**0.58**	0.02	0.12

In 2016, on the field site in Allershausen (AL), only weak correlations were observed at flowering and at silage maturity. The modified active ALS sensor showed better correlations compared to the Crop Circle and the Greenseeker but still revealed weaker relationships than the passive sensor. The best correlation observed at flowering were found at around 900 nm for the above ground biomass (LDW, BDW). The nitrogen uptake was best detected at wavelengths around 700 nm at silage maturity (Table 19).

Table 19: Best correlations (R^2) between **the means by cultivars x N levels** and of the non-destructively and destructively assessed parameters leaf and biomass dry weights, leaf and biomass nitrogen uptake at flowering and silage maturity abbreviated as LDW, BDW, LNU and BNU, respectively for the year 2016 on the field site in Allershausen.

	Flowering					**Silage maturity**				
Sensors	LDW	BDW	LNU	BNU	NNI	LDW	BDW	LNU	BNU	NNI
ALS900	0.26	0.42	0.14	0.10	0.01	0.12	0.02	0.02	0.00	0.04
R1100_1200	**0.70**	**0.54**	0.33	0.16	0.03	**0.62**	**0.59**	0.35	0.43	0.09
R900_970	**0.68**	**0.58**	0.30	0.16	0.02	**0.52**	**0.53**	0.26	0.34	0.06
WI	**0.68**	**0.57**	0.30	0.16	0.02	**0.50**	**0.50**	0.24	0.32	0.05
REIP	0.05	0.00	0.31	0.28	0.41					
NIR/NIR	0.12	0.00	0.38	0.34	0.33					

In 2016 on the field site in Dürnast among the active sensors, only the Crop-Circle (Cc) exhibited weak correlations, especially at 760/670 nm in contrast to the other active sensors revealing no correlations. The best HPS-correlations were again obtained at wavebands around 700 nm at flowering and silage maturity, with slightly lower correlations being observed at silage maturity. In general, both the parameters nitrogen uptake (R^2 = 0.76) and above ground biomass ($R^2 = 0.93$) indicated considerable correlations with enhanced relationships at flowering. During flowering best relationships were found for total biomass, however, this was reversed at silage maturity, where leaf dry weight was best assessed with the REIP index. Also moderate correlations were observed for the nitrogen nutrition index (NNI) where sensors performed best at silage maturity (Table 20).

Table 20: Best correlations (R^2) of **means by cultivars x N levels** and of the non-destructively and destructively assessed parameters leaf and biomass dry weights, leaf and biomass nitrogen uptake at flowering and silage maturity abbreviated as LDW, BDW, LNU and BNU, respectively, for the year 2016 in Dürnast.

	Flowering			**Silage maturity**				
Sensors	BDW	BNU	NNI	LDW	BDW	LNU	BNU	NNI
Nir/green	**0.93**	**0.65**	**0.56**	**0.73**	**0.66**	0.49	0.36	**0.53**
R760_730	**0.89**	**0.75**	**0.64**	**0.66**	**0.78**	**0.64**	**0.51**	**0.61**
R780_740	**0.90**	**0.74**	**0.63**					
NIR/red	**0.86**	0.31	0.28	**0.57**	0.26	0.15	0.03	0.15
YARA	**0.89**	**0.75**	**0.64**					
REIP	**0.88**	**0.76**	**0.65**					
R1100_1200	**0.88**	**0.54**	0.36	0.27	**0.57**	**0.76**	**0.66**	**0.56**
Nirr700	**0.92**	**0.63**	**0.54**	**0.72**	**0.61**	0.46	0.28	0.43

Very high heritability of 0.9 for the sensor indices could be achieved at flowering and silage maturity in all experimental field trials. The highest heritability up to 0.99 could be estimated across all fertilization levels and sampling dates in the year 2016 in the field site Dürnast. In contrast, at medium and high fertilization rates the heritability was decreased at flowering and silage maturity in the same year in Allershausen. An increased heritability of 0.90 was found at the lowest fertilization rate at flowering in Allershausen in 2016. Additionally, in the year 2015 for the field site Thalhausen with the lowest fertilization level (0.78) and medium fertilization level (0.88) weaker but still substantial heritabilities could be observed at flowering (Tables 21 and 22).

Table 21: Heritability (hÂ²) delivered by different sensors at flowering and silage maturity for the years 2015 in Thalhausen (TH), 2016 in Allershausen (AL) and 2016 in Dürnast (DU) at the nitrogen fertilization levels of 50 and 150 kg N ha^{-1}.

	Flowering			**Silage maturity**		
	2015	**2016**	**2016**	**2015**	**2016**	**2016**
Sensors	**TH_50**	**AL_50**	**DU_50**	**TH_50**	**AL_50**	**DU_50**
Cc730_670	0.74	0.60	0.91	0.84	0.00	0.90
Cc760_670	0.00	0.70	0.74	0.87	0.00	0.80
Cc760_730	0.78	0.60	0.90	0.12	0.00	0.74
HPS NDVI	0.68	0.90	0.57	0.9	0.29	0.99
HPS 730_670	0.71	0.90		0.95	0.50	
HPS 760_670	0.64	0.90		0.94	0.00	
HPS 760_730	0.72	0.80	0.76	0.46	0.00	0.82
HPS 780_740	0.66	0.80	0.82	0.72	0.00	0.80
HPS 742_764	0.00	0.80		0.66	0.00	
HPS REIP	0.63	0.80	0.82	0.66	0.00	0.80
Nir/green	0.74	0.90	0.76	0.53	0.00	0.90
YARA		0.80	0.75		0.00	0.80
R1100_1200	0.05	0.90	0.69	0.06	0.00	0.06
NIR/NIR		0.80			0.00	
WI		1.00			0.44	
R900_970	0.20	0.90	0.10	0.61	0.45	0.96
	2015	**2016**	**2016**	**2015**	**2016**	**2016**
Sensors	**TH_150**	**AL_150**	**DU_150**	**TH_150**	**AL_150**	**DU_150**
Cc730_670	0.00	0.65	0.72	0.74	0.65	0.80
Cc760_670	0.00	0.53	0.75	0.84	0.53	0.75
Cc760_730	0.00	0.35	0.44	0.90	0.35	0.86
HPS NDVI	0.83	0.03	0.85	0.90	0.03	0.92
HPS 730_670	0.88	0.43		0.90	0.43	
HPS 760_670	0.88	0.45		0.90	0.45	
HPS 760_730	0.84	0.30	0.92	0.90	0.35	0.77
HPS 780_740	0.83	0.33	0.93	0.90	0.36	0.69
HPS 742_764	0.83	0.27		0.89	0.27	
HPS REIP	0.62	0.00	0.94	0.91	0.00	0.70
Nir/green	0.87	0.32	0.95	0.98	0.33	0.88
YARA		0.29	0.93		0.29	0.74
R1100_1200	0.20		0.92	0.01		0.30
NIR/NIR		0.30			0.30	
WI		0.14			0.14	
R900_970	0.85	0.22	0.90	0.83	0.22	0.96

Table 22: Heritability (hÂ^2) delivered by different sensors at flowering and silage maturity for the years 2015 in Thalhausen (TH), 2016 in Allershausen (AL) and 2016 in Dürnast (DU) at the nitrogen fertilization level 250 kg N ha^{-1}.

	Flowering			**Silage maturity**		
	2015	**2016**	**2016**	**2015**	**2016**	**2016**
Sensors	**TH_250**	**AL_250**	**DU_250**	**TH_250**	**AL_250**	**DU_250**
Cc730_670	0.49	0.13	0.92	0.47	0.13	0.17
Cc760_670	0.00	0.19	0.96	0.94	0.19	0.00
Cc760_730	0.49	0.12	0.41	0.38	0.12	0.70
HPS NDVI	0.92		0.99	0.97	0.20	0.98
HPS 730_670	0.95	0.26		0.98	0.26	
HPS 760_670	0.95	0.05		0.97	0.05	
HPS 760_730	0.88	0.00	0.99	0.87		0.88
HPS 780_740	0.88	0.00	0.99	0.79	0.00	0.84
HPS 742_764	0.88	0.00		0.88	0.00	
HPS REIP	0.90	0.00	0.99	0.8	0.00	0.90
Nir/green	0.00	0.00	0.99	0.95	0.00	0.95
YARA		0.00	0.99		0.00	0.88
R1100_1200	0.15		0.87	0.00		0.04
NIR/NIR		0.00			0.00	
WI		0.35			0.35	
R900_970	0.49	0.33	0.94	0.9	0.34	0.98

Testing the relationships of destructive and non-destructive parameters at varying nitrogen fertilization rated, better correlations could be observed for selected organs in all years. In Tables 23, 24 & 25 the best correlations for indices and from all tested destructive parameters are presented. Across all years and field experiments leaf dry weight and leaf nitrogen uptake always exhibited the best correlations with the information delivered by the sensors, independent of weather and soil conditions.

In 2015 on the field site in Thalhausen, the best relationships were found around wavebands of 700 nm (demonstrated in contour maps and by indices correlation) at flowering and silage maturity. At the highest fertilization rate, correlations between non-destructive and destructive parameters were highest at flowering and silage maturity with improved correlations being observed at silage maturity (Table 23). Among the organs, leaf biomass dry weight and leaf nitrogen uptake could be best assessed at silage maturity with the same index R900_970.

Table 23: Destructive parameters leaves dry weight in kg ha^{-1} (LDW), above-ground biomass in t ha^{-1} (BDW) and nitrogen uptake of leaves (LNU) and above-ground biomass (BNU) in kg ha^{-1} being best correlated (R²) to reflectance information. Best indices for given fertilization rates at 50, 150 and 250 kg N ha^{-1} in 2015 on the field site in Thalhausen (TH) are indicated in bold. For BDW and BNU no noticeable differences were observed at flowering and silage maturity.

2015_TH

50 kg N ha^{-1}	**Flowering**				**Silage maturity stage**				
Sensors	LDW	BDW	LNU	BNU	Sensors	LDW	BDW	LNU	BNU
REIP	0.26				VARI	0.4			
REIP		0.3			**PRI**		**0.44**		
R780_740			0.46		HPS742_764			0.56	
R780_740				0.4	Globalrad-green				0.2

2015_TH

150 kg N ha^{-1}	**Flowering**				**Silage maturity stage**				
Sensors	LDW	BDW	LNU	BNU	Sensors	LDW	BDW	LNU	BNU
REIP	0.19				VARI	0.63			
HPS730_670		0.2			HPS730_670		0.16		
CC670			0.11		HPS760_730			0.6	
CC670				0.11	PRI				0.1

2015_TH

250 kg N ha^{-1}	**Flowering**				**Silage maturity stage**				
Sensors	LDW	BDW	LNU	BNU	Sensors	LDW	BDW	LNU	BNU
Cc730_670	**0.48**				**R900_970**	**0.75**			
R760_730		**0.45**			CC670_730		0.39		
Cc730_670			**0.5**		**R900_970**			**0.8**	
R1100_1200				**0.47**	**R760_730**				**0.44**

In general, relationships were weak at flowering and at silage maturity in 2016 for the field site in Thalhausen (TH) with slightly better correlations being observed for the leaf dry weight (R² = 0.61) at flowering compared to leaves dry weight at silage maturity. As well in 2015 on the field site in Thalhausen, best correlations were found at the highest fertilization rate at silage maturity in 2016 on the field site Allershausen. Also the assessment of the leaf dry weight (R² = 0.61) and biomass dry weight ($R^2 = 0.42$) was noticable at flowering at the lowest nitrogen fertilization level. Particularly the nitrogen uptake parameters leaf and biomass showed hardly any relationship to the sensed information at flowering but reached improved R^2-values at silage maturity at the highest fertilization level ($R^2 = 0.55$ for LNU and $R^2 = 0.37$ for BNU) (Table 24).

Better correlations at silage maturity were also observed in 2016 on the field site Dürnast, which is in agreement with the observations in 2015 on the field site Thalhausen (Table 23). In contrast to 2015 on the field site Thalhausen and in 2016 on the field site Allershausen above-ground biomass was better detected at flowering but still showed moderate relationships at silage maturity (Table 22). At the lowest fertilization level at flowering BDW showed an R^2 of 0.64 (Table 26).

Table 24: Correlations (R²) between the destructively assessed parameters leaf dry weight in kg ha^{-1} (LDW), above-ground biomass in t ha^{-1} (BDW) and nitrogen uptake of leaves (LNU) and above-ground biomass (BNU) in kg ha^{-1} and the best fitted sensor index within given nitrogen fertilization levels (50, 150 and 250 kg N ha^{-1}) in 2016 at the field site Allershausen. The Greenseeker active sensor is abbreviated with GS and the CropCircle active sensor as Cc.

2016_AL

50 kg N ha^{-1}	**Flowering**				**Silage maturity stage**				
Sensors	LDW	BDW	LNU	BNU	Sensors	LDW	BDW	LNU	BNU
R1100_1200	**0.61**				ALS760	0.04			
WI		0.42			R780_740		0.15		
R1100_1200			0.3		ALS970			0.05	
R1100_1200				0.09	R780_740				0.28

2016_AL

150 N ha^{-1}	**Flowering**				**Silage maturity stage**				
Sensors	LDW	BDW	LNU	BNU	Sensors	LDW	BDW	LNU	BNU
R900_970	0.58				RedGS	0.18			
WI		0.3			R742_764		0.11		
HPS760_670			0.4		RedGS			0.15	
NIRred				0.18	GNDVI				0.14

2016_AL

250 N ha^{-1}	**Flowering**				**Silage maturity stage**				
Sensors	LDW	BDW	LNU	BNU	Sensors	LDW	BDW	LNU	BNU
R1100_1200	0.39				**SI**	**0.55**			
ALS970		0.23			**Reip**		**0.48**		
R1100_1200			0.3		**Nir/Red**			**0.55**	
ALS970				0.18	**R780_740**				**0.37**

Table 26: Correlations (R^2) between the destructively assessed parameters leaf dry weight in kg ha^{-1} (LDW), above-ground biomass in t ha^{-1} (BDW), nitrogen uptake of leaves (LNU) and above-ground biomass (BNU) in kg ha^{-1}, and the best fitted sensor index within given fertilization levels (50, 150 and 250 kg N ha^{-1}) in 2016_DU. The Greenseeker active sensor is abbreviated as GS.

2015_DU

50 kg N ha^{-1}	**Flowering**		**Silage maturity**				
Sensors	BDW	BNU		LDW	BDW	LNU	BNU
R760_730	**0.64**		R900_970	0.28			
R760_730		**0.45**	**REIP**		**0.38**		
			REIP			0.38	
			REIP				**0.44**

2015_DU

150 kg N ha^{-1}	**Flowering**		**Silage maturity**				
Sensors	BDW	BNU		LDW	BDW	LNU	BNU
NIR green	0.62		**NDVI**	**0.42**			
red GS		0.45	R900_970		0.35		
			REIP			0.41	
			R900_970				0.31

2015_DU

250 kg N ha^{-1}	**Flowering**		**Silage maturity**				
Sensors	BDW	BNU		LDW	BDW	LNU	BNU
R760_730	0.47		RedGS	0.07			
Reip		0.17	R1100_1200		0.25		
			R900_970			0.3	
			RARSa				0.36

4.4.3 Partial Least Square Regression (PLSR)

4.4.3.1 PLSR analysis of spectral information obtained on the field site Thalhausen in 2015

In 2015 on the field site Thalhausen, the above-ground biomass ranged between 6.4-7.3 t ha^{-1} at flowering, while the cultivars Barros (9.6 t ha^{-1}) and Vitallo (8.8 t ha^{-1}) achieved the highest biomass dry weight. At silage maturity, biomass dry weights of 15.5 - 18.3 t ha^{-1} were reached by Barros and Cannavaro (22 t ha^{-1}). At flowering, a moderate total nitrogen uptake of 60- 80 kg ha^{-1} was observed and increased at silage maturity to 115-156 kg ha^{-1}. Solid relationships for the organ leaf biomass and nitrogen uptake were found at flowering and at silage maturity. Comparable to biomass dry weight, biomass nitrogen uptake showed better relationships at silage maturity compared to flowering. Relations to biomass dry weight and biomass nitrogen uptake were generally weaker compared to leaf dry weight and leaf nitrogen uptake. The most important wavelengths detecting biomass dry weight and leaf dry weight ranged between wavebands at 500-670 nm whereas the detection of nitrogen uptake was obtained at higher wavebands from 600-800 nm (Tables 27 and 28).

Table 27: Partial least square regressions (PLSR) calculated with the parameters BDW t ha^{-1} and BNU in kg ha^{-1} for the experimental site Thalhausen in 2015 at both sampling times.

		Total aboveground biomass				
		PC	Slope	Offset	RMSE	R²
Flowering	Dry weight	7	0.15	57.82	16.98	0.15
	N uptake	7	0.23	74.11	25.85	0.23
Silage maturity	Dry weight	7	0.45	54.87	24.37	0.45
	N uptake	7	0.56	69.45	30.1	0.56

Table 28: Partial least square regressions (PLSR) calculated with the parameter LDW in t ha^{-1} and LNU in kg ha^{-1} of the experimental site Thalhausen in 2015 at both sampling times.

		Leaves				
		PC	Slope	Offset	RMSE	R²
Flowering	Dry weight	7	0.6	0.46	0.14	0.68
	N uptake	7	0.54	27	14	0.54
Silage maturity	Dry weight	7	0.63	4.7	1.8	0.63
	N uptake	7	0.71	8.3	5.6	0.71

With the PLSR-model, a grouping of cultivars for the traits biomass dry weight, biomass nitrogen uptake, leaf dry weight and leaf nitrogen uptake was achieved at flowering and silage maturity with better classifications being observed at flowering. By creating score plots similarities with regard to the two main components of the different cultivars (expressed on the axis) are visually demonstrated. An example of cultivar grouping is shown in Figure one. Grouping with regard to the nitrogen fertilization levels was not possible for the parameters biomass dry weight, leaf dry weight, biomass nitrogen uptake and leaf nitrogen uptake at flowering and silage maturity (Fig 1).

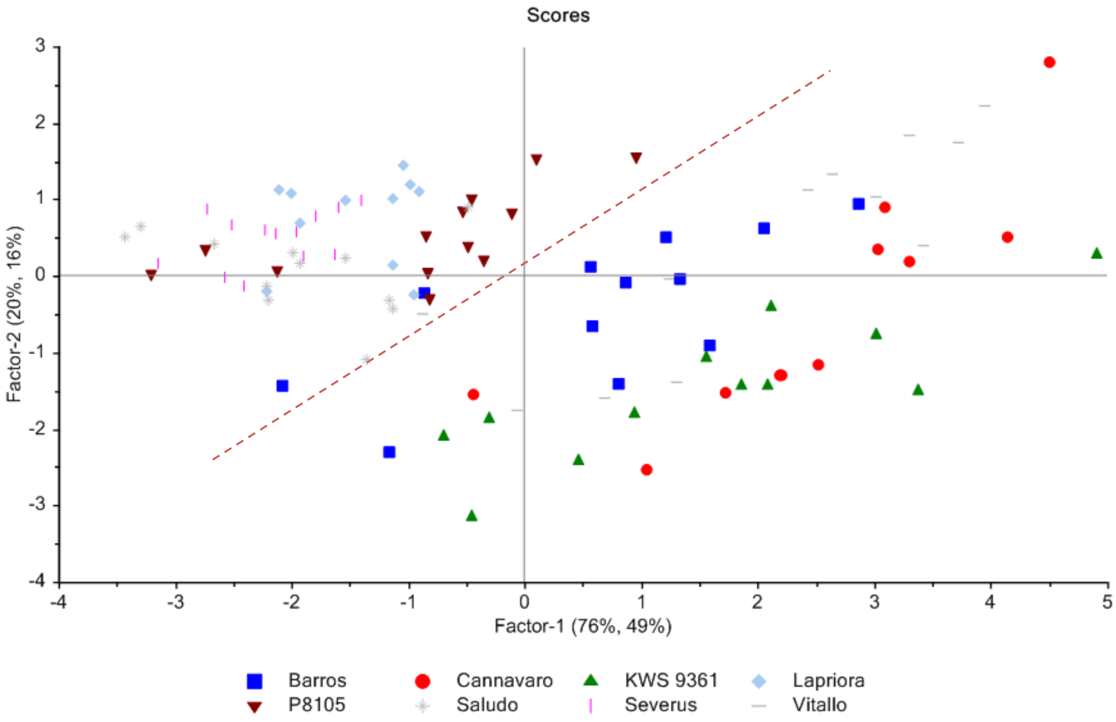

Fig 1: Grouping of different cultivars with regard to the trait leaf nitrogen uptake (LNU) on the site Thalhausen at flowering in 2015.The red line separates the groups. The two main components and the associated variances are illustrated on the axis.

4.4.3.2 PLSR analysis of spectral information from the field site Allershausen in 2016

In 2016, on the site Allershausen, the aboveground biomass at flowering reached an increase in biomass of 8.4-9.8 t ha^{-1} compared to 2015 in Thalhausen. The best growing cultivars were the late maturing cultivars Barros (9.5 t ha^{-1}), Cannavaro (12 t ha^{-1}) and Vitallo (9.4 t ha^{-1}). Nitrogen uptake at flowering exceeded the average with 130-190 kg ha^{-1} and also at silage maturity, an above- average nitrogen uptake of 280-340 kg ha^{-1} was found. At silage maturity, a final biomass yield of 30-38 t ha^{-1} was obtained with the cultivars Barros (41 t ha^{-1}) and Cannavaro (48 t ha^{-1}) exceeding the final yield average. The plant traits BDW ($R^2 = 0.5$) and BNU ($R^2 = 0.3$) could be detected best at silage maturity which was confirmed in 2015 on the field site Thalhausen. However the plant traits leaf dry weight ($R^2 = 0.6$) and leaf nitrogen uptake ($R^2 = 0.59$) were better detected at flowering. This was also observed in 2015 on the field site Thalhausen. The wavebands between 500-570 nm and 660-720 nm were most influential in distinguishing differences in biomass nitrogen uptake and leaf nitrogen uptake. The wavebands with best relationships to biomass (BDW and LDW) ranged between 530-600 nm and 660-706 nm (Appendix Tables 9–16). A grouping regarding cultivars (and maturity grade) was possible as shown in Figure 2 whereas a classification according to the nitrogen fertilization rates was not possible (Tables 29 and 30).

Table 29: Partial least square regressions (PLSR) calculated with the parameter BDW in t ha^{-1} and BNU in kg ha^{-1} for the experimental site Allershausen in 2016 at both sampling times.

		Total aboveground biomass				
		PC	Slope	Offset	RMSE	R²
Flowering	Dry weight	7	0.36	5.6	1.6	0.36
	N uptake	7	0.36	104.33	36.63	0.36
Silage maturity	Dry weight	7	0.5	17.5	6.17	0.5
	N uptake	7	0.3	252.42	88.64	0.3

Table 30: Partial least square regressions (PLSR) calculated with the parameter LDW in t ha^{-1} and LNU in kg ha^{-1} for the experimental site Allershausen in 2016 at both sampling times.

		Leaves				
		PC	Slope	Offset	RMSE	R²
Flowering	Dry weight	7	0.66	0.98	0.42	0.66
	N uptake	7	5.9	40.46	17.7	0.59
Silage maturity	Dry weight	7	0.23	2.7	1.02	0.23
	N uptake	7	0.29	52	26.3	0.29

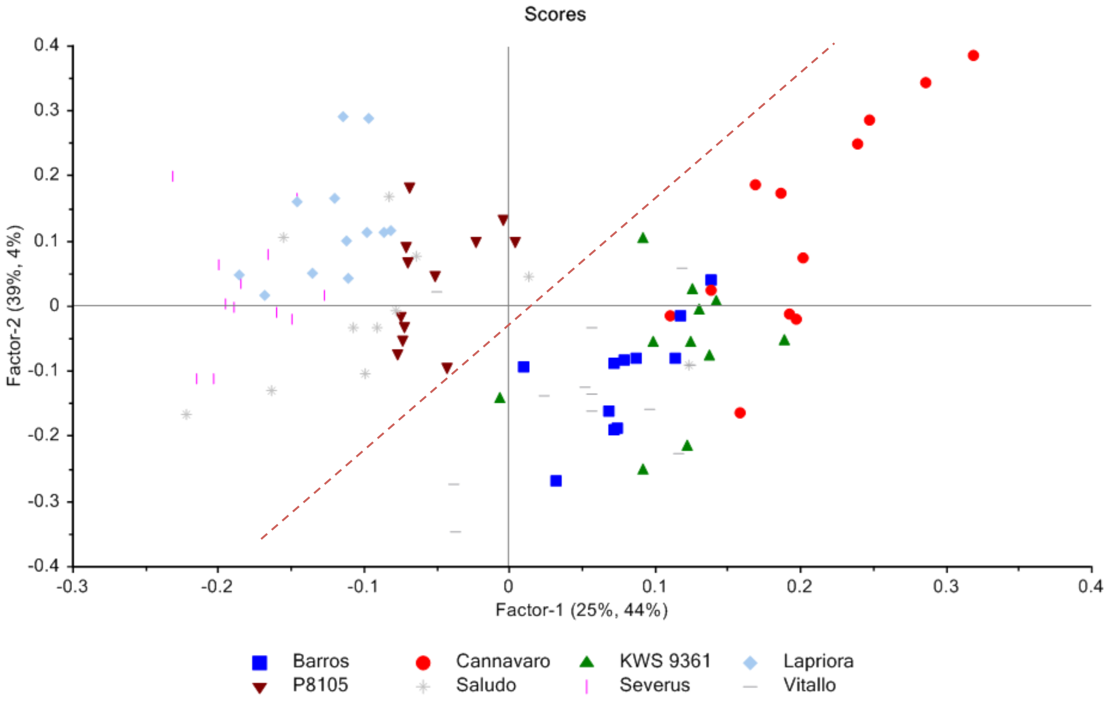

Fig 2: Grouping of differently maturing cultivars regarding the trait leaf dry weight (LDW) as obtained from the PLSR in 2015 on the field site Thalhausen at flowering. The red line separates groups. The two main components and the associated variances are illustrated on the axis.

4.4.3.3 PLSR analysis of spectral information from the field site Dürnast in 2016

In 2016 in Dürnast, an above-ground biomass of only 6-9 t ha^{-1} was obtained at flowering and also the yield at silage maturity was lower and reached only 16-28 t ha$^{- 1}$ in contrast to 2016 on the site in Allershausen. Also the nitrogen uptake was lower in Dürnast compared to Allershausen and ranged at flowering between 70- 150 kg ha^{-1} and at silage maturity around 200-260 kg ha^{-1}. The best performing cultivars were consistently Cannavaro and Vitallo at flowering (10 t ha $^{-1}$) and at silage maturity (25 t ha^{-1}). Rather close correlations were recorded at flowering as well as at silage maturity for all plant traits with always slightly better correlations found for both nitrogen uptake parameters. Best correlations between the sensed information and the total nitrogen uptake were observed at flowering ($R^2 = 0.84$) (Tables 31 and 32). The biomass detection could be best recorded with wavebands around 500-590 nm and 700- 730 nm. In contrast the most influential wavebands to detect nitrogen uptake were found between 600-650 nm, 700-720 nm and 720-750 nm (Appendix Tables 17-22). At silage maturity, a classification of cultivars or nitrogen fertilization levels was not possible and the PLSR models showed only tendencies of group building regarding the fertilization levels. In contrast, at flowering, a separation between the fertilization level 50 kg N ha^{-1} and the higher fertilization levels 150 and 250 kg N ha^{-1} could be observed (Fig. 3). Also a classification of the cultivars with regard to the biomass nitrogen uptake could be achieved and is shown in Figure 4.

Table 31: Partial least square regression (PLSR) calculated with the parameter above-ground biomass dry weight (BDW) in t ha^{-1} and total nitrogen uptake (TNU) in kg ha^{-1} for the experiment Dürnast in 2016 at both harvest samplings.

		Total aboveground biomass				
		PC	Slope	Offset	RMSE	R²
Flowering	Dry weight	7	0.76	1.9	1.09	0.76
	N uptake	7	0.84	18.25	17.8	0.84
Silage maturity	Dry weight	7	0.76	5.64	3.17	0.76
	N uptake	7	0.71	56.90	43.41	0.71

Table 32: Partial least square regression (PLSR) calculated with the parameter leaf dry weight (LDW) in t ha^{-1} and leaf nitrogen uptake (LNU) in kg ha^{-1} for the experiment Dürnast in 2016 at both harvest samplings.

		Leaves				
		PC	Slope	Offset	RMSE	R²
Silage maturity	Dry weight	7	0.63	0.81	0.4	0.63
	N uptake	7	0.75	10.78	0.78	0.75

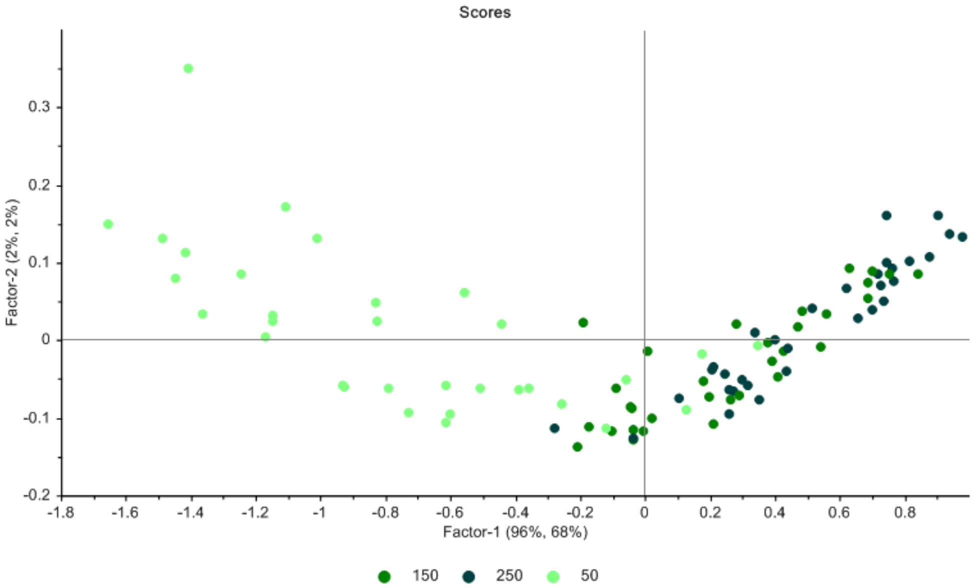

Figure 3: PLSR-model of data from 2016 from the field site Dürnast at flowering, illustrating the total biomass (BDW) distribution among the different fertilization levels 50, 150 and 250 kg N ha^{-1}. The two main components and the associated variances are illustrated on the axis.

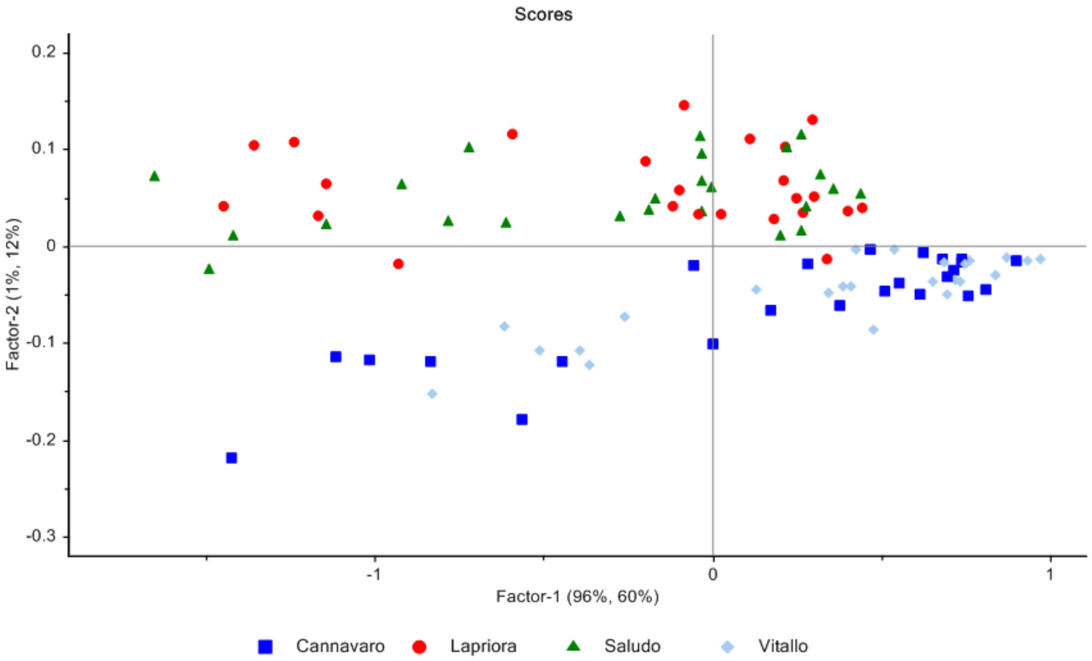

Figure 4: PLSR-model of data from 2016 in Dürnast at silage maturity, from the model for predicting BNU illustrating the total nitrogen uptake (BNU) distribution of different cultivars. The two main components and the associated variances are illustrated on the axis.

4.5 Discussion

Generally, for all sensors, the closest relationships were observed between spectral indices and the nitrogen status related parameters N content, aboveground N-uptake and NNI and these relationships are therefore primarily addressed. The evaluation of the correlation matrices revealed that an organ- and index-specific detection was not possible. Across all years and sampling dates, the R^2-values obtained for the relationships between the different sensors and the agronomic parameters differed. In agreement with Gitelson (1995) most of the destructively assessed parameters could be detected in the range around 700 nm whereas the indices around the near infra-red and the ratio 780_740 assessed destructive parameters best at flowering and silage maturity. These observations could be explained through different environmental influences throughout the years. Light intensity and the position of the sun could be a factor for a non-specific organ detection. Additionally, different ranges in yield ranges and differences in progressive senescence between the years could be a reason for the different performance of the indices.

In general, indices calculated from the passive sensors performed better compared to active sensors which confirms findings of Winterhalter et al. (2013) and Kipp et al. (2014b). Active sensors could not fully detect plant biomass due to a weaker light source than the natural sun light and particularly detection of nitrogen uptake at a large “sensor-to-target distance” by active sensors is rendered difficult in tall maize plants (Winterhalter et al., 2013). Elsayed (2015) and Jasper et al. (2009) also described poorer performance of active sensors caused by the lower penetration depth of the artificial light. Therefore, the discussion will be focused on the performance of passive sensors.

In all years, at given nitrogen fertilization levels, best correlations between the non-destructive and destructive measurements could be found at the lowest N level (R^2 varying from 0.38 to 0.64) and the highest N fertilization level (R^2 varying from 0.36 to 0.8). This was due to a higher differentiation of the cultivars in N-utpake and N translocation. However, differences over the years were observed with an improved sensor performance at silage maturity at the highest N fertilization rate in Thalhausen in the year 2015 possibly due to measurement errors at flowering. In 2015, a hot period during flowering could have affected the sensors´ performance and curled leaves resulting from heat stress could have influenced reflection from the maize canopy (Elsayed, 2015; Schlemmer et al., 2005). In contrast, improved detection was found at flowering at the lowest N fertilization rate in the year 2016 in Dürnast and in Allershausen due to highest differentiation among the cultivars and a delayed senescence of the leaves. A general observation for all fertilization levels showed moderate linear correlations with biomass dry weight ($R^2 = 0.58$) in the field trials in Thalhausen in 2015 and Allershausen in 2016. Similar relationships were observed for biomass dry weight with R^2 values of 0.47 by Udelhoven et al. (2013). On the contrary, in the field trial in Dürnast in 2016, a maximal biomass dry weight detection of $R^2 = 0.93$ in biomass dry weight was obtained possibly due to a stronger differentiation of the N fertilization levels caused by a very low residual nitrate availability. Since years and sampling dates showed differences in sensor performance, a detailed consideration of the years follows.

In 2015 at flowering in the field trial Thalhausen leaf dry weight and biomass dry weight detection was similar, with slightly relationships found for the nitrogen uptake parameters. However, leaf dry weight and leaf nitrogen uptake showed improved detection compared to biomass dry weight and biomass nitrogen uptake at silage maturity, which agrees with observations by Weber et al. (2012), who found better correlations at the milk-grain stage under drought stress compared to flowering. Since leaf senescence was already progressing at silage maturity and leaf dry weight and leaf nitrogen uptake detection showed the best correlations, it is evident that leaves were the dominant organs in maize plant detection (Winterhalter et al., 2012). This could also be confirmed by measurements in 2016 with improved sensor detection found at the maximum canopy size at flowering in both experiments. The weaker sensor performance during flowering, is possibly a result of heat stress causing increased reflectance by curled leaves, a plant defense mechanism for reducing energy absorption and to prevent temperature increase (Schlemmer et al., 2005; Weber et al., 2012). Weber et al. (2012) explained the increase in reflectance as a result of curled leaf blades for reducing water losses where a large amount of sun light was absorbed by the soil and surrounding environment thereby increasing environmental noise.

In contrast to Thalhausen in 2015, a better sensor performance was observed at flowering with enhanced leaf dry weight detection ($R^2 = 0.7$) in the field site Allershausen in 2016. Fairly close correlations with biomass dry weight ($R^2 = 0.72$) were observed in the year 2016 in the field site Dürnast as a consequence of a healthy and fully developed plant canopy allowing an improved sensor detection and decreased environmental noise (Weber et al., 2012). Decreased correlations were obtained at silage maturity as a result of enhanced leaf senescence and therefore decreased chlorophyll content (Peñuelas and Filella, 1998). This was also confirmed by Erdle et al. (2013a) who found that under accelerated senescence, wheat cultivars could not be differentiated satisfactorily by sensors since nearly all red light was reflected and led to saturation. However, a decreased detection of nitrogen uptake compared to biomass detection in both experimental field trials in 2016 was observed. This could be caused by the dilution effect of nitrogen as a result of an enhanced biomass production (Erdle et al., 2011). In contrast, the nitrogen uptake showed slightly higher correlations compared to the biomass detection in Thalhausen in 2015.

The best heritability of total biomass dry weight detection was observed at flowering in all three experimental field trials which could be explained through enhanced genotypic differences. This observation was also confirmed by sensors with increased heritability at flowering, and confirms that the indices allowed to distinguish genotypic differences among cultivars. Furthermore the heritability of the total biomass dry weight on the field site Allershausen was very weak which was also associated with decreased indices heritability on this field site. Differences among cultivars at the field site Allershausen can therefore not be explained by genotypic differences. In contrast to Dürnast in 2016, which showed a very strong heritability for biomass dry weight as well as for the non-destructive sensor detection at flowering and silage maturity. In contrast to Allershausen, an increased differentiation among cultivars in biomass production was found in Dürnast due to a decreased nitrogen mineralization. These observations and the strong heritability observed in biomass dry weight and for the sensing in Dürnast support this. Under nitrogen shortage, phenotypic differentiation among cultivars was possible and therefore could contribute to a targeted approach in breeding to increase the nitrogen use efficiency.

Compared to simple linear regressions between spectral indices and destructive parameters, Partial Least Square Regression (PLSR) showed similar R^2-values. Compared to total biomass dry weight detection, improved relationships for leaf dry weight and leaf nitrogen uptake detection at flowering were observed possibly due to the fully expanded and dominating leaf exposure. In contrast to flowering, enhanced biomass dry weight and biomass nitrogen uptake, recorded at silage maturity was observed which could be explained through already progressing leaf senescence and additional detection of the organ stem.

Across all years, group classification by spectral assessment of leaf dry weight and leaf nitrogen uptake was better enabled at flowering compared to silage maturity due to an improved trait differentiation of cultivars. Group formation on the basis of biomass dry weight and biomass nitrogen uptake showed only tendencies for the separation of plant organs and therefore showed weaker differentiation at flowering and silage maturity. A differentiation depending on the fertilization levels was only successful in the field trial in Dürnast in 2016, where the initial soil was very poor in residual nitrate and therefore N fertilization exerted a very significant influence on biomass production.

4.6 Conclusions

With increasing fertilization levels of 50, 150 and 250 kg N ha^{-1}, maize cultivars showed marked differences in individual yield components and final yield. Additionally, differences in final yield over the years could be explained trough environmental effects like weather and soil conditions. Spectral reflectance measurements were able to describe yield-related plant traits during grain filling. At flowering, for the parameters leaf dry weight and nitrogen uptake, best correlations due to fully expanded leaves were observed in the waveband range of 700 nm. Within the fertilization levels, best correlations were found at the lowest and highest fertilization level due to enhanced differentiation among cultivars regarding the nitrogen supply and delayed senescence. Partial least square regression showed the same correlations as linear regression models.

4.7 References

Aparicio, N., Villegas, D., Casadesus, J., Araus, J. L., and Royo, C. (2000). Spectral vegetation indices as nondestructive tools for determining durum wheat yield. Agronomy Journal 92, 83-91.

Barmeier, G., Mistele, B., and Schmidhalter, U. (2017). Referencing laser and ultrasonic height measurements of barley cultivars by using a herbometre as standard. Crop and Pasture Science 67, 1215-1222.

Barmeier, G., and Schmidhalter, U. (2016). High-throughput phenotyping of wheat and barley. Plants grown in single or few rows in small plots using active and passive spectral proximal sensing. Sensors 16, 1860.

Behmann, J., Steinrücken, J., & Plümer, L. (2014). Detection of early plant stress responses in hyperspectral images. ISPRS Journal of Photogrammetry and Remote Sensing, 93, 98-111.

Christensen, L. K., Upadhyaya, S. K., Jahn, B., Slaughter, D. C., Tan, E., and Hills, D. (2005). Determining the influence of water deficiency on NPK stress discrimination in maize using spectral and spatial information. Precision Agriculture 6, 539-550.

Elsayed, S. (2015). Comparing the performance of active and passive reflectance sensors to assess the normalized relative canopy temperature and grain yield of drought-stressed barley cultivars. Field Crops Research 177, 148-160.

Erdle, K., Mistele, B., and Schmidhalter, U. (2011). Comparison of active and passive spectral sensors in discriminating biomass parameters and nitrogen status in wheat cultivars. Field Crops Research 124, 74-84.

Erdle, K., Mistele, B., and Schmidhalter, U. (2013a). Spectral assessments of phenotypic differences in spike development during grain filling affected by varying N supply in wheat. Journal of Plant Nutrition and Soil Science 176, 952-963.

Erdle, K., Mistele, B., and Schmidhalter, U. (2013b). Spectral high-throughput assessments of phenotypic differences in biomass and nitrogen partitioning during grain filling of wheat under high yielding Western European conditions. Field Crops Research 141, 16-26.

Esbensen, K. H., Guyot, D., Westad, F., and Houmoller, L. P. (2002). "Multivariate data analysis: in practice: an introduction to multivariate data analysis and experimental design," Multivariate Data Analysis.

Furbank, R. T., and Tester, M. (2011). Phenomics–technologies to relieve the phenotyping bottleneck. Trends in plant science 16, 635-644.

Gamon, J. A., Peñuelas, J., and Field, C. B. (1992). A narrow-waveband spectral index that tracks diurnal changes in photosynthetic efficiency. Remote Sensing of Environment 41, 35-44.

Gitelson, A. A., Merzlyak, M. N., & Lichtenthaler, H. K. (1996). Detection of red edge position and chlorophyll content by reflectance measurements near 700 nm. Journal of Plant Physiology, 148(3-4), 501-508.

Guyot, G., Baret, F., and Major, D. (1988). High spectral resolution: Determination of spectral shifts between the red and the near infrared. International Archives of Photogrammetry and Remote Sensing 11.

Jasper, J., Reusch, S., and Link, A. (2009). Active sensing of the N status of wheat using optimized wavelength combination: impact of seed rate, variety and growth stage. Precision Agriculture 9, 23-30.

Kipp, S., Mistele, B., and Schmidhalter, U. (2014a). Identification of stay-green and early senescence phenotypes in high-yielding winter wheat, and their relationship to grain yield and grain protein concentration using high-throughput phenotyping techniques. Functional Plant Biology 41, 227-235.

Kipp, S., Mistele, B., and Schmidhalter, U. (2014b). The performance of active spectral reflectance sensors as influenced by measuring distance, device temperature and light intensity. Computers and Electronics in Agriculture 100, 24-33.

Mistele, B., and Schmidhalter, U. (2008). Spectral measurements of the total aerial N and biomass dry weight in maize using a quadrilateral-view optic. Field Crops Research 106, 94-103.

Mistele, B., and Schmidhalter, U. (2010). Tractor-based quadrilateral spectral reflectance measurements to detect biomass and total aerial nitrogen in winter wheat. Agronomy Journal 102, 499-506.

Montes, J. M., Melchinger, A. E., and Reif, J. C. (2007). Novel throughput phenotyping platforms in plant genetic studies. Trends in Plant Science 12, 433-436.

Montes, J. M., Technow, F., Dhillon, B. S., Mauch, F., and Melchinger, A. E. (2011). High-throughput non-destructive biomass determination during early plant development in maize under field conditions. Field Crops Research 121, 268-273.

Peñuelas, J., and Filella, I. (1998). Visible and near-infrared reflectance techniques for diagnosing plant physiological status. Trends in Plant Science 3, 151-156.

Peñuelas, J., Filella, I., Biel, C., Serrano, L., and Save, R. (1993). The reflectance at the 950–970 nm region as an indicator of plant water status. International Journal of Remote Sensing 14, 1887-1905.

Raun, W. R., Solie, J. B., Johnson, G. V., Stone, M. L., Lukina, E. V., Thomason, W. E., and Schepers, J. S. (2001). In-Season Prediction of Potential Grain Yield in Winter Wheat Using Canopy Reflectance Contribution of the Oklahoma Agric. Exp. Stn. Agronomy Journal 93, 131-138.

Rischbeck, P., Elsayed, S., Mistele, B., Barmeier, G., Heil, K., and Schmidhalter, U. (2016). Data fusion of spectral, thermal and canopy height parameters for improved yield prediction of drought stressed spring barley. European Journal of Agronomy 78, 44-59.

Schlemmer, M. R., Francis, D. D., Shanahan, J. F., and Schepers, J. S. (2005). Remotely measuring chlorophyll content in corn leaves with differing nitrogen levels and relative water content. Agronomy Journal 97, 106-112.

Singh, A., Ganapathysubramanian, B., Singh, A. K., and Sarkar, S. (2016). Machine learning for high-throughput stress phenotyping in plants. Trends in Plant Science 21, 110-124.

Singh, M., Ceccarelli, S., and Hamblin, J. (1993). Estimation of heritability from varietal trials data. Theoretical and Applied Genetics 86, 437-441.

Udelhoven, T., Delfosse, P., Bossung, C., Ronellenfitsch, F., Mayer, F., Schlerf, M., Machwitz, M., and Hoffmann, L. (2013). Retrieving the Bioenergy Potential from Maize Crops Using Hyperspectral Remote Sensing. Remote Sensing 5, 254-273.

Walter, A., Liebisch, F., and Hund, A. (2015). Plant phenotyping: from bean weighing to image analysis. Plant Methods 11(14). https://doi.org/10.1186/s13007-015-0056-8

Weber, V. S., Araus, J. L., Cairns, J. E., Sanchez, C., Melchinger, A. E., and Orsini, E. (2012). Prediction of grain yield using reflectance spectra of canopy and leaves in maize plants grown under different water regimes. Field Crops Research 128, 82-90.

White, J. W., Andrade-Sanchez, P., Gore, M. A., Bronson, K. F., Coffelt, T. A., Conley, M. M., Feldmann, K. A., French, A. N., Heun, J. T., and Hunsaker, D. J. (2012). Field-based phenomics for plant genetics research. Field Crops Research 133, 101-112.

Winterhalter, L., Mistele, B., Jampatong, S., and Schmidhalter, U. (2011a). High-throughput sensing of aerial biomass and above-ground nitrogen uptake in the vegetative stage of well-watered and drought stressed tropical maize hybrids. Crop Science 51, 479-489.

Winterhalter, L., Mistele, B., Jampatong, S., and Schmidhalter, U. (2011b). High throughput phenotyping of canopy water mass and canopy temperature in well-watered and drought stressed tropical maize hybrids in the vegetative stage. European Journal of Agronomy 35, 22-32.

Winterhalter, L., Mistele, B., and Schmidhalter, U. (2012). Assessing the vertical footprint of reflectance measurements to characterize nitrogen uptake and biomass distribution in maize canopies. Field Crops Research 129, 14-20.

Winterhalter, L., Mistele, B., and Schmidhalter, U. (2013). Evaluation of active and passive sensor systems in the field to phenotype maize hybrids with high-throughput. Field Crops Research 154, 236-245.

Wold, S., Sjöström, M., and Eriksson, L. (2001). PLS-regression: a basic tool of chemometrics. Chemometrics and Intelligent Laboratory Systems 58, 109-130.

4.8 Appendix

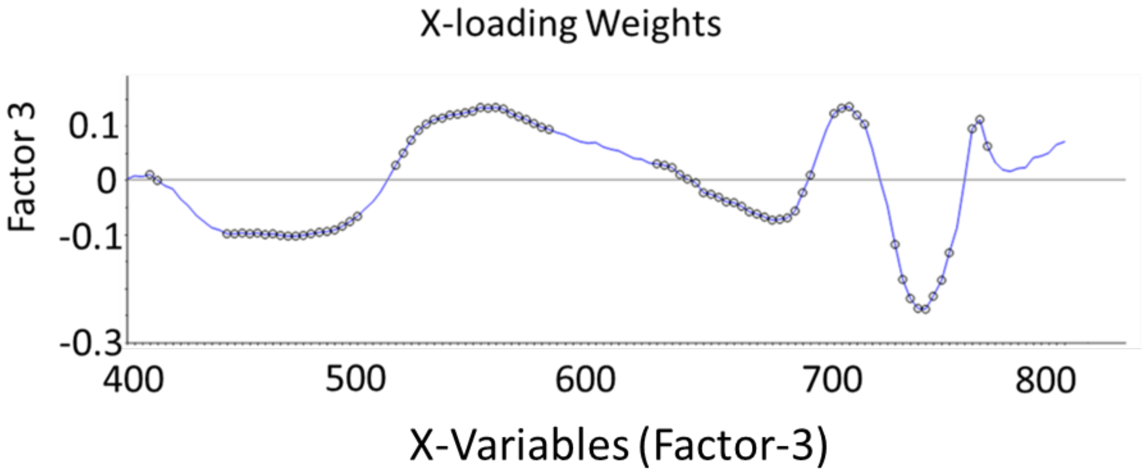

Fig. 1: Important variables for total biomass dry weight (t ha^{-1}) at flowering in Thalhausen in 2015.

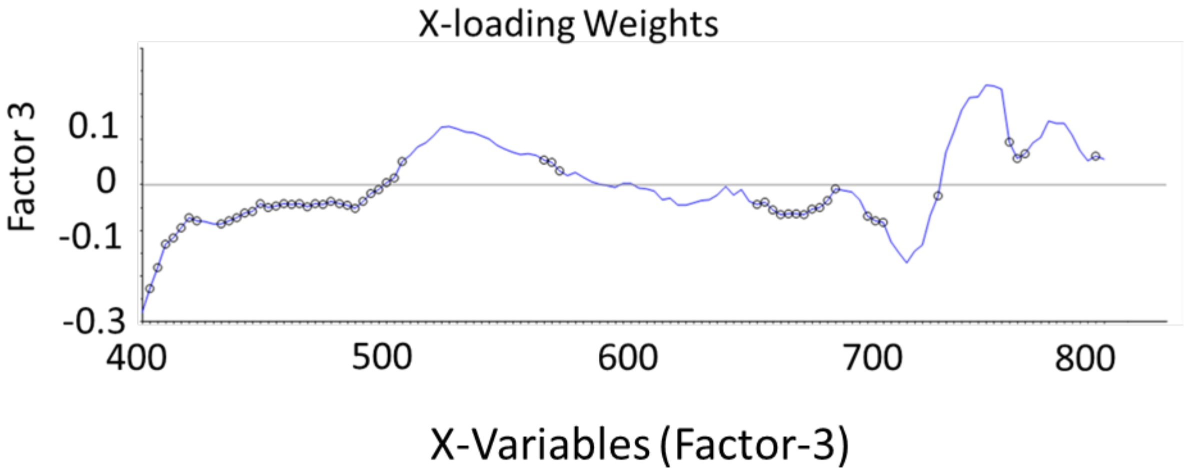

Fig. 2: Important variables for leaf dry weight (t ha^{-1}) detection at flowering in Thalhausen in 2015.

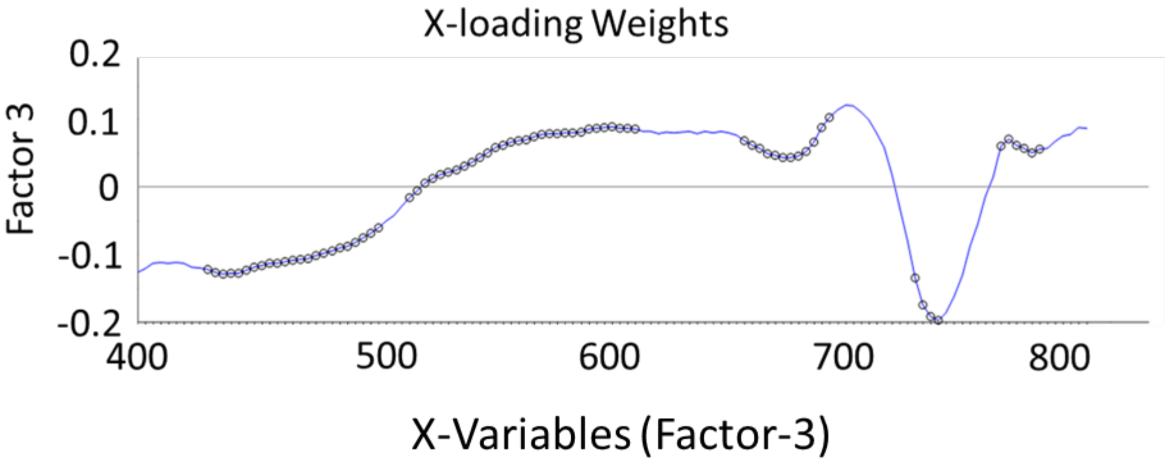

Fig. 3: Important variables for total nitrogen uptake (kg ha^{-1}) detection at flowering in Thalhausen in 2015.

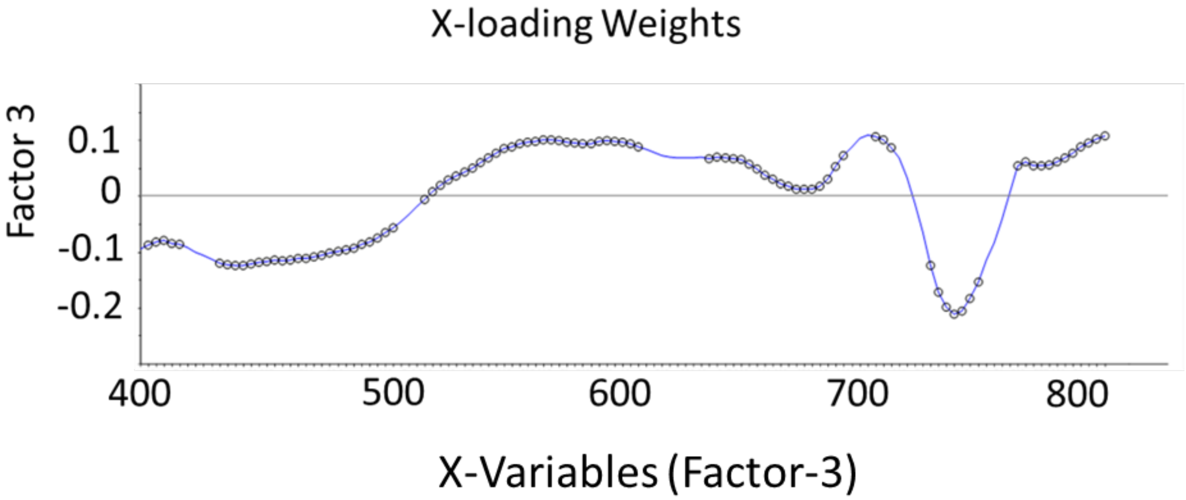

Fig. 4: Important variables for leaf nitrogen uptake (kg ha^{-1}) detection at flowering in Thalhausen in 2015.

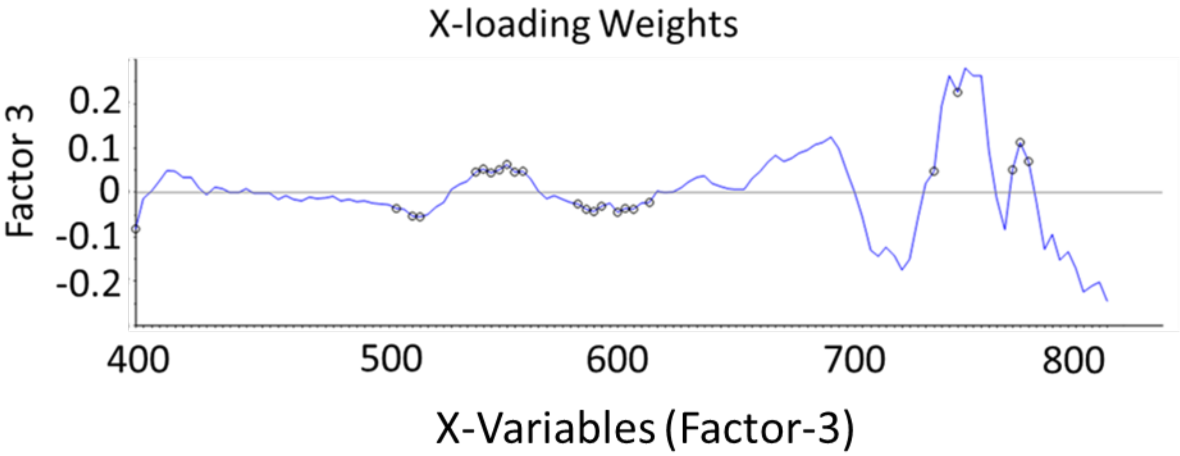

Fig. 5: Important variables for total biomass dry weight (t ha^{-1}) at silage maturity in Thalhausen in 2015.

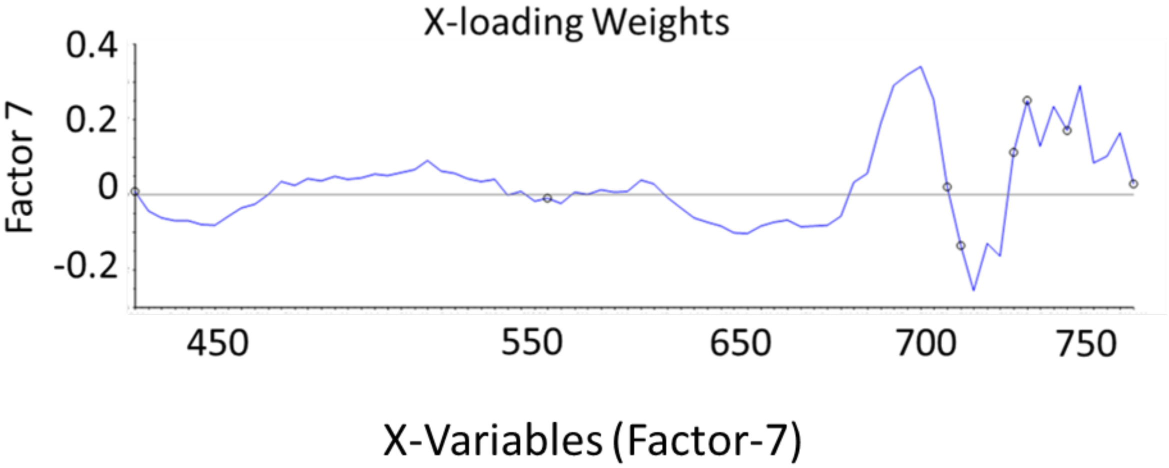

Fig. 6: Important variables for leaf dry weight (t ha^{-1}) detection at silage maturity in Thalhausen in 2015.

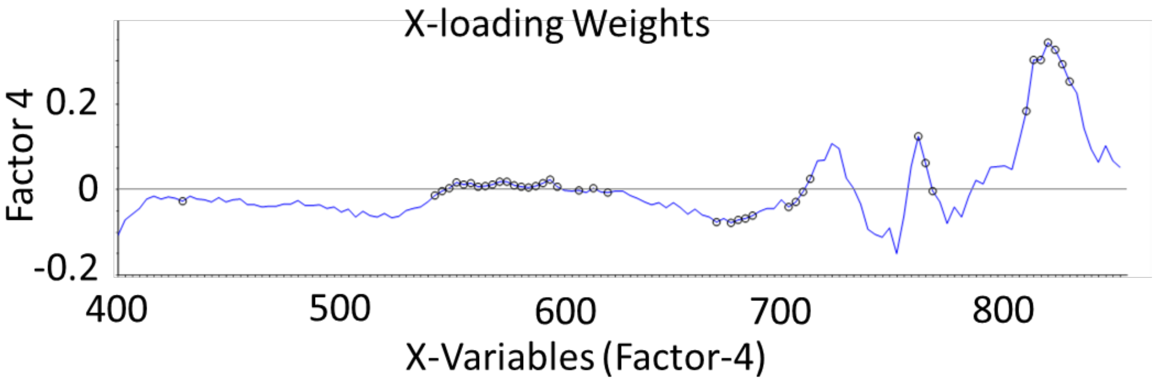

Fig. 7: Important variables for total nitrogen uptake (kg ha^{-1}) detection at silage maturity in Thalhausen in 2015.

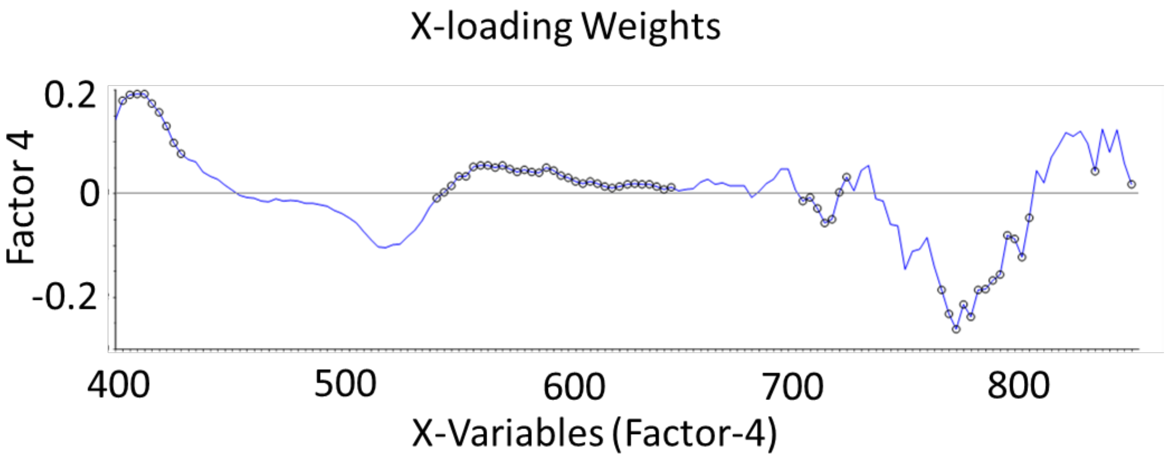

Fig. 8: Important variables for leaf nitrogen uptake (kg ha^{-1}) detection at silage maturity in Thalhausen in 2015.

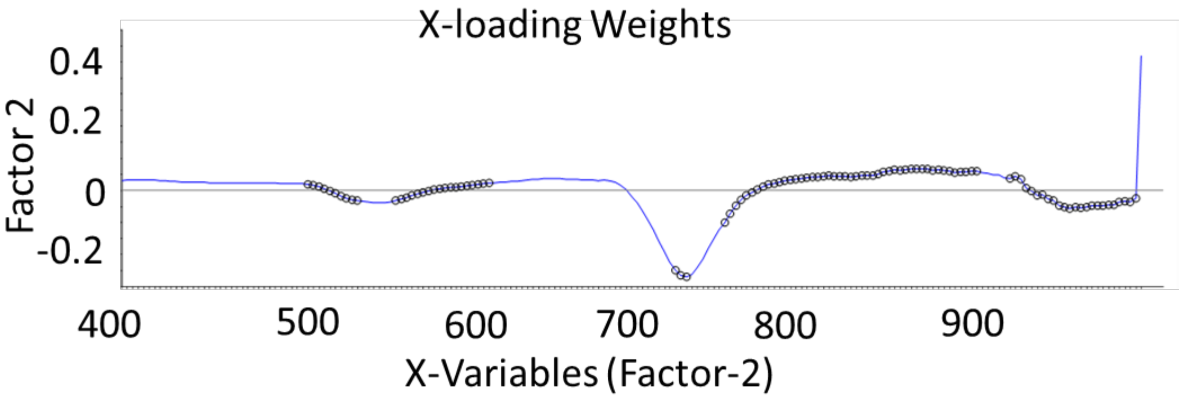

Fig. 9: Important variables of total biomass dry weight (t ha^{-1}) detection at flowering in Allershausen in 2016.

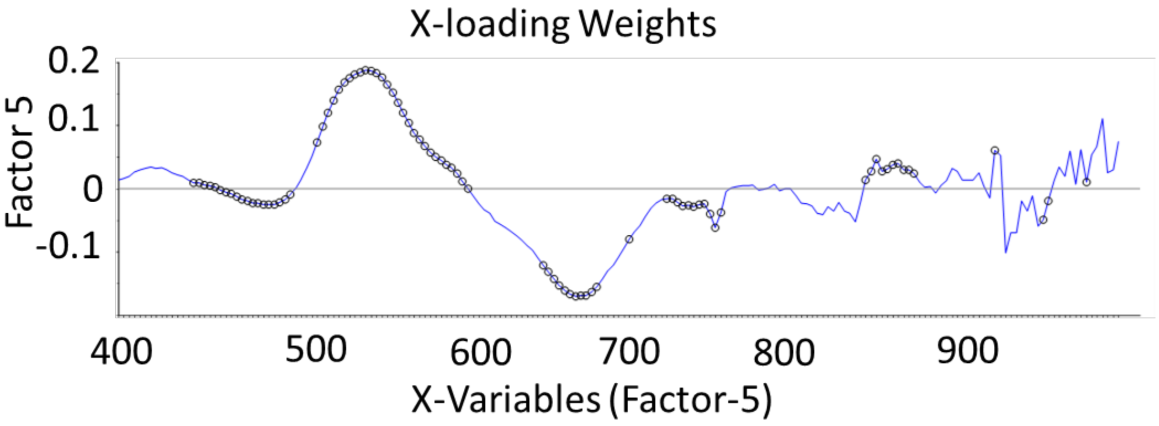

Fig. 10: Important variables of leaf dry weight (t ha^{-1}) detection at flowering in Allershausen in 2016.

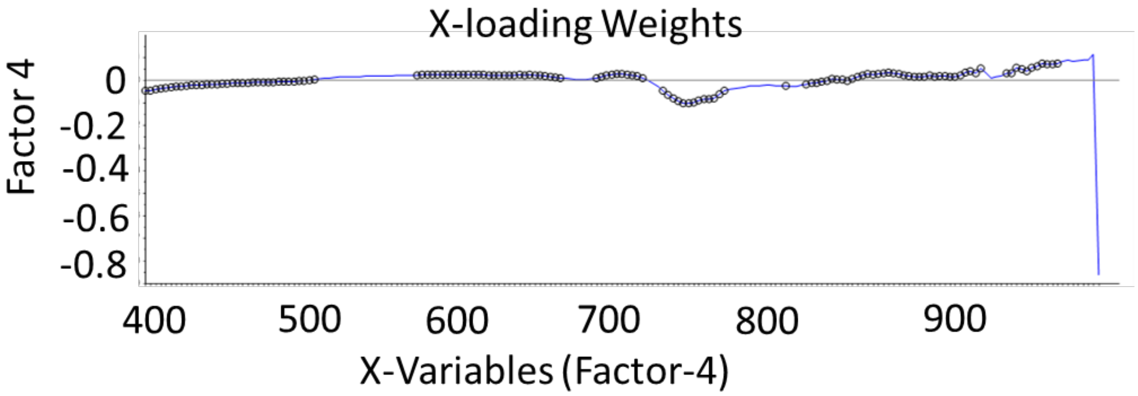

Fig. 11: Important variables of total nitrogen uptake (kg ha^{-1}) detection at flowering in Allershausen in 2016.

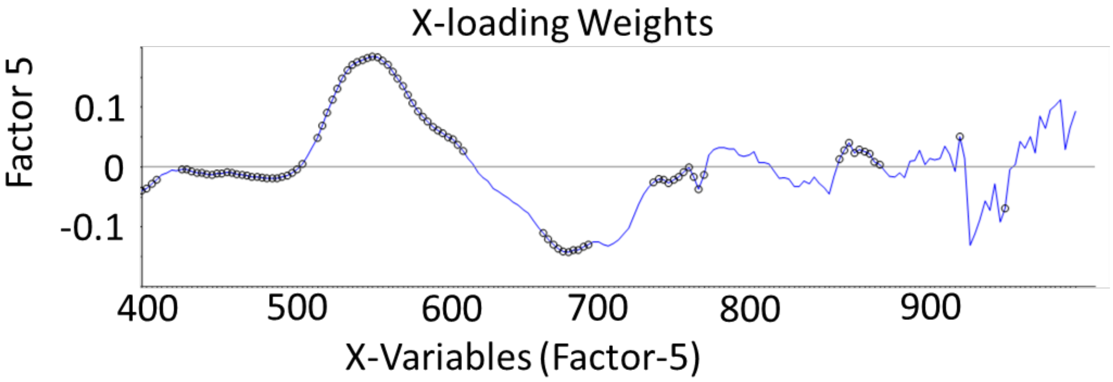

Fig.12: Important variables of leaf nitrogen uptake (kg ha^{-1}) detection at flowering in Allershausen in 2016.

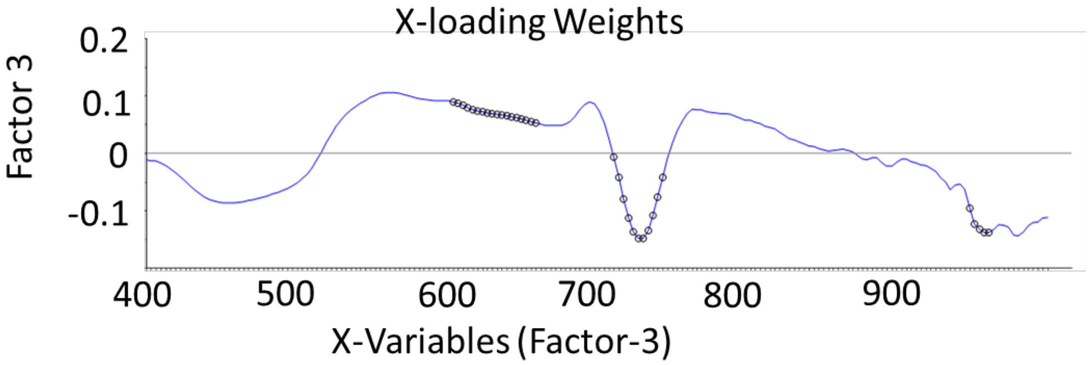

Fig. 13: Important variables of total biomass dry weight (t ha^{-1}) detection at silage maturity in Allershausen in 2016.

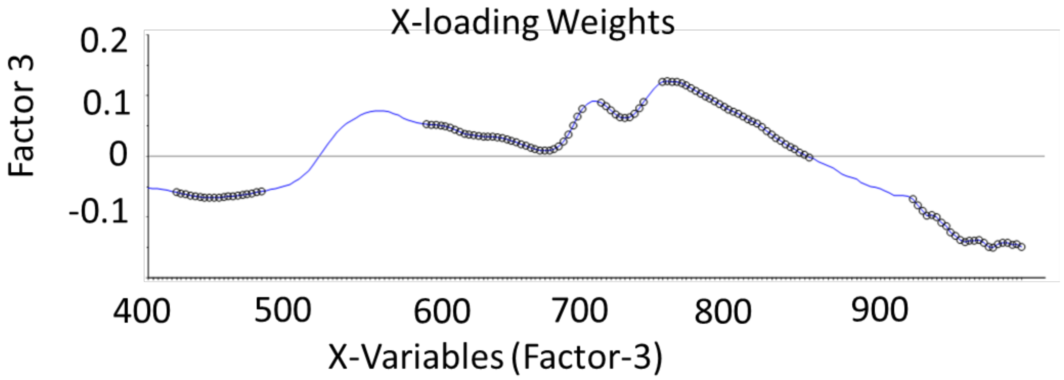

Fig. 14: Important variables of leaf dry weight (t ha^{-1}) detection at silage maturity in Allershausen in 2016.

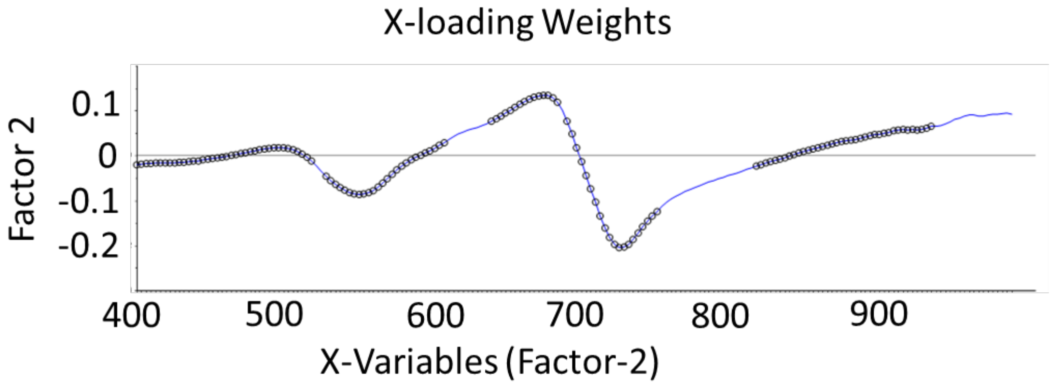

Fig. 15: Important variables of total nitrogen uptake (kg ha^{-1}) detection at silage maturity in Allershausen in 2016.

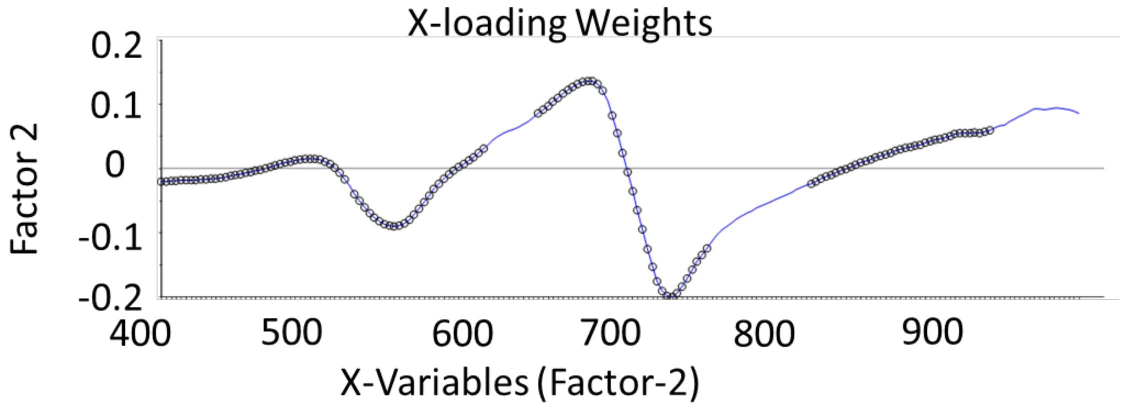

Fig. 16: Important variables of leaf nitrogen uptake (kg ha^{-1}) detection at silage maturity in Allershausen in 2016.

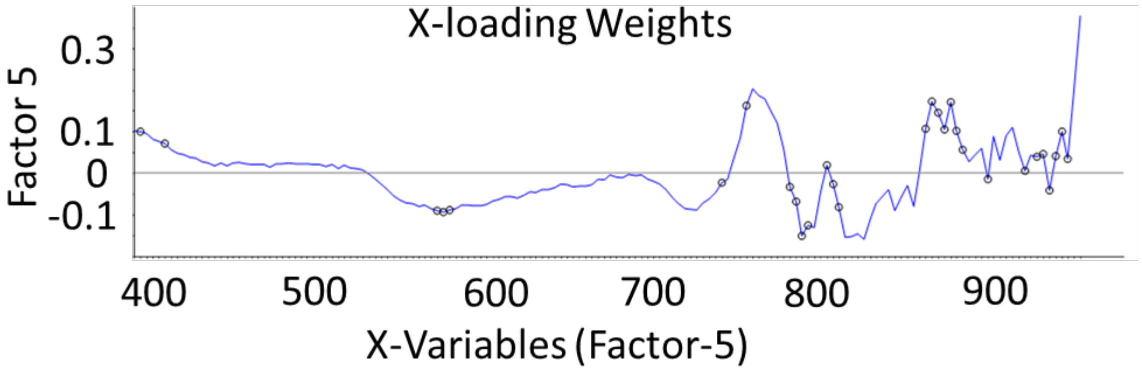

Fig. 17: Important variables of total biomass dry weight (t ha^{-1}) detection at flowering in Dürnast in 2016.

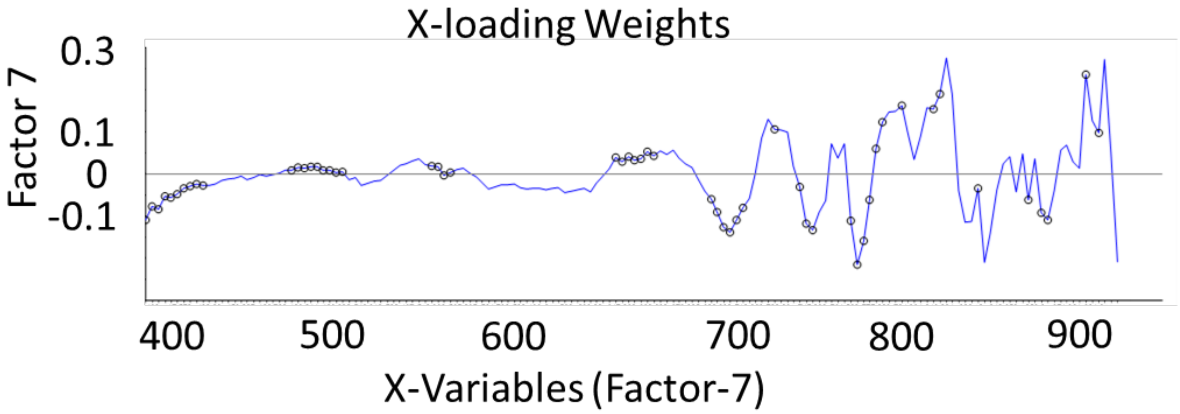

Fig. 18: Important variables of total nitrogen uptake (kg ha^{-1}) detection at flowering in Dürnast in 2016.

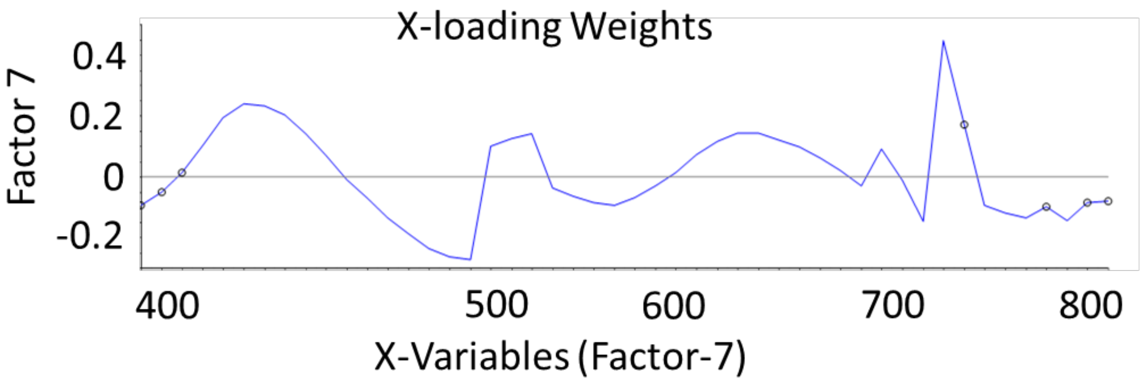

Fig. 19: Important variables of total biomass dry weight (t ha^{-1}) detection at silage maturity in Dürnast in 2016.

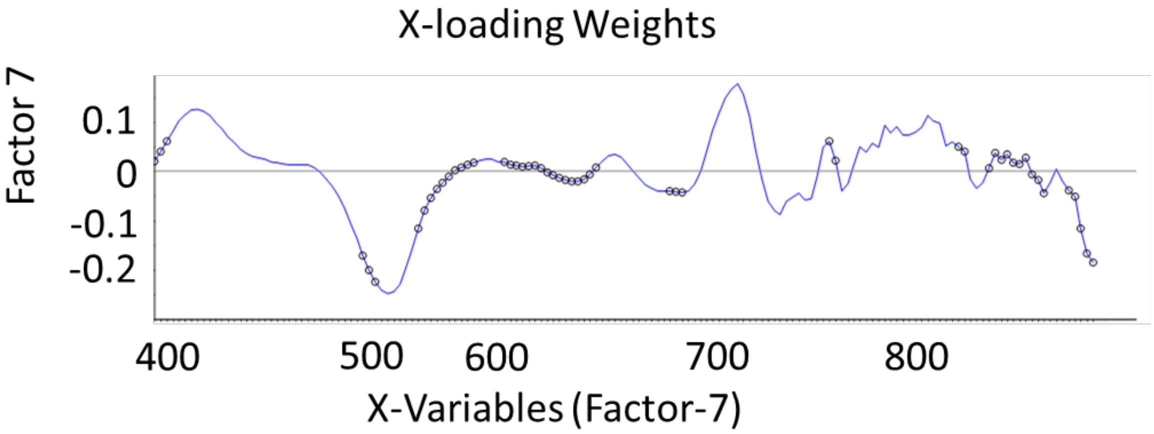

Fig. 20: Important variables of leaf dry weight (t ha^{-1}) detection at silage maturity in Dürnast in 2016.

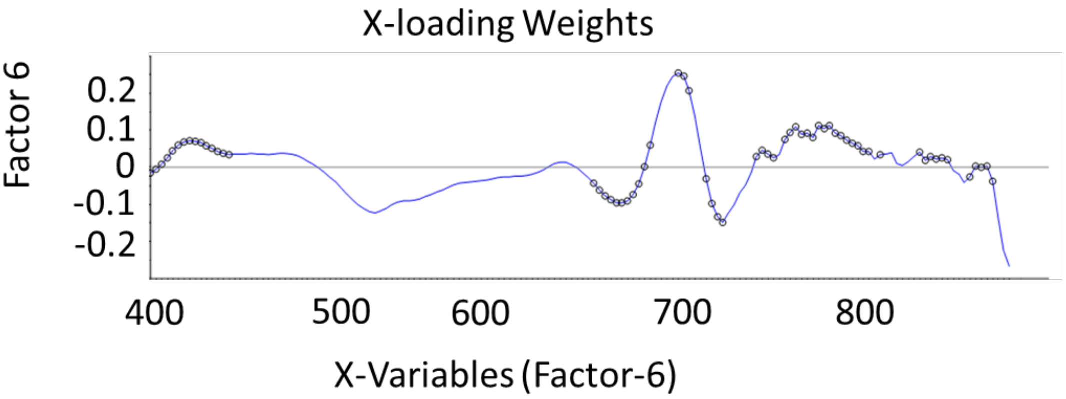

Fig. 21: Important variables of total nitrogen uptake (kg ha^{-1}) detection at silage maturity in Dürnast in 2016.

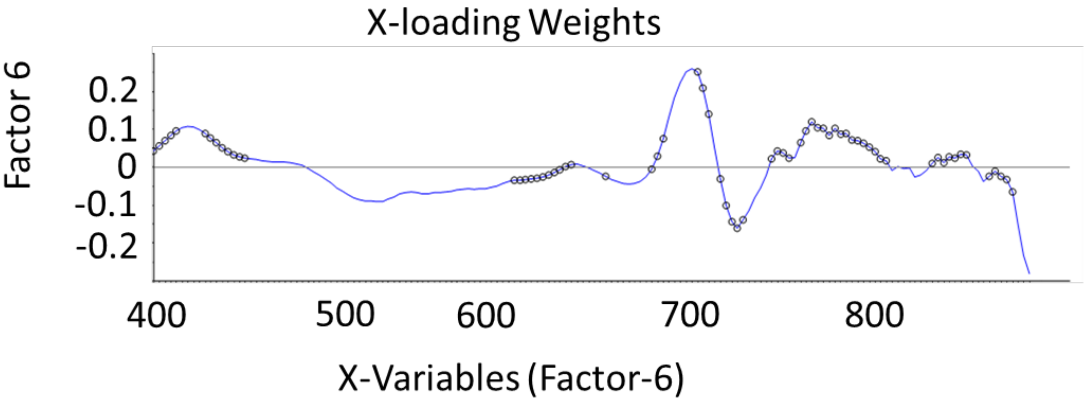

Fig. 22: Important variables of leaf nitrogen uptake (kg ha^{-1}) detection at silage maturity in Dürnast in 2016.

5 General Discussion

5.1 Tools for studying carbon and nitrogen allocation

There are various methods to estimate carbon and nitrogen allocation within a plant. Much knowledge about carbon and nitrogen allocation in plants was gained by means of stable isotopes, using both natural abundance and labelling experiments (Bowling et al., 2008; Dawson et al., 2002; Epron et al., 2012; Gallais et al., 2007; Peterson and Fry, 1987). Natural isotope abundance approaches take advantage of photosynthetic ^{13}C discrimination (Δ^{13}C) in C_3-plants, which leads to a pronounced difference in the δ^{13}C values of atmospheric CO_2 (source) and the photoassimilates (product) of about 20‰. Variation in leaf Δ^{13}C is controlled by the ratio of intercellular to atmospheric CO_2 concentration (c_i/c_a). Environmental conditions as drought stress potentially influence stomatal conductance and photosynthetic activity which leads to changes in the c_i/c_a ratio (Cernusak et al., 2013; Farquhar et al., 1982) and therefore reduces Δ^{13}C and increases δ^{13}C content in the assimilate. However, with increasing distance from leaves into the plants the δ^{13}C content becomes weaker (Brandes et al., 2006). Therefore labelling techniques with enriched ^{13}C and ^{15}N may be better alternatives in reflecting allocation processes in plants. Pulse labelling allows detecting transport velocities and the exact amount of carbon and nitrogen in the pool of several plant compartments (Epron et al., 2012). Pulse-labelling is usually applied in form of $^{13}CO_2$ which enters through photosynthetic activity into the leaves or $^{15}NH_3$ applied as fertilizer on soil assimilated directly from the roots. The information gained from the isotopes is restricted to the fate of CO_2 and NH_3 assimilated during the limited period of the label application (Blessing, 2014). Additionally, pulse-labelling experiments under controlled conditions for example climate chambers have been shown to be a reliable method to detect allocation processes within the plants. However, the application of label experiments into the fields are potentially more challenging due to heavy rainfall and accompanying losses of isotopes. Under non-controlled conditions and closed environmental systems the guarantee for complete isotope detection is not given.

In this thesis as method the assessment of the biomass dry weight differences at flowering (vegetative phase), silage and grain maturity (generative phase) in order to detect translocation processes through biomass displacement was used. This method was already successfully established in various previous studies (e.g. Ciampitti et al., 2013a; Ciampitti et al., 2013b; Ciampitti et al., 2013c, d; Hernandez-Ramirez et al., 2011; Pommel et al., 2006) and gives a good overview on transportation capacity and allocation systems. However, by comparing different maturing cultivars the time of harvest has to be chosen individually for all cultivars in order to ensure the same time-specific translocation capacity. Furthermore, biomass losses due to phenological differences are not considered and may lead to misinterpretation and therefore the exact amount of translocation capacity is not detected.

5.2 The importance of C- and N allocation in regard to breeding targets

Plant breeders have the goal to improve cultivars that suit the needs of the farmers (Duvick et al., 2010). These needs are constrained by certain requirements. There are various uses of maize: for example, as food and in livestock farming, where the focus is on a high energy density and digestibility (Argillier et al., 2000). In addition, grain maize with enhanced protein content is relevant in dairy cattle farming (Klopfenstein et al., 2013). However, through the use of maize as a renewable energy source (via the production of biogas) –the amount of methane has been gaining an increasing importance in today's breeding (Oslaj et al., 2010). By breeding maize as a potential energy crop the focus has shifted to higher dry weight biomass production and methane fermentation rates whereas corn crop proportion is neglected. This observation could lead to more precise breeding programs where silage and biogas maize are more separated. Beside the optimization of maize plant traits, official requirements, resource scarcity and field management force breeders to improve cultivars in their nutrient efficiency (P,N) (Ciampitti et al., 2013a; Hanway, 1962) and growth tolerance with regard to plant density (Ciampitti and Vyn, 2011). In order to meet all these requirements, a more in-depth understanding of carbon and nitrogen allocation in plants is inevitable. Only through a more detailed understanding of nitrogen and carbon uptake and remobilization capacity with regard to environmental changes, nutrient supply and longstanding breeding processes a better performance of cultivars can be achieved.

Additionally, it is already well-known that there is a close interaction between environment (E), genotype (G) and field management (M) (Ciampitti and Vyn, 2012). Nitrogen Use Efficiency is strongly influenced by climate conditions, fertilization rates and genomic variety (Ciampitti and Vyn, 2012). The strength of a cultivar cannot be identified through the phenotyping-years because environmental conditions do not stay consistent. A strong trait of a cultivar can be detected by changing the phenotyping location. The comparison of a cultivar under different environmental conditions, such as temperature, precipitation and soil could capture, enhanced environmental adaption of a cultivar. A high adaptation of plants can be recognized through their yield potential, yield stability and stress tolerance (Tollenaar and Lee, 2002). In contrast to the areal adaption of cultivars, the different strategies of producing dry matter and yield for different cultivars, such as stay green, late or early maturity cultivars depends on the year and the geographical location (Kosgey et al., 2013). The reproductive and remobilized N depends strongly on field management (M) and environmental conditions (E) (Ciampitti and Vyn, 2013). In addition, seed density and different fertilization rates influence nitrogen allocation in maize plants (Ciampitti et al., 2013b; Ciampitti et al., 2013c; Ciampitti and Vyn, 2011), too.

5.3 Future breeding targets

Since the implementation of maize hybrids on farmer fields in the early 1930s (Duvick et al., 2010), maize breeding has increased rapidly until today. However, breeding programs are going to be downsized or even eliminated in the future to the point that public maize breeding programs are going to be nearly irrelevant (Hallauer, 2009). The maize genome has already been sequenced and the molecular genetic research has advanced research with the Bt (Hutchison et al., 2010) and glyphosate resistance of maize (Sammons and Gaines, 2014). In the future, means will be provided to identify important genes to improve yield, pest tolerance, heat and drought tolerance of heterosis in hybrids (Hallauer, 2009) - a new time in breeding is about to start. However, to translate the information generated at the molecular level to the phenotype of corn in the field will be a tremendous challenge (Hallauer, 2009). Therefore, high-throughput phenotyping methods in classical field experiments must not lose sight because these methods provide also a wealth of information to combine genomic and phenomics as well as to complete and accelerate breeding targets.

5.4 Research questions revisited

This study contributes to the understanding of carbon and nitrogen allocation processes of maize plants in the reproductive phase with the help of high-throughput phenotyping techniques – using sensors and UAVs. One crucial aspect of nitrogen and carbon allocation is the link between uptake of both nutrients from leaves via photosynthesis and the roots until flowering and the effective redistribution to the reproductive organ – the corn. A deeper understanding of drivers and the close interaction of both allocations helps to predict nitrogen and carbon allocation patterns, critical plant physiological responses (e.g. under drought stress) and improves breeding targets. The experiments performed with different maize cultivars with different breeding targets grown under low (50 kg N ha^{-1}), medium (150 kg N ha^{-1}) and higher (250 kg N ha^{-1}) nitrogen fertilization levels has been shown to contribute to answering the research questions of the thesis.

1) In relation to claim settlement: can precision farming techniques as UAV and sensors help to asses economic related parameters like yield, post-emergence and nitrogen demand? And are they able to predict final yield increases in an early plant growth stage? Precision farming techniques have the potential to compensate losses with regard to yield, nutrient demand and field management. The successful detection of plant emergence and, thus, increased knowledge of plants amount and seed quantity is a reliable way to predict the final yield. Additionally, the estimation of series connection on a spatial and temporal dimension and the opportunity to estimate soil erosion grooves by image analysis support field management quality. Furthermore, nitrogen demand was successfully detected by image analysis and sensors. However, the estimation of more precise nutrient values is not possible through phenotyping methods, which cannot replace precise laboratory work.

2) With regard to the environmental aspect and official requirements: do sensors and image processing detect nitrogen demand in the exact dimensions for reliable field management. And do sensors and image processing provide the means for targeted and needs-oriented fertilizer approaches? The detection of aboveground biomass dry weight (BDW) and leaf biomass dry weight (LDW) was shown to be reliable. On soils with low nitrogen mineralization and a fertilization range of 50 to 250 kg N ha^{-1} correlations among BDW and indices reached up to $R^2 = 0.9$. Furthermore, biomass and leaf dry weight detection with lower nitrogen fertilization effects (due to rich soils) still reach correlations of around $R^2 = 0.5–0.6$ for BDW and 0.6-0.7 for LDW. Since sensors detected the nitrogen uptake of total aboveground biomass and leaves with correlations up to an R^2 of 0.7, the use of sensors for targeted and needs-oriented fertilization application is reasonable.

3) With respect to the breeding progress: is the utilization of sensors a reliable and potential tool to detect efficient traits of maize cultivars by providing accurate

maize performance forecasts and does it thereby accelerate the trustworthy breeding processes? Followed by the next question: How should future breeding targets consider physiological aspects? Sensor performance in breeding purposes is a useful tool to detect biomass yield and leaf mass, whereas detection of corn, cob and stem can be neglected due to maize plant architecture. Furthermore, the nitrogen uptake capacity of leaves and total above-ground biomass is an important parameter in breeding targets. Hence, time-consuming and costly laboratory measurements can be replaced through reliable ($R^2 = 0.7$) sensor detections.

However, besides above-ground biomass and leaf detection weaker or even no correlations were observed for other traits like corn amount and quality or stem nitrogen uptake and diameter. Therefore, sensor techniques can only partly replace maize scoring with regard to biomass and nitrogen uptake capacity, whereas leaf angle, corn production, stem diameter and many other traits still have to be done manually. However, sensor techniques provide information for preselection and drastically accelerated breeding.

4) Which importance do translocation processes have such as remobilized and reproductive N in future breeding targets and which loadings can be given to these two allocations? Can allocation processes be optimized, in regard to nitrogen use efficiency and the predicted environmental and climate changes? In the last years breeding targets were more focused on reproductive N together with an increase in yield, whereas NUPsilk decreased from a percentage uptake of 75% before 1999 to 46% after 1999 in “new era” cultivars. However, remobilized N in the generative phase should not be underestimated due to a significant increase of Nrem under drought stress conditions during the corn filling period.

Therefore, a close interaction between remobilized and reproductive N is given and both nitrogen translocations contribute their part to maintain grain filling. In breeding programs which optimize nitrogen use efficiency, remobilized N is a relevant parameter due to an effective use of nitrogen which is first stored in any plant organ (stem or leaf) and with starting senescence is used to fill corn. In contrast, with enhanced reproductive N yield increased, too, but to scoop fully the potential of reproductive N, environmental conditions and sufficient soil N has to prevail. The post flowering N uptake depends strongly on optimal weather conditions and soil N content. The complete need on nitrogen is not fully covered by remobilized N but future breeding should consider enhanced remobilization strength in maize plants to compensate post flowering nitrogen uptake losses.

5.5 References

Argillier, O., Méchin, V., and Barri e ` re, Y. (2000). Inbred line evaluation and breeding for digestibility-related traits in forage maize. Crop Science 40, 1596-1600.

Blessing, C. H. (2014). Carbon Allocation from the Canopy to the Soil/Root System in Response to Environmental Stress (Doctoral dissertation).

Bowling, D. R., Pataki, D. E., and Randerson, J. T. (2008). Carbon isotopes in terrestrial ecosystem pools and CO2 fluxes. New Phytologist 178, 24-40.

Brandes, E., Kodama, N., Whittaker, K., Weston, C., Rennenberg, H., Keitel, C., Adams, M. A., and Gessler, A. (2006). Short-term variation in the isotopic composition of organic matter allocated from the leaves to the stem of Pinus sylvestris: effects of photosynthetic and postphotosynthetic carbon isotope fractionation. Global Change Biology 12, 1922-1939.

Cernusak, L. A., Ubierna, N., Winter, K., Holtum, J. A., Marshall, J. D., and Farquhar, G. D. (2013). Environmental and physiological determinants of carbon isotope discrimination in terrestrial plants. New Phytologist 200, 950-965.

Ciampitti, I. A., Camberato, J. J., Murrell, S. T., and Vyn, T. J. (2013a). Maize nutrient accumulation and partitioning in response to plant density and nitrogen rate: I. Macronutrients. Agronomy Journal 105, 783-795.

Ciampitti, I. A., Murrell, S. T., Camberato, J. J., Tuinstra, M., Xia, Y., Friedemann, P., and Vyn, T. J. (2013b). Physiological dynamics of maize nitrogen uptake and partitioning in response to plant density and nitrogen stress factors: II. Reproductive phase. Crop Science 53, 2588-2602.

Ciampitti, I. A., Murrell, S. T., Camberato, J. J., Tuinstra, M., Xia, Y. B., Friedemann, P., and Vyn, T. J. (2013c). Physiological dynamics of maize nitrogen uptake and partitioning in response to plant density and N stress factors: I. Vegetative Phase. Crop Science 53, 2105-2119.

Ciampitti, I. A., Murrell, S. T., Camberato, J. J., Tuinstra, M., Xia, Y. B., Friedemann, P., and Vyn, T. J. (2013d). Physiological dynamics of maize nitrogen uptake and partitioning in response to plant density and nitrogen stress factors: II. Reproductive Phase. Crop Science 53, 2588-2602.

Ciampitti, I. A., and Vyn, T. J. (2011). A comprehensive study of plant density consequences on nitrogen uptake dynamics of maize plants from vegetative to reproductive stages. Field Crops Research 121, 2-18.

Ciampitti, I. A., and Vyn, T. J. (2012). Physiological perspectives of changes over time in maize yield dependency on nitrogen uptake and associated nitrogen efficiencies: A review. Field Crops Research 133, 48-67.

Ciampitti, I. A., and Vyn, T. J. (2013). Grain nitrogen source changes over time in maize: A Review. Crop Science 53, 366-377.

Dawson, T. E., Mambelli, S., Plamboeck, A. H., Templer, P. H., and Tu, K. P. (2002). Stable isotopes in plant ecology. Annual Review of Ecology and Systematics 33, 507-559.

Duvick, D., Smith, J., and Cooper, M. (2010). Long-term selection in a commercial hybrid maize breeding program. Janick. I. Plant Breeding Reviews. Part 2, 109-152.

Epron, D., Bahn, M., Derrien, D., Lattanzi, F. A., Pumpanen, J., Gessler, A., Högberg, P., Maillard, P., Dannoura, M., and Gérant, D. (2012). Pulse-labelling trees to study carbon allocation dynamics: a review of methods, current knowledge and future prospects. Tree Physiology 32, 776-798.

Farquhar, G. D., O'Leary, M. H., and Berry, J. A. (1982). On the relationship between carbon isotope discrimination and the intercellular carbon dioxide concentration in leaves. Functional Plant Biology 9, 121-137.

Gallais, A., Coque, M., Le Gouis, J., Prioul, J., Hirel, B., and Quillere, I. (2007). Estimating the proportion of nitrogen remobilization and of postsilking nitrogen uptake allocated to maize kernels by nitrogen-15 labeling. Crop Science 47, 685-691.

Hallauer, A. R. (2009). “Corn breeding”. Iowa State Research Farm Progress Reports, 475.

Hanway, J. (1962). Corn growth and composition in relation to soil fertility: II. Uptake of N, P, and K and their distribution in different plant parts during the growing season. Agronomy Journal 54, 217-222.

Hernandez-Ramirez, G., Brouder, S. M., Smith, D. R., and Van Scoyoc, G. E. (2011). Nitrogen partitioning and utilization in corn cropping systems: Rotation, N source, and N timing. European Journal of Agronomy 34, 190-195.

Hutchison, W. D., Burkness, E., Mitchell, P., Moon, R., Leslie, T., Fleischer, S. J., Abrahamson, M., Hamilton, K., Steffey, K. L., and Gray, M. (2010). Area wide suppression of European corn borer with Bt maize reaps savings to non-Bt maize growers. Science 330, 222-225.

Klopfenstein, T. J., Erickson, G. E., and Berger, L. L. (2013). Maize is a critically important source of food, feed, energy and forage in the USA. Field Crops Research 153, 5-11.

Kosgey, J. R., Moot, D. J., Fletcher, A. L., and McKenzie, B. A. (2013). Dry matter accumulation and post-silking N economy of 'stay-green' maize (*Zea mays* L.) hybrids. European Journal of Agronomy 51, 43-52.

Oslaj, M., Mursec, B., and Vindis, P. (2010). Biogas production from maize hybrids. Biomass and Bioenergy 34, 1538-1545.

Peterson, B. J., and Fry, B. (1987). Stable isotopes in ecosystem studies. Annual Review of Ecology and Systematics 18, 293-320.

Pommel, B., Gallais, A., Coque, M., Quillere, I., Hirel, B., Prioul, J. L., Andrieu, B., and Floriot, M. (2006). Carbon and nitrogen allocation and grain filling in three maize hybrids differing in leaf senescence. European Journal of Agronomy 24, 203-211.

Sammons, R. D., and Gaines, T. A. (2014). Glyphosate resistance: state of knowledge. Pest Management Science 70, 1367-1377.

Tollenaar, M., and Lee, E. (2002). Yield potential, yield stability and stress tolerance in maize. Field Crops Research 75, 161-169.

Curriculum vitae

PERSONAL PROFILE

EDUCATION

08 2014 – 08 2017	*Ph.D. in agricultural sciences at the* Technical University of Munich (TUM) Munich, Germany Topic: High-Throughput Phenotyping of different maize cultivars (*Zea mays* L.) under nitrogen discrimination
09 2007 – 09 2013	*Diploma (equivalent to MA) in* Geoökologie *(Environmental Science) at the* Karlsruher Institute of Technology (KIT) Karlsruhe, Germany Main focus: Ecosystem research, plant physiology
09 2012 – 04 2013	*Master thesis written at the* *Swiss Federal Institute of Technology Zürich (ETH)* Zürich, Switzerland Topic: Diurnal transport and storage of recently fixed carbohydrates in beans (*Phaseolus vulgaris* L.)
03 2010 – 07 2010	*Academic semester abroad at the* Universidade do Paraná with a DAAD scholarship, Curitiba, Brazil

REMUNERATED WORK EXPERIENCE

08 2014 – 08 2017	*Research Assistant at the Technical University of Munich (TUM)* Munich, Germany
03 2012 – 08 2012	*Practical experiences at Investment Ethics Research & Advisory AG (INVERA),* Zürich, Switzerland
08 2010 – 11 2010	*Research Assistant at Instituto Nacional de Pesquisas da Amazônia (INPA)*,Manaus, Brazil
10 2008 – 12 2010	*Evaluation Assistant at the Federal Agency of Hydraulic Engineering* Karlsruhe, Germany

CONFERENCE CONTRIBUTIONS AND RESAERCH STAYS

09 2017	*Poste*r at the VDLUFA-Congress; Standortgerechte Landnutzung- Umweltverträglich und wirtschaftlich, Digitale Erfassung von Maispflanzen mit Drohnenbildern, Freising
12 2016	*Talk* at the International Nitrogen Initiative Conference, Discriminating Nitrogen Status Parameters of Maize Cultivars with High-throughput Phenotyping, Melbourne, Australia

09 2016	*Talk* at the DGP International Conference, Discriminating Nitrogen Status Parameters of Maize Cultivars with High-throughput Phenotyping, Hohenheim Stuttgart, Germany
07 2016	*Summer School*, Image Analysis for Plant Phenotyping, Wageningen, Netherlands
11 2015	*Poste*r at the conference – Regulation of soil organic matter and nutrient turnover in agriculture; Challenges in future breeding methods: How to detect nitrogen use efficiency of different maize cultivars, Kassel Germany